ISBN 978-82-326-0890-4 (printed version)
ISBN 978-82-326-0891-1 (electronic version)
ISSN 1503-8181

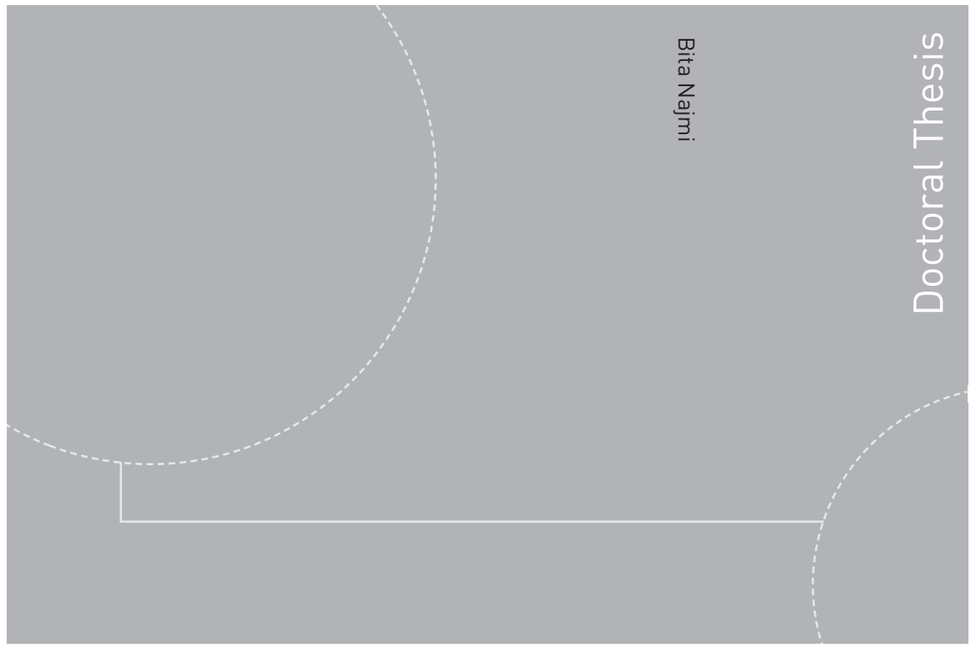

Doctoral theses at NTNU, 2015:117

Bita Najmi

Operation of power cycles with integrated CO_2 capture using advanced high-temperature technologies

NTNU
Norwegian University of Science and Technology
Faculty of Engineering Science and Technology
Department of Energy and Process Engineering

NTNU – Trondheim
Norwegian University of
Science and Technology

Doctoral theses at NTNU, 2015:117

NTNU

NTNU – Trondheim
Norwegian University of
Science and Technology

Bita Najmi

Operation of power cycles with integrated CO_2 capture using advanced high-temperature technologies

Thesis for the degree of Philosophiae Doctor

Trondheim, May 2015

Norwegian University of Science and Technology
Faculty of Engineering Science and Technology
Department of Energy and Process Engineering

NTNU – Trondheim
Norwegian University of
Science and Technology

NTNU
Norwegian University of Science and Technology

Thesis for the degree of Philosophiae Doctor

Faculty of Engineering Science and Technology
Department of Energy and Process Engineering

ISBN 978-82-326-0890-4 (printed version)
ISBN 978-82-326-0891-1 (electronic version)
ISSN 1503-8181

Doctoral theses at NTNU, 2015:117

Printed by Skipnes Kommunikasjon as

To my dear family

Abstract

One of the routes for CO_2 capture from power plants is to remove carbon content of the fuel before combustion takes place, known as pre-combustion CO_2 capture. A typical pre-combustion CO_2 capture method consists of two stages of Water Gas Shift (WGS) reactors at two different temperature levels, followed by a CO_2 capture unit. The CO_2 capture process is usually based on physical absorption at low temperature. A novel pre-combustion CO_2 capture technology, so-called Sorption Enhanced Water Gas Shift (SEWGS), combines both the WGS reaction and CO_2 capture in one single unit, at elevated temperatures. The equilibrium-controlled WGS reaction is hence enhanced towards higher conversions of CO into CO_2. The CO_2 is adsorbed simultaneously on the solid adsorbent.

This thesis deals with dynamic performance assessment of an Integrated Gasification Combined Cycle (IGCC) power plant, incorporating a SEWGS process for pre-combustion CO_2 capture. This is to examine how well the IGCC with SEWGS can perform under load variations.

Syngas from a coal gasifier is sent to the SEWGS system after going through solids and H_2S removal units. A multi-train SEWGS system treats the feed syngas being produced continuously in a gasifer of the IGCC. Each SEWGS train consists of eight reactors, working in parallel and packed with a mixture of the WGS reaction catalyst and CO_2 adsorbent. Each SEWGS reactor undergoes a fixed sequence of processing steps, repeated in a cyclic manner, based on a Pressure Swing Adsorption (PSA) process. The PSA process steps consist of feed, rinse, three pressure equalization, depressurization, purge and repressurization steps. The SEWGS reactors are interacting with each other in all the cycle steps, except during depressurization and purge step. The interconnection between the reactors is carried out using valves. Steam is assumed to be extracted from the steam cycle and used as the rinse and purge gas. A H_2-rich stream is produced during the feed step, where the WGS reaction and CO_2 adsorption take place simultaneously. Part of the H_2-rich being produced during the feed step is used for the repressurization step. A CO_2-rich gas is recovered during the depressurization and purge step. The H_2-rich product is used as a fuel in a GT within the IGCC power plant. Cyclic operation manner of the SEWGS process means that the system is inherently dynamic and therefore studying dynamic performance of such a system is necessary, particularly when such a process is incorporated into a power plant. Also, the SEWGS system dynamic characteristic at different flow rates of feed syngas is interesting for further investigation of the load-following performance of the IGCC power plant at different GT load levels.

A one-dimensional, non-isothermal, homogeneous dynamic model of a PSA-based SEWGS system of multiple dispersed plug-flow reactors has been carried out. Operation schedule of the SEWGS system, including aspects such as transition from one PSA processing step to another for a given reactor and switching of the connections between the reactors using interconnecting valves, is implemented by the modeling approach.

The designed SEWGS process gives a CO_2 recovery rate of 95%, with around 99% purity of the recovered CO_2. The H_2-rich product purity achieved is around 81%. The H_2-rich stream flow rate,

produced from a SEWGS train, is found to undergo a periodic fluctuation of around ±33%, due to using part of the H_2-rich product stream repeatedly during the re-pressurization step. While, the GT requires a smooth fuel heat input (flow rate, composition) at any given load of operation, it is essential to dampen the H_2-rich product flow rate fluctuations as much as necessary. A schedule is developed to initiate operation of the trains with time lags and evaluate its impact on improving the H_2-rich fuel fluctuation. Two different scheduled operation schemes are applied and time lags between the operation of trains are optimized. The fluctuations of the H_2-rich stream flow rate are decreased from ±33% to ~±14% and ~±11% for the first and second operation scheme, respectively.

A closed-loop control strategy including a buffer tank followed by a control valve, before the GT is implemented to further smooth out the fluctuations in the H_2-rich fuel flow rate and composition. The control system is also designed to control the H_2-rich fuel at full-load and part-load operations of the GT, complying with the fuel flow rate and heating value requirements of a modern GT.

Performance simulation of the IGCC integrated with the SEWGS system, incorporating the fuel control strategy is first carried out at full-load operation of the GT. For evaluating part-load performances, four different cases, introducing various load change strategies for the GT and gasifier are studied. Step/ramp changes of the GT and gasifier, unplanned/planned GT load changes and same/different GT and gasifier load change occurrence time are all addressed through these four cases. Simulation results indicate that the designed control strategy functions properly and is able to control the H_2-rich fuel as per GT requirements at different part-loads, while keeping the buffer tank pressure within the desired range. Dynamic characteristics of the SEWGS system is revealed from the SEWGS simulations at different feed syngas flow rates and compared with those of the gasifier and GT. Using the buffer tank between the SEWGS and the GT, improves part-load operation flexibility of the GT. Smooth operation and load-following capability of the IGCC integrated with the SEWGS system is achievable, depending on the load change strategy, taking into account the limited load gradient of the SEWGS and gasifier units compared to the GT.

Preface

This thesis is submitted to the Norwegian University of Science and Technology (NTNU) for partial fulfillment of the requirements for the degree of *philosophiae doctor* (PhD).

The work was carried out at the Department of Energy and Process Engineering at the Faculty of Engineering Science and Technology of NTNU, Trondheim, Norway. Professor Olav Bolland has been the main supervisor and Dr. Konrad Eichhorn Colombo as the co-supervisor.

Acknowledgments

First and foremost, I would like to thank my supervisor Professor Olav Bolland for offering me the opportunity to pursue my PhD at Energy and Process Engineering Department. He gave me the freedom I needed to move on. His constructive comments, insightful discussions and generous support made my PhD thesis to be finished successfully. I sincerely appreciate all his contributions of time, ideas and funding throughout my PhD work.

I would also like to thank my co-supervisor, Dr. Konrad Eichhorn Colombo, for sharing his experience and knowledge with me, for his fruitful discussions and friendly advice. He was a good source of encouragement during my PhD work.

My gratitude and thanks to Professor Hugo Atle Jakobsen for his time and insightful advice on the stage of mathematical modeling of the SEWGS process.

I also wish to thank Professor Sigurd Skogestad for his useful Plantwide Process Control course, and his insightful suggestions on the process control.

I would also like to give my thanks to Snorre Foss Westman, for his help and contribution in simulation of the SEWGS.

I am indebted to many friends and colleagues at the department. Zeinab, Amlaku, Neda, Danahe, Mehdi, Renga. I have enjoyed talking to them, listening to them, drinking with them and in one word being friend with them.

A special feeling of gratitude to my loving mom, my first teacher and my best friend, she is always there for me with her unconditional support.

And special thanks to my siblings, in particular Vahid, for their kindness and encouraging me along my way. I am grateful of having them.

Table of Contents

Nomenclature

a	Langmuir isotherm parameter (-)
a_{k_z}	Constant of the empirical correlation of the effective thermal conductivity (-)
c	Total gas-phase concentration (mole gas/m^3 gas)
d_p	Catalyst and adsorbent particle diameter (m)
d_t	Internal diameter of reactor (m)
c_i	Gas-phase concentration of component i in gas mixture (mole /m^3 gas)
C_v	Flow coefficient (m^3/(s $bar^{1/2}$))
$C_{p,ads}$	Adsorbent specific heat capacity at constant pressure (J/ (kg adsorbent K))
$C_{p,cat}$	Catalyst specific heat capacity at constant pressure (J/ (kg catalyst K))
$C_{p,gas}$	Gas-phase molar specific heat capacity at constant pressure (J/ (mole K))
D_{ax}	Molecular diffusion coefficient (m^2/s)
F_c	Flow coefficient (mole/(s Pa))
h_i	Enthalpy of component i (J/mole)
k_g	Gas-phase thermal conductivity (J/(mole K))
k_{LDF}	LDF mass transfer coefficient (1/s)
k_z	Effective axial thermal conductivity (W/ (m^2K))
K_C	Langmuir isotherm parameter (1/Pa)
K_R	Langmuir isotherm parameter (1/Pa)
K_C^0	Pre-exponential factor-Langmuir isotherm parameter (1/Pa)
K_R^0	Pre-exponential factor-Langmuir isotherm parameter (1/Pa)
m	Monolayer capacity for CO_2 chemisorption (mole/kg)
Mw	Molecular Weight (kg /kmole)
P_0	Buffer tank pressure (bar)
P_1	Downstream fuel control valve pressure (bar)

P_{CO2}	CO_2 partial pressure (bar)
Pr	Prandtl number (-)
q_{CO_2}	Adsorbent loading of CO_2 (mole CO_2 adsorbed/kg adsorbent)
$q^*_{CO_2}$	Equilibrium adsorbent loading of CO_2 (mole CO_2 adsorbed/kg adsorbent)
r	Reaction rate of forward WGS reaction (mole/(kg catalyst s))
R	Gas constant (L bar/K mole)
Re	Reynolds number (-)
T	Temperature (K)
T_{wall}	Reactor wall temperature (K)
u_0	Inlet feed gas velocity (m/s)
U	Overall bed-to-wall heat transfer coefficient (W/ (m^2 K))
V_{tank}	Buffer tank volume (m^3)
x_{valve}	Valve opening (stem position) (-)
y_i	Gas-phase gas molar fraction of component i (-)
$\dot{m}_{in,tank}$	Mass flow rate to the buffer tank (kg/ s)
$\dot{m}_{out,tank}$	Mass flow rate out of the tank (kg/ s)
$\dot{m}_{valve}$	Mass flow rate through the fuel control valve (kg/ s)
$\dot{n}_{valve}$	Valve molar flow rate (mole/s)
ΔH_R	Heat of reaction (J/mole)
ΔH_{ads}	Isosteric heat of adsorption of CO_2 (J/mole CO_2 adsorbed)
ΔP	Valve pressure difference (Pa)

Greek Letters

ε_t	Total void fraction of reactor bed (total gas volume/reactor volume) (m^3 gas/m^3 reactor)
ε_b	Void fraction of bed (inter particle gas volume/reactor volume)(m^3 gas in bed/m^3 reactor)
η_i	Catalyst efficiency for component i (-)
μ	Gas-phase dynamic viscosity (Pa. s)
λ_s	Shape factor of catalyst and adsorbent particles (-)

ρ_{gas}	Gas-phase density (kg/m^3)
$\rho_{b,ads}$	Adsorbent bulk density in reactor bed (kg adsorbent/m^3 reactor)
$\rho_{b,cat}$	Catalyst bulk density in reactor bed (kg catalyst/m^3 reactor)

Abbreviations

AC	Activated Carbon
AGR	Acid Gas Removal
ASU	Air Separation Unit
ATR	AutoThermal Reforming
CCGT	Combined Cycle Gas Turbine
CCP	CO_2 Capture Project
CCS	Carbon Capture and Storage
CNT	Carbon NanoTube
CSS	Cyclic Steady State
D	Depressurization
DOE	Department of Energy
EBTF	European Benchmark Task Force
ECN	Energy research Centre of the Netherlands
Eq, REq	Equalization and Re-Equalization
F	Feed
FI	Flow Indicator
FT	Flow Transmitter
GHG	GreenHouse Gas
GT	Gas Turbine
HP	High Pressure
HRSG	Heat Recovery Steam Generator
HTC	HydroTalCite
HTS	High Temperature Shift

IGCC	Integrated Gasification Combined Cycle
LDF	Linear Driving Force
LDH	Layered Double Hydroxide
LOS	Lithium Orthosilicate
LP	Low Pressure
LTS	Low Temperature Shift
LZC	Lithium Zirconate
M	Mixer
MDEA	MethylDiEthanolAmine
MEA	MonoEthanolAmine
MOF	Metal Organic Framework
MS	Molecular Sieve
NGCC	Natural Gas Combined Cycle
P	Purge
PC	Pulverized Coal
PDAE	Partial Differential Algebraic Equation
PI	Proportional Integral
PI	Pressure Indicator
PSA	Pressure Swing Adsorption
PT	Pressure Transmitter
R	Rinse
RP	Re-Pressurization
SER	Sorption Enhanced Reaction
SEWGS	Sorption Enhanced Water Gas Shift
SMR	Steam Methane Reforming
SR	Steam Reforming
ST	Steam Turbine
S/C	Steam to Carbon ratio

TIT	Turbine Inlet Temperature
TOT	Turbine Outlet Temperature
TSA	Temperature Swing Adsorption
V	Valve
WGS	Water Gas Shift

Chapter 1

1. Introduction

1.1. Carbon capture and storage

Solar radiation passes easily through the atmosphere and reaches the earth. Land, water and vegetation at the earth's surface, absorb approximately 51% of the radiation. Some of this energy is emitted back from the earth's surface in the form of infrared radiation [1].

CO_2 as an important greenhouse gas has a long residence time in the earth's atmosphere and unlike N_2 and O_2, the primary gas components in the atmosphere; it is not transparent to infrared radiation. It absorbs outgoing infrared radiation from the earth's surface. This causes the earth to get warmer and so-called greenhouse gas (GHG) effect occurs with the increase of the concentration of the GHGs in the atmosphere and gradual global climate change. There are strong evidences on global climate change as a result of the increasing anthropogenic emissions of GHGs [2].

Human activities are interfering with the earth's carbon cycle, resulting in rising CO_2 concentrations in the atmosphere. The primary man-made source of the CO_2 emissions worldwide are combustion of fossil fuels (coal, natural gas, oil) in power plants for electricity production (accounting for about 60% of the total CO_2 emissions) [1]. According to the World Energy Outlook 2011 [3], the use of coal as the main fuel source for power generation has remarkably increased over the past decades. The global move towards the use of renewable energy sources, i.e. wind, solar, geothermal and liquid biofuels proceeds slowly and cannot follow the rapidly increasing world's energy demand. Therefore, the use of coal as a cheap energy source remains important.

On the other hand, fossil-fuelled combustion within power generation plants is the major contributor to CO_2 emissions [4]. This prompts substantial research on effective technologies and methods to reduce the CO_2 emissions from power plants. The CO_2, once captured, can then be prepared for transportation and geological, ocean or mineralization storage [5].

1.1.1. CO_2 capture technologies

CO_2 capture technologies are classified under three main routes of post-combustion, pre-combustion and oxy-combustion technologies as shown schematically in Fig. 1-1. These categories are applicable to both fossil fuels and biomass. Different CO_2 removal processes, such as solid adsorption, chemical, physical or hybrid absorption into a liquid solvent and membranes can be considered, when employing the CO_2 capture routes [6, 3, 5, 7-10]. Post-combustion refers to capture of CO_2 from flue gas produced by the combustion of fossil fuels. Chemical absorption-based processes such as monoethanolamine (MEA) are the most commercialized and well-established CO_2 removal process. The decarbonized flue gas is discharged to the atmosphere and the captured CO_2 is prepared for storage. In the pre-combustion technology, the fuel is converted to syngas (a mixture of mainly CO

and H_2) via coal gasification/steam reforming. CO is further converted into CO_2 in shift reactors. CO_2 is then removed from shifted syngas before combustion takes place. A H_2-rich fuel is produced and burned in the combustion chamber. The most common CO_2 capture process is based on a physical absorption process. Oxy-combustion technology is characterized by the use of nearly pure oxygen for combustion, instead of air, and a flue gas mainly composed of CO_2 and H_2O is produced. A low temperature cryogenic air separation process is typically employed for oxygen production. A summary of principle advantages and disadvantages of the three different CO_2 capture routes is presented in Table 1-1 [2, 8].

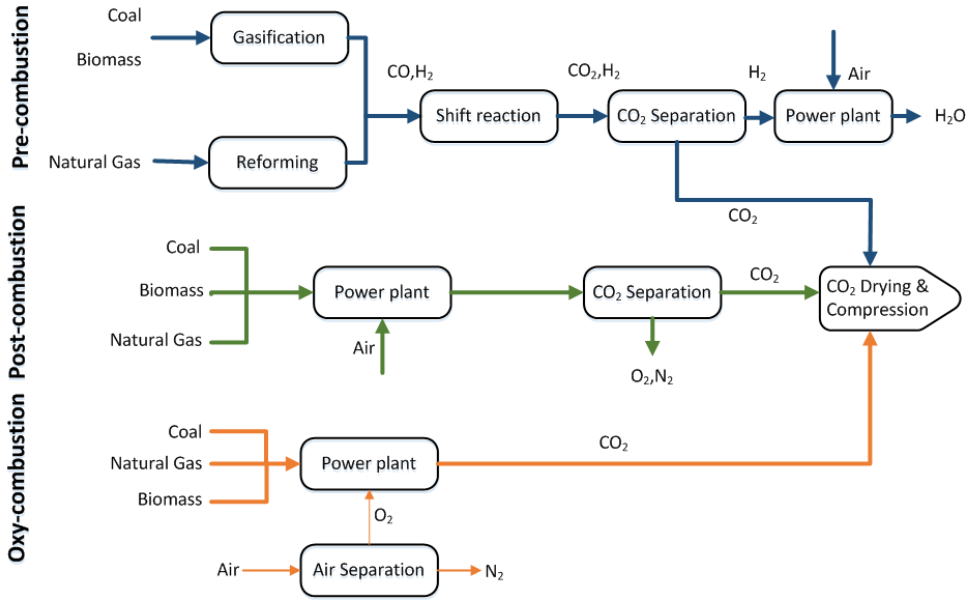

Fig. 1-1. General scheme of the different CO_2 capture routes [11]

Regardless of the technology used for the CO_2 capture, the efficiency of the capture process is determined by the energy consumption of the process in terms of electric power consumption and heating/cooling duties required for the capture process. Chemical solvents, as an example, have lower electric power consumption due to the lower flow rate of chemical solvents compared to physical solvents and in consequence less power is required for solvent circulation. But for instance chemical solvents require more heat for regeneration than physical solvents, due to the chemical reaction involved [12].

Different CO_2 capture technologies are not equivalent or at the same stage of development. It is therefore difficult to make a general decision about the best CO_2 capture process.

In a technical and economic estimation study it was concluded that pre-combustion CO_2 capture by physical absorption suits integrated gasification combined cycle (IGCC) the best, oxy-combustion should be considered for pulverized coal-fired (PC) power plant and post-combustion capture by chemical absorption is the best choice of CO_2 capture process for natural gas combined cycle (NGCC) [8, 12].

In a simulation work on IGCC plants with pre-combustion CO_2 capture technologies using both chemical and physical solvents for CO_2 absorption, it was found that the use of physical solvent, Selexol, for CO_2 capture is more energy efficient, compared to other physical (Rectisol and Purisol) and chemical methyldiethanolamine (MDEA) solvents. This is mainly due to the lower energy (heat) consumption for solvent regeneration and more simplified process configuration of the Selexol-based CO_2 capture process [12].

Some major characteristics of different CO_2 capture processes including absorption, membrane and adsorption based technologies are outlined in Table 1-2.

Table 1-1. Principle advantages and disadvantages of the different CO_2 capture approaches [2, 8, 13, 14]

	Advantages	Drawbacks
Post-combustion	• Mature technology, long history in chemical and petroleum industries. • Applicable to the majority of existing power plants (existing plants can be equipped with the technology) • The technology is highly flexible with respect to load changes in the power plant • Shorter time for construction • Higher net power plant efficiency than pre- combustion and most oxy-combustion cycles • High purity CO_2 (>99 %), produced at high CO_2 capture ratio (90 %)	• Large volumetric flow rate of flue gas at essentially atmospheric pressure, with CO_2 at low partial pressure (3-15 mbar) • Energy required to heat, cool, and pump non-reactive carrier liquid (usually water) is often significant (**Absorption)** • Equipment corrosion and possible negative environmental impact (**Absorption)** • Thermal and oxidative degradation of the solvent **(Absorption)** • Large amount of energy to regenerate solvents and release CO_2 **(Absorption)**

Pre-combustion	• Generation of H_2-rich fuel, which can be also used as a chemical feedstock (in a fuel cell or hydrogen industry) • High CO_2 concentrations produced by the shift reactor (typically 15 to 60%) and high partial pressures range • Applicability of pressure reduction technologies for CO_2 separation rather than heating, due to high pressure operating condition • CO_2/H_2 separation is inherently easier to perform than CO_2/N_2 or O_2/N_2 separation, due to the larger differences in the polarizability and quadrupole moment of the molecules • Possibility of combined CO_2/H_2S capture	• Initial fuel conversion steps (gasification, reforming) are more elaborate and costly than in post-combustion (technical complexity of the process) • Less flexible with respect to load changes • Retrofitting with pre-combustion capture is not possible • Capability to combust H_2-rich (>50%) in gas turbine (GT) • The most mature technology based on using physical solvents is a low temperature technology which requires cooling of syngas before capture process and heating again before the GT, causing efficiency loss
Oxy-combustion	• Easy separation of CO_2/H_2O by condensation • Less or no chemicals are necessary, compared to pre-combustion and post-combustion • Possible to retrofit in conventional coal fired plants	• Depending on the purity of the oxygen stream, the CO_2 content in the product is between 65–90 %. Further CO_2 purification step may be required. • Cost of air separation unit and flue gas recirculation reduces the economic benefit (may reduce net plant output by up to 25%) • Consumes large amounts of oxygen coming from an air separation unit • More complicated combustors due to pure oxygen combustion compared to air combustion

Table 1-2. Different CO_2 capture processes characteristics [1, 8, 12, 15, 16, 17, 18, 19, 20]

Absorption
Physical (CO_2 is physically absorbed into a solvent in the absence of chemical reactions)
• Applicable to pre-combustion CO_2 capture • Low vapor pressure, low toxicity, low capacity and less corrosive solvent
Chemical (CO_2 is chemically absorbed by a solvent via chemical reactions of ionic nature)
• Applicable to both pre-combustion and post-combustion capture • Most-established process for post-combustion technology • Thermal regeneration by heat consumption (steam) • Corrosive nature
Membrane
• Applicable to post-combustion, pre-combustion and oxy-combustion • Needs to be resistant to the gas contaminants • Creating pressure difference across the membrane demands power • Permeability and selectivity are two important parameters • No need for regeneration process • Limitation on the operating temperature • Plug of membranes by impurities in the gas stream • Not proven industrially • Modular system
Adsorption
• Applicable to post-combustion and pre-combustion • Regeneration by pressure swing adsorption (PSA) or temperature swing adsorption (TSA) • Thermal, chemical, and mechanical stability and cyclic capacity are important • Lower regeneration energy • More efficient heat recovery (compared to liquid amines) • Complex gas/solid reactor system • Able to operate at higher temperatures than solvents, avoids additional equipment for syngas cooling (in pre-combustion case)

In general, physical solvents are more appropriate at CO_2 partial pressures higher than about 8 bars (CO_2 concentration: ~40%), while chemical solvents are more suitable for CO_2 partial pressures lower than about 8 bars (CO_2 concentration: 4-8% in natural gas-fired vs. 12-15% in coal-fired power plant). Chemical processes based on the primary amines, such as MEA, are favored at very low (less than 1 bar) partial pressures of CO_2. Whereas, chemical processes based on the tertiary amines such as MDEA are preferred when the partial pressure of the CO_2 is slightly higher due to their easier regeneration at higher pressure conditions. The absorption capacity of the amines increases, at pressures lower than about 8 bar, with the partial pressure of the CO_2. It then begins to saturate at a partial pressure of about 8 bar [8, 15].

1.1.2. Pre-combustion CO_2 capture technologies

Applying CO_2 capture technologies to existing power plants, CO_2 needs to be removed from a diluted (<15% by volume) large flue gas stream at low pressure, i.e. the post-combustion capture method (Fig.1-1). In alternative power plant designs, the fuel is first converted in a reforming or gasification process and a subsequent shift-reaction into a high pressure gaseous mixture essentially consists of

CO_2 and H_2, called shifted syngas. At this stage, CO_2 can be selectively separated from the shifted syngas prior to be sent to a GT for power generation, which is the concept for pre-combustion CO_2 capture (Fig. 1-1). In this case the gas stream is at high pressure and contains a high concentration of CO_2. This facilitates the CO_2 removal process. The use of physical solvents such as Selexol or Rectisol, is the most developed and mature technology for CO_2 capture from syngas [8, 12, 21, 22]. Recently, solid adsorption-based processes, as an alternative to physical absorption-based processes, with the potential to lower the CO_2 capture capital and operating costs, have attracted a lot of attention [23, 24, 25, 26, 27]. Given the fact that, in the pre-combustion capture applications the gas pressure and CO_2 fraction in the gas to be treated are high (~35 bars, ~40% CO_2), adsorption-based processes, in particular PSA processes, have promising features [26].

1.2. IGCC power plant with/without CO_2 capture

IGCC is an electrical power generation system in which a solid feedstock (coal, lignite, pet coke, biomass, solid waste, etc.) is partially oxidized at high temperature and pressure with oxygen (produced by an air separation unit (ASU)) and steam to produce syngas. Syngas is primarily a mixture of carbon monoxide and hydrogen along with smaller quantities of other components (e.g. carbon dioxide, water vapor, hydrogen sulphide, ammonia, etc.). Conversion of the solid feedstocks to syngas is accomplished through a gasification process. Entrained flow, oxygen-blown gasifiers, which normally operate at high temperatures (1000-1500 °C) and pressures (30-70 bars) have been identified as the most suitable and promising gasifier type applied for an IGCC plant. Typically they pose a high conversion of solid fuels (~99%). Shell's gasifier is one of the most efficient gasifiers of this type [28]. The main differences between this and other gasification technologies are: the coal feed (being dry or slurry), number of the gasifier stages (one or two), syngas cooling (water quench or heat exchangers) and air vs. oxygen-blown [27, 29, 30, 31, 32]. The dry feed design has typically a higher plant energy efficiency compared with the slurry feed design. Oxygen-blown gasifiers produce syngas with a higher calorific value as well as utilize smaller size of the downstream components due to the absence of the N_2 volume and its diluent effect [33]. In conventional IGCC plants, the syngas generated by the gasifier is further treated for particulates and hydrogen sulphide removal and then it is sent to a combined cycle gas turbine (CCGT) for electric power generation. The hot flue gas from the combustion of the syngas in the GT is then used to produce steam in Heat Recovery Steam Generator (HRSG). The resulting steam is expanded in a steam turbine of the combined cycle to generate additional electrical power [29, 34]. An example of an IGCC power plant without CO_2 capture is schematically shown in Fig. 1-2.

IGCC power plants offer a number of advantages over conventional PC power plants as follows [12, 35, 36]:

- High thermal efficiency, low NO_x, SO_x and solids emissions.
- The possibility of using lower grade coals in IGCC plants, which makes them commercially advantageous.
- Opportunities to produce power as well as synthetic fuels and chemicals.

- High-pressure syngas (H_2, CO), produced by coal gasification can be shifted to a CO_2/H_2 mixture, via a catalytic reactor, resulting in high partial pressure of CO_2, in favor of the capture process.

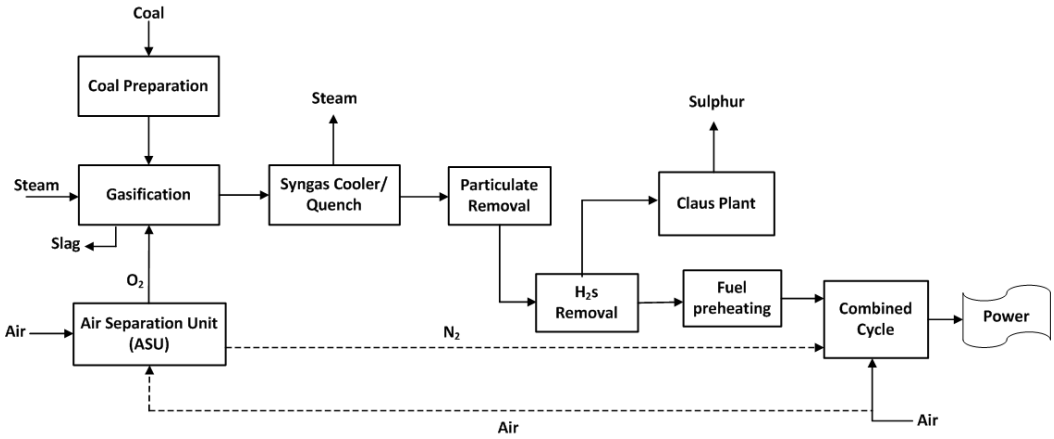

Fig. 1-2. Conventional IGCC power plant without CO_2 capture

Their main drawback, on the other hand, is the production of comparatively large amounts of CO_2, released to the atmosphere [12]. Therefore, development of the carbon capture and storage (CCS) technologies in the coal-fired power plants must be taken into consideration to avoid/reduce the CO_2 emissions. To apply a pre-combustion CO_2 capture process, the conventional IGCC plant layout is modified by adding two main units: A CO shift conversion unit downstream the particulate removal unit and a subsequent CO_2 separation and compression unit as shown in Fig. 1-3. The shift conversion unit is the reaction of converting CO in the raw syngas into CO_2 by shifting the CO over steam in a catalytic bed. When H_2S removal unit is downstream of the shift conversion unit, it is called sour water gas shift (WGS) conversion (Fig. 1-3). An alternative is to use a sweet WGS reaction, where the H_2S removal unit is upstream of the shift conversion.

Most of the studies on pre-combustion CO_2 capture from IGCC plants employ physical or chemical solvents, such as Selexol, Rectisol or MEA. These solvent-based absorption processes operate at a fairly low temperature. Thus, the gas stream entering the absorber must be significantly cooled down. This results in either loss of high amount of the available energy or high capital costs to recuperate heat [37]. It is therefore worth to investigate alternative more efficient CO_2 capture processes for IGCC applications with potentially lower energy penalties than the low-temperature capture processes.

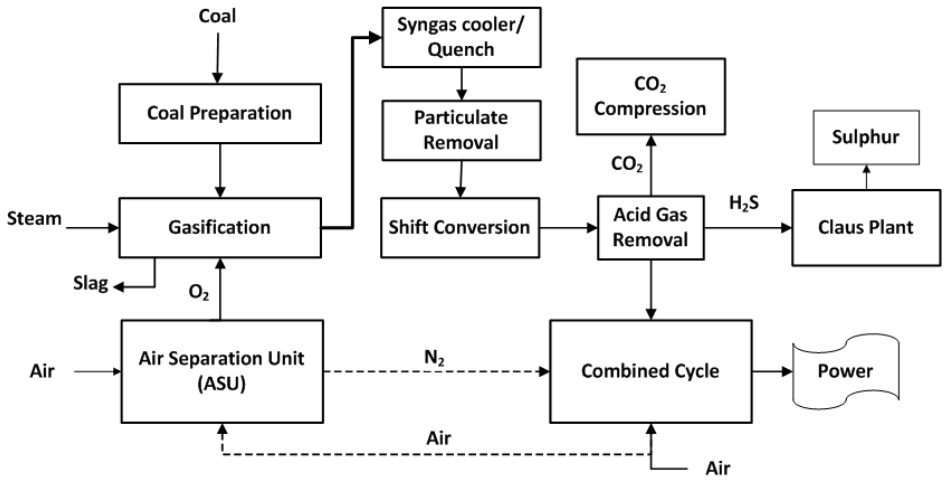

Fig. 1-3. Classical IGCC with pre-combustion CO_2 capture [31]

1.3. Adsorption-based CO_2 capture technologies

Adsorption is a selective process in which molecules contained in liquid or gaseous mixtures adhere on a solid surface of the adsorbent. The adsorption quality is determined by the properties of adsorbed particles such as molecular size, molecular weight and polarity as well as the adsorbent surface (polarity, pore size and spacing). This is a different process from absorption in which atoms, molecules or ions are dissolved in a bulk phase (volume), not on the surface. Depending on the adsorbents regeneration method, two types of adsorption processes can be distinguished: PSA and TSA processes. The PSA process is based on a pressure change to release the adsorbed gas (adsorption at high pressure and desorption at low pressure), while the TSA process swings the temperature to drive off the adsorbed gas (adsorption at low temperature and desorption at high temperature). In other words, equilibrium capacity of the adsorbents is reduced either at low pressure or high temperature, which is the basis for the regeneration methods by PSA and TSA, respectively. The main drawback of the TSA methods is the long regeneration time. Hours, compared to seconds for the PSA processes [38]. The PSA regeneration methods, in general, are technically and economically more viable than the TSA regeneration methods [5, 9, 10]. The PSA technology is in particular attractive where a high degree of gas purity is required [18].

For the successful evaluation of solid adsorbent-based CO_2 capture processes, finding a proper adsorbent material with suitable properties to be employed for CO_2 capture is crucial. Besides, other equally important parameters such as adsorption reactor, regeneration process and overall process integration of the capture system (e.g. thermal integration with the power plant) need to be fully addressed [7]. Some important parameters to be investigated about CO_2 adsorbent materials are [7, 16, 25, 27, 39]:

(a) Adsorption capacity for CO_2
(b) Selectivity for CO_2
(c) Equilibrium adsorption isotherm
(d) Adsorption/desorption kinetics
(e) Chemical stability/tolerance to impurities
(f) Effect of presence of specific gas components (contaminants) on adsorbent capacity
(g) Mechanical and thermal stability
(h) Cost/ease of adsorbent synthesis
(i) Regenerability (ease of regeneration, in terms of energy required & time) and multicycle stability

In practice, when choosing a CO_2 adsorbent candidate material, there should be a trade-off because all the mentioned properties may not be satisfied in the meantime. Each adsorbent's strengths and weaknesses must be considered in the context of a practical adsorption process for effective CO_2 separation. In general, fast adsorption and desorption kinetics, large adsorption capacity, infinite regenerability and stability, and a wide range of operating window define an ideal hypothetical adsorbent.

1.3.1. Classification of CO_2 adsorbent materials

With respect to adsorption/desorption temperature, CO_2 adsorbents can be classified into three groups of low (below 200 °C), intermediate (200-400 °C) and high temperature (above 400 °C) adsorbents.

1.3.1.1. Low temperature CO2 adsorbents (below 200 °C)

1.3.1.1.1. Carbon-based adsorbents:

Activated carbon (AC) and molecular sieves (MS) are examples of the carbon-based adsorbent materials. Their main advantages are low cost, high surface area, high amenability to pore structure modification and surface functionalization (easy to make) and relative ease of regeneration. They are chemically and hydrothermally stable, but they have a low selectivity for CO_2 in the presence of other gases (e.g. CH_4, N_2, H_2, etc.). Their CO_2 adsorption mechanism is physical and weak (heat of adsorption is relatively low). The CO_2 uptake and selectivity of these materials at low pressures and ambient temperatures are relatively low. Methods of enhancing the adsorbate-adsorbent interaction and CO_2 selectivity are under further research works [23, 40]. For example, the adsorption properties of the AC can be significantly improved by incorporation of amine functional groups into their porous structure. This results in an increase of the CO_2 capacity at high temperatures, while at lower temperatures, physisorption is predominant [39, 41]

Development of new carbon-based materials with improved CO_2 uptake is in progress. Carbon nanotubes (CNT) for low-pressure carbon capture processes are one example of these materials.

1.3.1.1.2. Zeolite-based adsorbents

The CO_2 adsorption mechanism on zeolites is based on physical adsorption and additionally a relatively strong bound of carbonate species. Their CO_2 selectivity over other gases (N_2, CH_4, H_2O, etc.) is quite low and their adsorption capacity rapidly declines with increasing temperature above 30

°C and becomes negligible above 200 °C [42]. In general they are characterized by a relatively high CO_2 capacity at low pressure [39]. Moisture presence is also another challenge for zeolite-based CO_2 adsorbents, which may compete with CO_2 for the active adsorption sites and weaken the interaction of CO_2 with the adsorbent (cations), as well as adversely affect the stability of the zeolites [43]. Regarding carbon capture applications, type X and A zeolites have been widely investigated. Zeolite 13X has shown the best performance in PSA-based processes for post-combustion CO_2 capture [39, 44].

1.3.1.1.3. Alkali metal carbonate-based adsorbents

Examples of these adsorbents are $NaCO_3$ and K_2CO_3. The optimum adsorption temperatures for these materials are within the range of 50–100 °C, while an effective regeneration takes place in the range of 120–200 °C. They are suitable for treatment of flue gases at temperatures below 200 °C [16]. Their CO_2 adsorption mechanism is based on two reversible and highly exothermic carbonation reactions, which make the energy management for this type of the adsorbents important [45]. The overall rate of reaction is low. Methods such as using $NaCO_3/K_2CO_3$ composite materials, dispersed on a support such as Al_2O_3 have been investigated to enhance the adsorption rate of these materials [46]. CO_2 adsorption of these materials decreases with temperature increase. Still some issues including long term stability/durability, presence of contaminants in the gas mixture, carbonation reaction rate and energy management should be addressed about these adsorbent materials [16].

1.3.1.1.4. Metal Organic Frameworks (MOFs)

MOFs are a class of crystalline porous materials with high surface area. There is also the possibility to modify their structures and functional properties (adjustable chemical functionality). This feature provides an advantage to control pore dimension and chemical potential of the surface, which ultimately provides the possibility of developing adsorbents with the desired adsorption properties. In general, MOFs indicate higher CO_2 capacity at high pressures, compared to zeolites. However, at low pressures, their CO_2 capture capacity is relatively low. The high thermal stability and reversible CO_2 adsorption make use of these materials promising for pressure swing processes. Their CO_2 selectivity and heat of adsorption are generally higher than those of zeolites. The water presence has a detrimental effect on the CO_2 capture capacity of these adsorbent types [26, 27, 39].

1.3.1.2. Intermediate CO_2 adsorbents (200-400 ºC)

Layered double hydroxides (LDHs), also known as hydrotalcite-like compounds (HTCs) or anionic clays are layered basic solids. Among various intermediate-temperature CO_2 adsorbents, HTCs have been well investigated and are believed to be the most promising adsorbent candidates. They have a high surface area and abundant surface basic sites (with different strength for adsorption) [47]. The interaction between the adsorbed CO_2 and the basic adsorption sites on the surface of the material is stronger than that of the zeolites, but weaker than the alkali metal carbonates. Their adsorption operating temperature is around 200 °C and above. Regeneration temperature is typically about 400 °C. Relatively low adsorption capacity is an issue for this type of the adsorbents. The presence of water in the feed gas mixture has a positive effect on the CO_2 adsorption capacity. Whereas, the presence of sulphur compounds has a negative effect as it may compete with the CO_2 on the adsorption sites [48]. The CO_2 adsorption capacity of these materials is improved with increasing the

pressure. Addition of alkali metal carbonates (e.g. K_2CO_3) in HTCs is an effective approach to improve the CO_2 adsorption capacity and kinetics of these materials. Potassium ions (K^+) could strongly interact with the HTC and consequently generate surface basic sites, which could adsorb CO_2 reversibly at high temperatures [49, 50]. The long-term stability of the HTCs during the PSA based CO_2 adsorption/desorption cyclic operation is also an issue, which is yet to be addressed. More detailed explanation about this class of adsorbents is provided in chapter 2.

1.3.1.3. High temperature solid adsorbents (above 400 °C)

1.3.1.3.1. Ca-based adsorbents

Ca-based materials are known as the good candidate CO_2 adsorbent materials due to their high reactivity with CO_2 according to the reversible carbonation reaction: $CaO + CO_2 \leftrightarrow CaCO_3$, high capacity and low cost [51]. The carbonation reaction is simple and the heat of the highly exothermic reaction can be efficiently recovered. The high adsorption temperature, as well as the substantial increase of the volume from CaO to $CaCO_3$, on the other hand, cause sintering of the adsorbent particles (textural degradation) and as a result, loss of the reversibility [52]. Therefore their durability and cyclic stability need to be improved for practical application of these materials.

1.3.1.3.2. Alkali ceramic-based adsorbents

Alkali metal (Li, Na, K, etc.) containing ceramics (e.g. Li_2ZrO_3) are another type of the high temperature CO_2-adsorbents. There is only a small volume change during the CO_2 adsorption/desorption cycles. The adsorption process is described by the mobility (diffusion) of the alkali metals from the core of the particle in the ceramic-based adsorbent to the surface and reaction with CO_2. The mobility of the Na is larger than that of Li. Therefore composite alkali ceramic-based adsorbents such as LiNa ceramic-based have an improved CO_2 adsorption capacity than the Li ceramic-based materials (Li_2ZrO_3). Production of the Li_2CO_3 from reaction of the CO_2 with the Li_2ZrO_3, limits the rate of the CO_2 adsorption on the adsorbent material. The main drawback about Li_2ZrO_3 adsorbents is their kinetic limitation [16].

A different classification of materials presented in [53], defines four groups of CO_2 adsorbent materials: (1) micro-porous and meso-porous inorganic and organic materials such as zeolites, silica gel, alumina and AC, (2) mixed oxide materials such as CaO (3) lithium metal oxides such as lithium zirconate (LZC) and lithium Orthosilicate (LOS) and (4) HTC materials. The first group of the materials show high CO_2 adsorption capacities and physical adsorption rate at low (near ambient) temperature. However, the CO_2 working capacity decreases to very low values at temperatures above 250 °C. Polar adsorbents such as zeolites, silica gel and alumina show very poor CO_2 selectivity, in the presence of polar gases such as steam. Even water selectivity of these adsorbents may take over the CO_2 selectivity. The CaO adsorbent in the second group can react with the CO_2 in a bulk chemical carbonation reaction. This material shows high CO_2 adsorption rate at temperatures above 500 ºC. Regeneration of the CaO requires high temperatures (about 900 °C) to maintain the CO_2 capture capacity at high levels. This may result in sintering of the CaO active surface. Due to the formation of the $CaCO_3$, cyclic stability of this adsorbent material is reduced [54, 55]. In the third group, LZC and LOS show good CO_2 chemisorption capacity at high temperature. However, their

main drawback is the slow adsorption kinetics and high regeneration temperature (about 900 °C for LZC and 700 °C for LOS), due to the strong chemical bonding to the CO_2 [53]. The fourth group, HTC materials own some characteristics such as adequate working capacity at high temperature of 400-450 °C, good cyclic stability, fast adsorption/desorption kinetics and high selectivity as well as an enhanced capacity for the CO_2 in the presence of steam [49, 56, 57].

1.4. PSA processes

1.4.1. Configuration

Historically PSA processes have been widely used in industry for various applications including air separation, drying, toxic gaseous removal and hydrogen purification [37]. However, their application for CO_2 capture is still under investigation and has not been demonstrated on a commercial scale [58, 59, 60]. One of the first PSA process configurations applied for the air separation on industrial scale, is a twin-bed, four-step configuration, as shown in Fig. 1-4. This is a basic PSA cycle proposed by Skarstorm, in which each bed undergoes four fundamental steps including pressurization by feed, adsorption, countercurrent depressurization and purge [61].

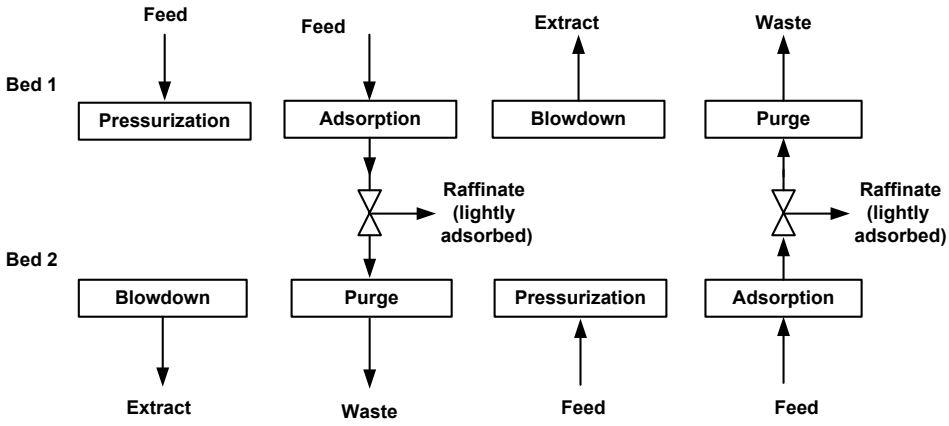

Fig. 1-4. Operating principle of a basic twin-bed PSA cycle (Skarstorm) [61]

The PSA process concept and configuration is based on the purity requirement of the components being separated. In most of the industrial PSA applications, so-called stripping PSA process, high purity of the weakly adsorbed gas (light product) on the solid adsorbent is pursued, while, the strongly adsorbed gas may not be recovered with high purity (Fig. 1-5a). On the other hand, to achieve a high purity of the strongly adsorbed component (heavy product) another process configuration, so-called rectifying PSA process, is considered (Fig. 1-5b). Where the purity of the both light and heavy products is desired, two process configurations are combined, which is called dual-reflux PSA process (Fig. 1-5c) [62].

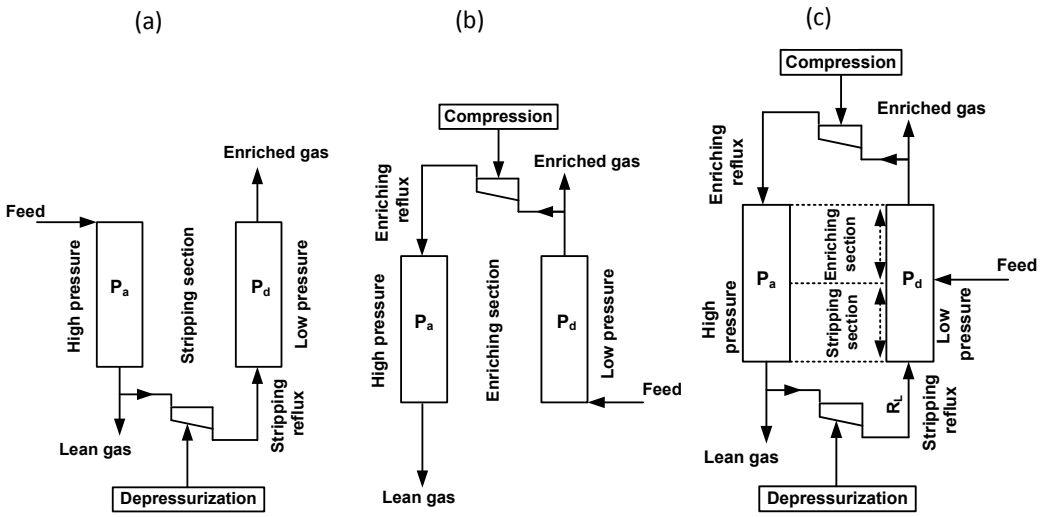

Fig. 1-5. Three different PSA process configurations (a): stripping PSA, (b): rectifying PSA and (c): dual-reflux PSA [62]

In a simple twin-bed process both products cannot simultaneously be achieved at high purities and one product may not be recovered well. Such configurations are employed mainly when the feed gas is inexpensive and so the recovery rate of either of products is not an issue. A wide variety of PSA process configurations adopted from the Skarstorm cycle has been employed for various applications. More complex cycles may be achieved by increasing the number of beds, addition of various pressure equalization and purge steps. This results in achieving higher productivity of the adsorbent, higher purity of both the gas streams, continuous production of the separated gas streams and utilization of the pressure energy of the incoming feed. However, employing additional beds and pressure equalization steps creates more complexity in the structure and operation of the system with additional flow-switching valves and piping [14].

Most of the modern PSA process systems employ a multi-bed process, which includes additional steps compared to the basic Skarstom configuration. The main purpose of using the multiple bed system is to maintain at least one bed available to serve the incoming feed gas for the adsorption step, while releasing a purified gas from another saturated bed. When a PSA process is applied as a pre-combustion CO_2 capture to an IGCC plant the number of pressure equalization steps is the governing parameter for the number of the adsorption columns [14, 63]. Additional beds, i.e. using pressure equalization steps, will be beneficial to utilize the energy available in the high pressure feed stream as much as possible. This will reduce the compression energy required to increase the pressure in an already regenerated bed to the feed pressure for starting a new cycle. Also additional pressure equalization steps improve the purity of the product streams. However, it increases complexity of the piping and valve network.

1.4.2. Operation

PSA is an inherently intermittent process, which reaches a cyclic steady state (CSS) mode. The CSS is a state that process would progressively achieve after operating a certain number of cycles after the start-up of the process. Thereafter, almost an identical pattern of variations in product gas thermodynamic properties is observed repeatedly in each cycle [14, 64]. This is unlike many gas separation processes which reach steady state mode and outlet properties such as flow rate, composition and thermodynamic parameters become stable thereafter.

For design of PSA-based CO_2 capture processes using solid adsorbents, the main objectives are 1) development of adsorbents with a high cyclic capacity and selectivity for CO_2 and 2) determining optimal operating conditions. The adsorbent properties such as capacity, heat of the adsorption and kinetics are not only important for the efficient performance of the process from thermodynamic point of view, but also play an important role on the equipment size and costs of the process. For instance the volume of the adsorbent determines the size of the bed, the heat of adsorption determines the amount of energy required for regeneration and the adsorbent equilibrium and kinetics properties affect the cycle time.

Among different CO_2 capture processes, PSA processes are in particular of interest for pre-combustion CO_2 capture from IGCC plants, where the syngas from a coal gasification process is already at high pressure and CO_2 concentration [65].

A number of principle advantages and drawbacks of the PSA processes for CO_2 capture are listed in Table 1-3.

Table 1-3. PSA-based CO_2 capture processes, main advantages and drawbacks [14, 65]

Advantages
• Potentially lower energy penalty for CO_2 capture compared to solvent processes • Absence of any rotating machines/circulating solvents • Many design options
Drawbacks
• Large energy to compress the low pressure CO_2 for transportation & storage, resulted from regeneration process (either by PSA or vacuum swing adsorption (VSA)) at low pressure • Requirement of large size adsorption beds, which is a function of syngas feed flow rate and the cycle duration • Requirement for a large number of valves to start/stop gas flow and switch it from a bed to another. The valves of a PSA process have to be actuated for a couple of times/per cycle • The piping/adsorption beds are subject to cyclic stresses, generated from periodic pressurization depressurization

IGCC power plants with pre-combustion CO_2 capture, applying PSA processes comprise some features as outlined [14, 28, 65]:

- The entire IGCC can be divided into two different islands; hydrogen island and power island. Hydrogen, which is the lightly adsorbed component, is the desired product of the hydrogen

island and used as a GT fuel. High degrees of the hydrogen recovery are therefore desired to maximize the power production.

- Unlike the industrial hydrogen purification PSA processes, hydrogen purity is not considered the top priority as the hydrogen is diluted in a GT inlet to control turbine inlet temperature (TIT). The purity of the CO_2 (the strongly adsorbing component) on the other hand, is important, in view of reducing the GHG emissions. Therefore a conventional stripping PSA process (e.g. a Skarstrom cycle) may not be applicable, and a rectifying PSA or a dual-reflux PSA process has to be considered [66]

- The feed gas used for most of the processes developed up to date for hydrogen purification contains more than 70% hydrogen (typically the steam methane reforming off-gas or the refinery off-gases), whereas the hydrogen composition in the syngas feed stream in the pre-combustion IGCC process is no more than 55 %.

- Due to the dynamic nature of the PSA process, which reaches a CSS, with a repeated pattern of variation in flow rate, composition and thermodynamic parameters, the recovery and purity of the H_2 and CO_2 are actually the time-averaged values, while the process is in CSS [14].

- IGCC concept can be modified for hydrogen production along with the power production [37, 64].

1.5. PSA-based sorption enhanced water gas shift process

The sorption enhanced water gas shift (SEWGS) technology, is a novel high temperature combined reaction-adsorption process for CO_2 capture and hydrogen production. This technology is attractive for pre-combustion CO_2 capture from power plants. Conventional pre-combustion technologies, incorporate two WGS reactors (high temperature shift (HTS) and low temperature shift (LTS)) followed by an absorption-based CO_2 capture process. Applying the SEWGS technology, the WGS reactor(s) and CO_2 removal unit are replaced with the SEWGS process. A H_2-rich fuel gas is produced during the simultaneous WGS reaction and CO_2 adsorption and sent to a GT for combustion. The equilibrium controlled WGS reaction is hence enhanced towards higher conversions of CO into CO_2. A separate CO_2-rich gas stream, as the secondary product of the SEWGS system, is recovered during the regeneration of the adsorbent, based on a PSA process. In this work, the SEWGS process system is designed to be employed as a pre-combustion CO_2 capture process and remove carbon content of a given amount of feed syngas being produced continuously in a coal gasifier within an IGCC reference case [68]. The SEWGS system has a multi-train arrangement. Each train is composed of eight packed-bed reactors, filled with a mixture of the WGS catalyst and CO_2 adsorbent, working in parallel and undergoing a sequence of PSA processing steps. More detail about the SEWGS process, design, history and development is provided in Chapter 2.

1.6. Motivation

Application of the novel high temperature PSA-based SEWGS technology for pre-combustion CO_2 capture from IGCC power plants has attracted a growing attention lately. However, it is still far from being considered as a well-developed technology. So far, a majority of the research work on the SEWGS process has focused on developing/selecting a suitable CO_2 adsorbent material under the conditions of the SEWGS process.

Besides the development/selection of an adsorbent material, designing a PSA-based SEWGS system is also an important step to reveal the operational characteristics of the process. Many design options can be achieved by including and combining different basic PSA process steps and using alternative streams with different flow directions. A model-based design is thus beneficial to reduce doing enormous experimental efforts. Availability of some advanced modeling and simulation tools (e.g. gPROMS) facilitates development of complex process flowsheet models, such as PSA processes and applying numerical solution methods to simulate dynamic behavior of such processes.

So far, the theoretical studies on the SEWGS process have focused only on the steady-state performance of the system. Still a rigorous model of a PSA-based SEWGS process, accounting the complexities of the modern PSA processes, such as the network of flow switching valves in an interconnected multi-bed process system, has not been published in the open literature. Moreover, cyclic operation manner of the SEWGS process means that the system is inherently dynamic and therefore studying dynamic performance of such a system is necessary, for evaluating dynamic performance and load-following capabilities of an IGCC power plant integrated with the SEWGS process.

Moreover, with addition of other resources such as wind, solar to the electric power supply network, a general requirement for fossil fuel power plants with CCS, i.e. IGCC with SEWGS in this work, is to be able to operate with varying load. This necessitates examining the load-following capacity of IGCC with SEWGS and how well an IGCC using SEWGS can follow load changes.

1.7. Thesis objective

The main objective of this work is to conduct a detailed study on dynamic performance assessment of an IGCC power plant, equipped with a PSA-based SEWGS system for pre-combustion CO_2 capture. This assessment includes aspects such as:

- Load-following performance and operation flexibility of the IGCC with SEWGS, at different part-loads, taking into account the limited load gradients of the gasifier and SEWGS, compared to relatively fast dynamics of the GT.
- Controllability of the IGCC with SEWGS at full-load and part-load operation modes, by incorporating possible control strategies, due to the addition of SEWGS process with its cyclic operation manner.
- Sufficient performance of the SEWGS process unit in terms of the CO_2 recovery rate and purity, when the SEWGS process is part of the IGCC power plant for pre-combustion CO_2 capture.

A number of tasks, in connection with the main objective of the work, are carried out. First, a good understanding about the dynamic characteristics of SEWGS system is required. The reason is that the pre-combustion SEWGS unit is located at the heart of the power plant and is responsible for the supply of H_2-rich fuel to the GT as well as CO_2 capture. Therefore, the operation of the entire plant is largely affected by the operation of the SEWGS unit.
The H_2-rich stream flow rate and composition, produced from the SEWGS system, is found to undergo a periodic fluctuation, associated with using part of the H_2-rich product repeatedly for repressurization step. To integrate the SEWGS system into the IGCC power plant, possible control strategies of the multi-train SEWGS operation, with the aim of reducing the H_2-rich stream fluctuations are considered. In addition, a fuel control system, including a buffer tank is designed, with the objective of further control of the H_2-rich fuel, with respect to mass flow rate as well as pressure and composition at different GT loads. This is to comply with the fuel flow rate and heating value requirements of the GT. Finally, dynamic performance of the IGCC with SEWGS is investigated by introducing a number of part-load operation scenarios with respect to time constants of: the coal gasifier and GT and unplanned vs. planned GT load change occurrence.

1.8. Thesis outline

This thesis comprises 4 chapters and 4 papers. In chapter 1, **a**n introduction to the subject is given. CO_2 capture and storage concept and technologies, in particular pre-combustion CO_2 capture technology are introduced. IGCC power plants, the importance of the CO_2 capture and state-of-the-art CO_2 capture processes from such plants are discussed. An overview of the solid adsorption-based CO_2 capture technologies and characteristics of different class of adsorbent materials are discussed. The SEWGS process is briefly introduced. The motivation, objective, list of papers, working process of the thesis as well as achievements is presented. In chapter 2, SEWGS concept is presented in detail. Relevant works from the literature are reported as well. Chapter 3 includes the system description and methodology used in this work. Chapter 4 outlines the main conclusion of the thesis and recommendations for future work. Papers are enclosed at the end of the thesis.

1.9. List of papers

- Paper I

Najmi, B., Bolland, O., Westman, S. F., 2013. Simulation of the cyclic operation of a PSA-based SEWGS process for hydrogen production with CO_2 capture, Energy Procedia, 37, 2293– 2302.

A dynamic one-dimensional homogeneous model for multiple bed Sorption Enhanced Water Gas Shift (SEWGS) system has been developed in this work. The SEWGS system under consideration is based on a Pressure Swing Adsorption (PSA) process which operates in a cyclic manner. During the reaction/adsorption step, CO_2 produced by Water Gas Shift (WGS) reaction is simultaneously adsorbed on a highly CO_2-selective solid adsorbent and removed from the gas phase, enhancing the WGS reaction toward higher reaction conversion and hydrogen production. The periodic adsorption and desorption of CO_2 is induced by a pressure swing cycle, and the cyclic capacity can be amplified by purging with steam. Simulation results enable tracking the operation of the system over sequence of steps. As it is expected, high levels of CO conversion and CO_2 capture ratio are achieved by

enhancing the equilibrium reaction of WGS with adsorbents. Moreover there is no need to reheat the hydrogen product before it enters the GT due to operability of SEWGS system at high temperature of approximately 400°C. Hydrogen production undergoes repeating fluctuations over cycle time which is associated with using part of the H_2 product for repressurization step.

- Paper II

Najmi, B., Bolland, O., Colombo, K. E., 2015. A systematic approach to the modeling and simulation of a Sorption Enhanced Water Gas Shift (SEWGS) process for CO_2 capture, Submitted manuscript to Separation & Purification Technology Journal (minor revision requested).

Dynamic operation of a Sorption Enhanced Water Gas Shift (SEWGS) system, based on a Pressure Swing Adsorption (PSA) process, is investigated by detailed dynamic modeling and simulation. The SEWGS system is a multi-train system, where each train consists of eight reactors working in parallel. The reactors are packed with a mixture of Water Gas Shift (WGS) reaction catalyst and CO_2 adsorbent. Syngas is converted to a H_2-rich product by an enhanced WGS reaction and a separate CO_2-rich stream is also produced. The SEWGS system considered in this work is designed to be integrated in an Integrated Gasification Combined Cycle (IGCC) power plant as a pre-combustion CO_2 capture process. Therefore the operating conditions of the system are compatible with those of an IGCC power plant. Moreover, the SEWGS system dynamic characteristic at different loads of feed syngas is interesting for further investigation of the performance of an IGCC power plant at different GT load levels. Simulation results reveal performance of the system in terms of components breakthrough curves and steam consumption of the system with a CO_2 recovery rate of 95% and 99% purity of the recovered CO_2. The H_2-rich product purity achieved is around 81%. It is found that changing the rinse and purge steam amount affects the CO_2 purity and recovery rate. However, the H_2-rich product purity remains almost unchanged. Simulation of the SEWGS system at different loads of feed syngas shows that to maintain the CO_2 recovery and purity of the design case as the target performance, in addition to changing the rinse and purge steam loads, duration of the feed step and thus the cycle time should be varied as well. The H_2-rich stream flow rate produced by the SEWGS train undergoes large fluctuations of around ±33%, which should be minimized due to the requirements of the GT. It is tried in this work to reduce the fluctuations by scheduling operation of the different trains with time lags. Two different configurations (five sets of double trains and two sets of pentuple trains) are considered and operation of the SEWGS system under these configurations is compared with the basic configuration. Applying these two operation strategies, H_2-rich stream flow rate fluctuations are decreased from ~±33% in the basic configuration to ~±14% and ~±11% in the first and second configuration respectively. However, compared to the basic configuration, the H_2-rich stream overall production rate drops around 5.5% and 6.2% on average, respectively. This is due to the time lags considered in the scheduled operation strategy of the trains, compared to the train operation strategy in the basic configuration with no time lag.

- Paper III

Najmi, B., Bolland, O., Colombo, K. E., 2015. Load-following performance of IGCC with integrated CO_2 capture using SEWGS pre-combustion technology, International Journal of Greenhouse Gas Control, 35, 30–46.

The performance assessment of an Integrated Gasification Combined Cycle (IGCC) integrated with the Sorption Enhanced Water Gas Shift (SEWGS) technology for pre-combustion CO_2 capture at full-load and part-load modes of operation is investigated. Syngas from a coal gasifier is sent to the SEWGS system after going through solids and H_2S removal units. A H_2-rich stream is produced by the SEWGS system and used in a GT for combustion. A control strategy including a buffer tank followed by a control valve, between the SEWGS system and the GT is implemented to smooth out the fluctuations in the H_2-rich fuel flow rate, resulted from the cyclic operation of the PSA-based SEWGS system. Simulation of the IGCC integrated with the SEWGS system is first performed at full-load operation of the GT. For evaluating part-load performances, four different cases, introducing various load change strategies for the GT and gasifier are studied. Step/ramp changes of the GT and gasifier, unplanned/planned GT load changes and same/different GT and gasifier load change occurrence time are all addressed through these four cases. Simulation results indicate that the designed control strategy is able to minimize the H_2-rich fuel flow rate fluctuations and dampen the fuel composition variations, while keeping the buffer tank pressure within the desired range. Dynamic characteristics of the SEWGS system is revealed and compared with those of the gasifier and the GT. Using the buffer tank between the SEWGS and the GT, improves part-load operation flexibility of the GT. Smooth operation and load following capability of the IGCC integrated with the SEWGS system is achievable, depending on the GT part-load level and load change strategy, taking into account the limited load gradient of the gasifier and the SEWGS units compared to the GT.

- Paper IV

Najmi, B., Bolland, O., 2014. Operability of Integrated Gasification Combined Cycle Power Plant with SEWGS Technology for Pre-combustion CO_2 Capture, Energy Procedia, 63, 1986-1995.

This paper investigates the performance of an integrated gasification combined cycle (IGCC) power plant incorporating a sorption enhanced water gas shift (SEWGS) process for pre-combustion CO_2 capture at part-load conditions. The multi-train SEWGS process operates on a cyclic manner based on a pressure swing adsorption (PSA) process and reaches a cyclic steady state. Each train consists of eight SEWGS vessels. A H_2-rich stream which is produced at high temperature and pressure is sent to a GT as an almost carbon-free fuel for power generation. A CO_2-rich stream, the secondary product of the SEWGS process, is released from the solid adsorbent at low pressure. Dynamic mathematical modeling of the SEWGS system developed previously is used to simulate the performance of the SEWGS system at different part-loads. A control strategy including a buffer tank and a closed-loop proportional integral (PI) controller is designed to provide the required amount of the fuel to the GT at full-load and part-load modes of operation. The control system performance is very important to provide a fuel from the SEWGS system that fulfils the requirement of the GT with respect to fuel pressure and heating value variations. Simulation results show when the GT load is changed, the control system functions properly and provides the corresponding GT fuel flow after a new steady-

state condition is reached. The H_2-rich stream flow rate fluctuation, associated with the cyclic operation of the SEWGS process, is reduced from ~±14% to ~±1% under the effect of the designed PI controller. On the other hand, when a load change is given to the GT, operation of the entire IGCC plant is dictated by the rate of change of the SEWGS system. The load gradient of the SEWGS process achieved from the part-load simulations is ~2% load/min. The SEWGS system is not able to respond to load changes as rapid as the GT. This will reduce the operation flexibility of the entire IGCC Plant. However, the addition of the intermediate buffer tank improves the operation flexibility of the GT as long as the pressure variation in the tank falls within the acceptable range.

1.10. Working process

This work undertakes an interaction between chemical process engineering, process control and applied mathematics as shown in Fig. 1-6.

The sequence of the steps carried out to achieve the objectives presented in section 1.7 is as follows:

I. Screening study in the literature to select an appropriate CO_2 adsorption material for the design of the SEWGS process.

II. Adopting a flowsheet for the IGCC integrated with a SEWGS pre-combustion CO_2 capture process from an available conventional IGCC flowsheet.

III. Defining/setting the SEWGS process design parameters, including the cycle configuration, cycle time, volume of the SEWGS reactor and adsorbent/catalyst particles.

IV. Development of a non-isothermal, one dimensional homogenous dynamic model for a single SEWGS reactor, taking into account mass, energy and momentum balances; implementing the model in gPROMS and numerical simulation of the system of partial differential algebraic equations (PDAE).

V. Development of a process flowsheet model for the multiple interconnected SEWGS reactors, including the flow switching valves and mixtures/splitters, implementing the model in gPROMS and numerical simulation of the PDAE equations.

VI. Scheduling the SEWGS trains operation with time lags between the operations of trains and evaluating its impact on improving the H_2-rich fuel fluctuations.

VII. Design and implementation of a model-based fuel control strategy including a buffer tank and a PI control valve, to control the GT fuel at different part-loads.

VIII. Applying the various part-load operation strategies and investigate dynamic performance analysis of the IGCC with SEWGS**.**

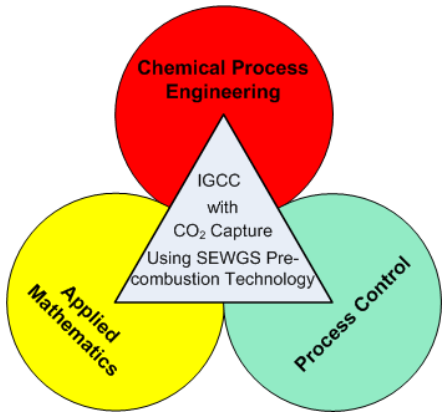

Fig. 1-6. Multidisciplinary approach for the analysis of IGCC with SEWGS technology

1.11. Achievements

- Using the SEWGS detailed dynamic modeling and simulation approach, transients occurring in the SEWGS reactors, while going through different PSA process steps as well as impact of the SEWGS operation parameters such as feed syngas flow rate, rinse/purge gas consumption and cycle time on the SEWGS system performance are understood, (Paper I, II).

- The SEWGS system dynamic response to load changes is identified and compared with that of the gasifier, by conducting SEWGS simulations at different part loads (paper IV).

- The H_2-rich product flow rate and composition fluctuation is observed. This necessitates applying further control strategies to reduce the fluctuations and prepare the H_2-rich fuel according to the GT requirements, when the SEWGS system is added to the IGCC.

- The developed strategy to operate the multi-train SEWGS system with time lags, is capable of reducing about 60% of the H_2-rich fuel flow rate fluctuation (paper II).

- The designed closed-loop, model-based fuel control system, incorporating a buffer tank and a control valve, controls the H_2-rich fuel in terms of flow rate, pressure and composition at different GT part-loads (paper III).

- The buffer tank, which is designed as part of the fuel control system, improves operation flexibility of the IGCC with SEWGS, dampens a large portion of the H_2-rich fuel flow rate and composition variations (paper III, IV).

- Operability and controllability of the IGCC with SEWGS at different GT part-load levels are discussed. Smooth operation and load-following capability of the IGCC integrated with the SEWGS system is achievable, depending on the load change strategy (paper III).

Chapter 2

2. SEWGS background

2.1. Development of SEWGS technology

The sorption enhanced reaction (SER) concept is based on the Le Chatelier's principle that states (a) the conversion of reactants to products and (b) the rate of forward reaction in an equilibrium controlled reaction can be increased by selectively removing reaction product(s) from the reaction zone (gas phase) by adsorption on a solid material. This shifts the reaction towards the product side [69, 70]. The SER concept was basically applied to the steam methane reforming (SMR) by Air Products and Chemicals Inc. in the 1990s and used to produce a high purity hydrogen (95+ % mole) at a lower reaction temperature than that of the conventional equilibrium controlled endothermic SMR reactor [71, 72]. A fixed bed reactor packed with a mixture of a SMR catalyst and a chemisorbent was employed for the SER concept. The chemisorbent, which was a K_2CO_3-promoted HTC-based material, selectively removed the undesired SMR reaction product (CO_2) at a temperature of 300-500 ºC (in the presence of excess steam) and thus enhanced the conversion of the CH_4 to the H_2 (82%). The SER concept showed a high potential to remove the need for high-temperature reactor metallurgy as well as reduce/eliminate the need for additional H_2 purification units. Following these promising results, further experimental and theoretical studies of the SER concept for the SMR application were performed [56, 58, 70, 73, 74, 75].

The SER concept has been further expanded for the WGS reaction application and ongoing research works are being carried out to investigate the application of this novel technology for pre-combustion CO_2 capture from power plants [76, 77, 78, 79, 80, 81].

The so-called sorption enhanced water gas shift (SEWGS) concept, combines the equilibrium WGS reaction with CO_2 adsorption on solid materials. The WGS reaction is thermodynamically controlled and slightly exothermic (41 kJ/kmole CO_2). The equilibrium constant of the WGS reaction decreases and the reaction rate constant increases with the increase of the temperature [82]. The optimum practical temperature for the WGS reaction is between 200 and 400 ºC.

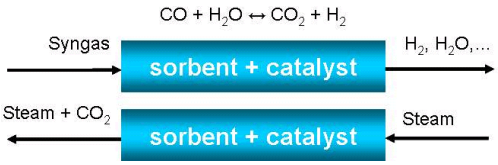

Fig. 2-1. SEWGS principle, (upper) adsorption and reaction at high pressure (lower) desorption at low pressure [84]

H_2 and CO_2 are the products of the WGS reaction. In the SEWGS principle as shown in Fig. 2-1, the CO_2, once produced is adsorbed simultaneously on a solid CO_2 adsorbent material. This shifts the equilibrium WGS reaction towards an enhanced conversion from CO to CO_2 and leaves a gas phase, mainly consists of H_2 and steam. The CO_2, as a separate by-product, can then be recovered from the adsorbent by regenerating the bed based on a PSA process [76, 83]. As a basic requirement for the SEWGS process, adsorbent needs to be regenerable and usable during many reaction/adsorption and regeneration cycles to make the SEWGS process profitable.

CO_2 Capture Project (CCP), a major joint industry effort, working with Air Products and Chemicals, carried out development of the novel SEWGS technology for pre-combustion fuel decarbonization [78, 85]. The CCP's work in two phases, focused on providing technical and scientific knowledge to reassure that the CO_2 can be stored securely and the costs of the CO_2 capture can be reduced. In this regard, in the second phase the focus was in particular on developing different capture technologies such as the SEWGS, in gas-fired power plants. During CACHET (Carbon dioxide Capture and Hydrogen production from gaseous fuels), a project under the European sixth Framework Programme (FP6), further study and optimization of the SEWGS process were carried out. The project mainly focused on novel pre-combustion capture technologies and hydrogen production from natural gas-fired power plants that could significantly reduce the costs of the CO_2 capture. Energy research Centre of the Netherlands (ECN) constructed and operated both a single and multiple column SEWGS unit operations. Experimental data from the full cyclic operation of the multi-column SEWGS were complex and difficult to analyze and calibrate a model to fit. However, the enhancement of the WGS reaction by simultaneous CO_2 adsorption was observed. Degradation of the CO_2 adsorbent materials was also observed which demanded further improvement and investigation of the appropriate high temperature CO_2 adsorbents. [86, 87].

Within the seventh Framework Programme (FP7), three main EU projects continued working on the CO_2 capture [84, 88, 89]. A base case and common parameters were defined for system simulation to have consistent and comparable results [68]. Further development of the SEWGS technology for natural gas, coal and blast furnace applications was defined within the scope of the FP7 project [84, 87]. The overall objective was reducing the energy penalty and costs of the CO_2 capture relative to the CACHET project, by development of the improved and more efficient adsorbent materials [83, 90, 91], optimized cycle configurations, reactor design and integration of the SEWGS process with power plants [83, 79].

2.2. SEWGS process concept and configuration

The new high temperature SEWGS technology is mainly attractive for decarbonizing a GT fuel and pre-combustion CO_2 capture in power plants. Unlike the common pre-combustion technologies, where the syngas is typically passed through a two-stage HTS (at 350 °C) and LTS (190-210 °C) reactors and a downstream CO_2 removal unit, the SEWGS process combines the WGS reactor(s) and the CO_2 capture process in a single unit. The syngas generated from a coal gasifier or a natural gas reformer is mixed with steam and enters the SEWGS reactor at high temperature and pressure (~400 °C, 20-30 bar). However, the SEWGS reactor used in the literature is fed by a partially shifted

syngas, which has already passed through an upstream HTS reactor [76]. The reason for having a HTS reactor upstream of the SEWGS reactor is explained to avoid the high temperatures in the SEWGS reactor caused by the exothermic WGS reaction.

The CO_2 produced from the WGS reaction in the SEWGS system, is adsorbed simultaneously on a solid adsorbent and the H_2 production is increased. The main equipment in this process is the WGS reactor, which is typically packed with a mixture of the CO_2 adsorbent and the WGS catalyst as shown in Fig. 2-2. A single SEWGS reactor is a batch process, which produces a H_2-rich product and operates until the CO_2 adsorbent is saturated by the CO_2 (or a pre-determined level of the CO_2 breakthrough is reached). Then the feed to the SEWGS reactor is disconnected (usually directed to another reactor), the reactor bed is regenerated and the adsorbed CO_2 is recovered. The regeneration of the adsorbent is normally based on a PSA process and consists of a sequence of various processing steps, which defines the SEWGS cycle configuration. To achieve a continuous production of the H_2-rich and CO_2-rich products out of the batch SEWGS single reactor process, it is common to use a multiple reactor system for the PSA-based SEWGS process.

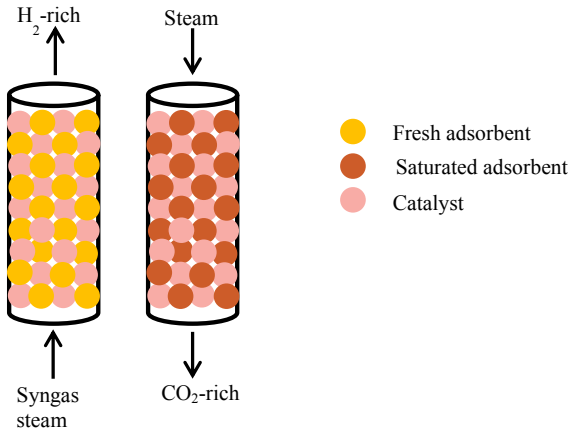

Fig. 2-2. A single catalyst-adsorbent packed SEWGS reactor scheme, fresh adsorbent at the start and saturated adsorbent at the end of the batch process.

Referring to Fig. 2-3 as an example of a SEWGS cycle configuration and taking the reactor #1, the SEWGS process starts with a feed step in which the WGS reaction and CO_2 adsorption take place. A H_2-rich stream essentially at feed pressure and higher temperature (than the feed syngas temperature) is produced during the feed step. The regeneration consists of a number of steps. A rinse step is usually carried out at feed pressure following the feed step, by sending a rinse gas to the reactor to sweep the gases left in the reactor and recycle them to the feed of another reactor. This will maximize the recovery of the H_2, as well as the CO_2 product purity and prevents contamination of the CO_2 product by the H_2 left in the reactor. The rinse step has been used in most of the works on the SEWGS process in the literature [76, 77, 78, 79, 80, 83, 86, 92]. Using a counter-current high pressure (HP) steam has a better performance than a co-current CO_2 or N_2 rinse gas [77, 78, 92]. On

the other hand, the amount of rinse steam is a trade-off between the desired CO_2 purity/H_2 recovery and power penalty resulted from the HP steam extraction from a steam cycle. Following the rinse step, the reactor pressure is reduced by using a number of steps known as equalization, whereby the feed end of the vessel is connected to that of another vessel. Doing so, the pressure energy in the vessel(s) undergoing the pressure-reduction steps can be recovered and used to repressurize the vessel(s) after regeneration. Further displacement of the residual gases from the reactor continues during the equalization steps. Therefore, using more equalization steps allows reducing the rinse gas consumption, while meeting the target CO_2 purity/H_2 recovery. On the other hand, additional equalization steps necessitate higher number of the SEWGS reactors to operate the cycle, increasing the equipment cost and complexity of the process.

Recovery of the CO_2 is obtained in the two subsequent steps named depressurization and purge steps. The depressurization step, also known as blow down is conducted counter-currently down to the CO_2 recovery pressure. Then a low pressure (LP) steam is sent to the reactor counter-currently to purge the bed. The steam can be either bled from the steam turbine or produced with a dedicated level in the HRSG (when the SEWGS is part of a power plant for CO_2 capture). The effluent gas from the purge step is a low-pressure CO_2/steam mixture at around 400 °C. The mixture is cooled down to around 35 °C to condensate the steam and be prepared for the CO_2 compression.

Once the purge step is terminated, the SEWGS vessel is repressurized, first by accepting gas from other vessels undergoing the equalization step(s), and then by receiving part of the product gas counter-currently. The reactor is then ready to restart a new SEWGS cycle.

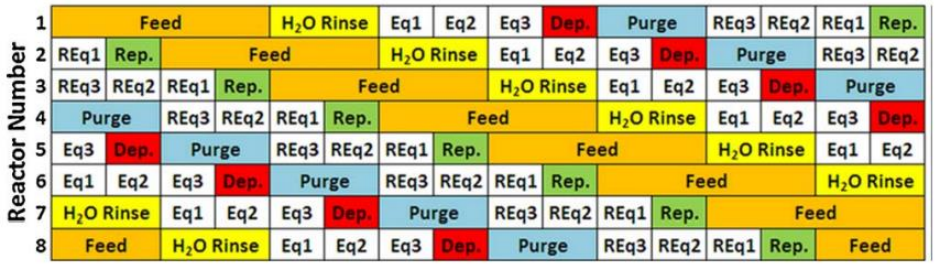

Fig. 2-3. A SEWGS cycle configuration, the sequence of steps consists of feed, rinse, three equalization steps (Eq1-Eq3), depressurization (Dep.), purge, three equalization steps for repressurizing the reactors (REq3-RE1) and repressurization (Rep) [76]

A higher number of the SEWGS reactors can ensure continuity of the product streams and achieving a desired extent of separation. The optimal number of the SEWGS reactors is usually between six to eight, all connected with flow switching valves [76].

In commercial-scale SEWGS systems, where a large amount of the syngas needs to be treated, usually multiple reactor trains arranged in parallel would need to be employed. This is to limit the size of the single SEWGS reactors by distributing the feed syngas among the reactor trains. Each train consists of a number of the SEWGS reactors, which operate according to a defined cycle

configuration. Two separate streams of the H_2-rich and CO_2-rich are produced from each train. The total product of the SEWGS system is the sum of products from each reactor train. An example of an installed multi-bed multi-train SEWGS system is shown in Fig. 2-4.

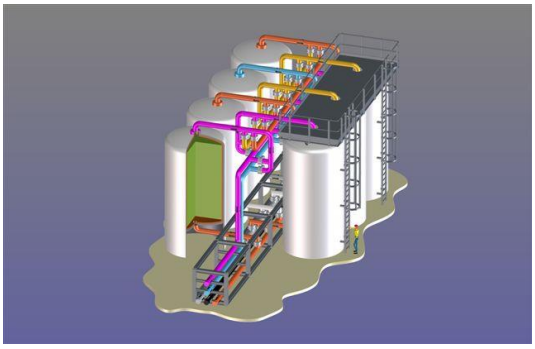

Fig. 2-4. A 3D design for a commercial size SEWGS unit [93]

2.3. Material development

One of the main issues with SEWGS process, is to find an adequate adsorbent to capture the CO_2 under the conditions typical for the SEWGS process (temperature ~350-550 °C, pressure 20-30 bar and at the presence of water vapor) [76, 83].

On the basis of ongoing research activities conducted so far, HTC-based materials have been recognized as the most promising CO_2 adsorbent material for the SEWGS pre-combustion CO_2 capture technology [56, 57, 86, 94, 95].

HTCs also known as LDHs or "anionic clays" are composed of positively charged brucite-like layer, e.g. $Mg(OH)_2$ and negatively charged interlayer, e.g.CO_3^{2-}, as shown in Fig. 2-5. The positive charge is formed from the trivalent cations partially substituting the divalent cations in the brucite structure. The excess positive charge is balanced by the anions and water molecules present in the interlayer [53]. The general formula for the HTCs is: $[M^{2+}_{1-x}M^{3+}_{x}(OH)_2]^{x+}(A^{n-}_{x/n})\ mH_2O$, in which x is normally 0.1-0.3. For the HTCs used in the CO_2 adsorption processes at high temperatures, the divalent ion (M^{2+}) is Mg^{2+}, the trivalent ion (M^{3+}) is Al^{3+} and the interlayer anion (A) is CO_3^{2-}: $(Mg_{1-x}Al_x(OH)_2(CO_3)_{x/n}\ mH_2O)$ [53]. The final property of the material can change with different combinations of the cations, anions, the ratio of cations M^{2+}/M^{3+}, preparation and activation methods [96]. They can be transformed into basic mixed oxides with increased surface area and pore volume after thermal decomposition (at temperatures beyond 300 ºC). This will enhance their CO_2 capture capacity [97, 98]. A specific feature about the HTCs is the so-called "structural memory effect" by which these materials can recover their original structure from the mixed oxides upon contact with water or aqueous solutions containing certain anions. This property is the key to successful application of these materials as anion exchanges and catalyst support precursors [99, 100].

The CO_2 capture capacities of the HTCs can be improved by impregnation with alkali metal carbonates such as K_2CO_3 [49, 53, 57, 94]. However, high degrees of the K_2CO_3 loading (beyond an

optimum value) block some active CO_2 adsorption pores on the surface and negatively impact the CO_2 adsorption capacity [96].

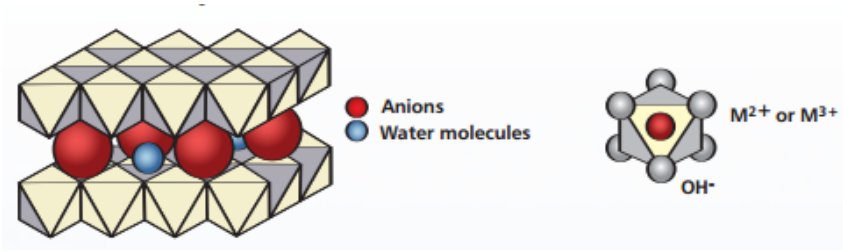

Fig. 2-5. Layered double hydroxide (LDH) or hydrotalcite (HTC) structure [101]

A screening study was carried out on different samples of the HTC materials from the commercial HTCs to the alkali modified HTCs: impregnated commercial HTCs with potassium and cesium. The HTC impregnated with potassium showed the highest CO_2 capture capacity at temperatures of about 400 ºC, CO_2 partial pressure (P_{CO2}) of 0.4 bar and in the presence of steam among the other samples tested [49].

The CO_2 capture capacities of the potassium-promoted HTCs at the presence of water are higher than the dry condition. For example, according to Ding and Alpay [56], the positive effect of the presence of water on the CO_2 capture capacity of the potassium-promoted HTC is visible even at low water concentrations. The positive effect of the presence of water on the adsorption capacity of the potassium-promoted HTC was also reported by Oliveira et al. [49]. The maximum CO_2 capture capacity achieved was 0.75 mole/kg at the presence of minimum 16% water, T=400 °C and P_{CO2} = 0.4 bar. In contrast, there are few reports about the negative effect and ineffectiveness of the water presence on the CO_2 capture capacity of the potassium-promoted HTCs as well. Ficicilar and Dogu reported a CO_2 capture capacity reduction for the potassium-promoted HTC in the presence of 20% water due to diffusion resistance of the CO_2 to the active sites [102]. Allam et al. and Hufton et al., on the other hand, reported no change in the CO_2 capture capacity of such materials in the presence of 15-18% steam in the feed gas [78, 69]. A more recent work was carried out to investigate the CO_2 capture mechanism of three different commercial K_2CO_3-doped HTC-based materials with different Mg/Al ratio and potassium content in the temperature range of 300-600 ºC and steam pressures 0-4.55 bar [95]. First, by reviewing different studies in the literature on the CO_2 capture capacity of the HTC materials, the authors stated that the CO_2 capture mechanism on the K-promoted HTC for application in the SEWGS process might be influenced by a critical CO_2/steam pressure. At high CO_2 and steam pressures and steam to CO_2 partial pressure ratio close to one, formation of the $MgCO_3$ is the dominant mechanism. However, recently it has been reported that this causes reduction of the carbon capture rate over time [91]. At low steam pressures, on the other hand, the most generally accepted hypothesis for the CO_2 adsorption mechanism is a two-step process, one fast reversible chemical reaction, followed by slow reversible reaction(s), where different carbonated species are

involved. Then, by doing experiments, the authors concluded that the formation of K-dawsonite ($KAl(CO_3)(OH)_2$) was the main identified capture mechanism, when the feed was dry or with low water contents. However, at increased values of the available steam in the reaction system up to 35% (by volume), the CO_2 capture capacities of the adsorbents increased drastically and reached values as high as 9 mole/kg adsorbent. The reasons attributing to these high capture capacities as stated by the authors were more likely: the reconstruction of the HTC at high temperatures (300 °C), the hydration of potassium carbonate to form the hydrogen carbonate hydrate $K_4H_2(CO_3)_3 \times 1.5H_2O$ and the formation of magnesium carbonate during the capture process conditions (300 °C and 13 bar). According to their findings, absolute values of steam and CO_2 partial pressures and their ratio play a crucial role in the CO_2 capture mechanisms and efficiencies of the potassium-promoted HTC-based adsorbents for their application in the SEWGS processes [95].

A potassium-promoted HTC material was used as the CO_2 adsorbent for application in a bench scale SEWGS process, operating at 400–450 °C and 25 bar under high CO_2 and steam pressure [92]. The adsorbent only-filled vessels were employed to determine the breakthrough capacities and stability of the adsorbent under cyclic operation condition. The adsorbent-catalyst filled vessels were used to demonstrate the SEWGS concept and stability of the adsorbent-catalyst mixture over cyclic operation. The potassium-promoted HTC-based material showed breakthrough capacities of 1.3-1.4 mmole/gr at around 400 ºC and a good stability over 4000 cycles. It was reported that the CO_2 capture capacity of the potassium-promoted HTCs was improved with the increase of the CO_2 partial pressure as well as the presence of steam in the feed gas. It was also reported that the CO_2 capture capacity of the adsorbent greater than 8 mmole/g was achievable if the CO_2 and H_2O partial pressures in the feed were sufficiently high. The authors stated that this high capacity was associated with the formation of the $MgCO_3$ in the bulk of the adsorbent material. However, the kinetics of this chemisorption was too slow to utilize in a PSA-based SEWGS process. The formation of the $MgCO_3$ in the potassium-promoted HTC at high CO_2 and steam pressures and magnesium content (Mg/Al=2.9) was demonstrated in another work and mentioned as the important factor in achieving high CO_2 capture capacities [103].

An experimental work was carried out to investigate the cyclic and breakthrough capacity of a potassium-promoted HTC-based material for two different cases of adsorption only and adsorption/reaction system [86]. A fixed bed reactor (two meter tall) was first filled with the tablets of potassium-promoted HTC-based material and exposed to a mixture of CO_2, steam and N_2 at 400 °C. The typical breakthrough capacity of 1.4 mmole/g was obtained. Also, purging the bed with a low pressure superheated steam resulted in additional CO_2 removal. Stable CO_2 recoveries well above 90% were achieved for more than 1400 cycles of adsorption/desorption with the cyclic capacity of ~0.66 mmole/g. In the next series of the experiments the concept of the SEWGS system was demonstrated. The bed was filled with a mixture of commercial iron-chromium shift catalyst and the potassium-promoted HTC, and was exposed to a mixture of CO_2, CO, steam, H_2 and N_2. Enhanced CO conversion up to 100% and stable rate of the CO_2 capture for 300 cycles of the adsorption/reaction and desorption were observed.

The K_2CO_3-promoted HTC-based adsorbents used during the CACHET project (K-MG70) suffered from two main issues (1) the mechanical strength failure of the adsorbent pellets over several hundred cycles [4], (2) an increasing slip of the CO_2 in the H_2 product appeared over the cycles, under realistic process conditions, i.e. elevated CO_2 and steam partial pressures. The formation of the considerable amounts of $MgCO_3$ was found to be the main reason for these issues. Later, in the FP7 project, new adsorbents were developed with increased cyclic capacity and mechanical strength compared against its predecessor in the CACHET. The new adsorbent was a k_2CO_3-promoted HTC-based material with lower magnesium content, noted as K-MG30 (30 wt.% Mg, compared to 70% in the CACHET project) [91].

Investigations on the HTC properties as CO_2 adsorbent material mainly focused on sweet SEWGS condition. In other words, the sulphur from the syngas is removed upstream the SEWGS process. At the final stages of the FP7 project a research work was conducted on the CO_2 capture capacity and behavior of the HTC-like materials in the presence of the H_2S, which exists in higher quantities in the syngas generated from a coal gasifier, rather than the natural gas reforming process. It was shown that a 20 wt% K_2CO_3-promoted HTC-based was capable of co-adsorption of the H_2S along with the CO_2. In other words, the SEWGS system employed at sour conditions had the potential for simultaneous decarbonation and desulphurization of the sour syngas generated from the coal gasification. However, an additional desulphurization unit might be required for separation of the CO_2 and H_2S, which would need further investigations in terms of the efficiency penalty of the power plant. Moreover, adsorbents with different contents of the K_2CO_3 and MgO might demonstrate different characteristics with respect to H_2S adsorption which was left to be further investigated [104].

Catalytic properties of a K_2CO_3-promoted HTC adsorbent has also been reported in an experimental work [93]. The conversion of CO to CO_2 during the breakthrough experiments with the adsorbent and in the absence of the WGS catalyst was the main evidence. The authors state that this property could add commercial and technical benefits to the use of the SEWGS technology for pre-combustion compared to the conventional technologies.

2.4. CO_2 chemisorption equilibria

The K_2CO_3-promoted HTC material has been found as the outstanding CO_2 adsorbent material for the SEWGS application [49, 50, 53, 56, 57, 59, 76, 78, 80, 86, 92-96, 99, 100, 101, 103-105]. There is still discussion in the literature about the characteristics of the K_2CO_3-promoted HTC material in terms of the CO_2 chemisorption isotherms and kinetics at different temperatures, with the presence of water. Different adsorption mechanisms such as simple Langmuir description [56, 58], Freundlich isotherm [53], nonequilibrium coupled reactions [94], CO_2 complexation reactions [106] and coupled exothermic-endothermic reactions [49] have been suggested in the literature to describe the CO_2 adsorption on the K_2CO_3-promoted HTCs. The adsorption capacity of the HTC-based materials in general is a function of the number of surface basic sites, which are variable with the chemical composition (e.g. Mg/Al ratio) and the degree of impregnation with alkali metal carbonate such as K_2CO_3.

Ding and Alpay used a Langmuirian isotherm to fit the equilibrium adsorption data on K_2CO_3-promoted HTC at 400 °C and CO_2 partial pressures up to 0.6 bar. The maximum monolayer capacity achieved was 0.65 mole/kg at wet conditions [56].

Reijers et al. [105] studied CO_2 adsorption on a 22% K_2CO_3-promoted HTC sample, noted as PURAL MG70, at 400 °C. They employed the Freundlich isotherm to present their CO_2 uptake data in a low pressure region (CO_2 partial pressure between 0.02-0.25 bar).

Oliveira et al. [49] screened different HTC samples (PURALMG30, MG50, MG70) promoted with K or Cs in the temperature range of 403-510 °C. A bi-Langmuirian isotherm was considered for describing the CO_2 adsorption capacity on the different samples (CO_2 partial pressures up to 0.5 bar). The bi-Langmuirian isotherm takes into account two types of available adsorption sites on the surface. One is related to physical adsorption with low isosteric adsorption enthalpy (40 kJ/mol). The second part is associated with the chemisorption through an endothermic chemical reaction with an enthalpy of 130.8 kJ/mole.

Halabi et al. [53] investigated the adsorption of CO_2 on a K_2CO_3-promoted HTC at 400-500 °C and the CO_2 partial pressure of 0.85 bar, experimentally. The equilibrium adsorption data obtained was described by Freundlich isotherm. A loss of 8% took place in the fresh adsorbent capacity due to an irreversible chemisorption. However, a stable working capacity of about 0.89 mole/kg was preserved.

An analytical equilibrium model was developed by Lee et al. [57] with the purpose of providing further insight into the mechanism of the CO_2 chemisorption on the k_2CO_3-promoted HTCs. The authors state that the isotherms used in the earlier K_2CO_3-promoted HTC adsorption schemes are not accurate enough in predicting the CO_2 adsorption mechanism, especially at higher partial pressures of the CO_2, which is typical for the SEWGS operating condition. They presented an analytical isotherm composed of two simultaneous mechanisms for the chemisorption process (a) Langmuirian term in the low pressure region ($P_{CO2} < 0.2$ bar) and (b) chemical complexation reaction term, which accounts for the higher pressures. The chemical complexation term considers a reaction between the gaseous CO_2 and the adsorbed CO_2 on the solid adsorbent. The monolayer capacity obtained at 400 °C was relatively low (0.25 mole/kg). However, the adsorbent demonstrated a total capacity of 0.875 mole/kg. This model is presented by equation (1):

$$q^*_{CO_2}\left(P_{CO_2}, T\right) = \frac{mK_C P_{CO_2}\left[1+(a+1)K_R P^a_{CO_2}\right]}{1+K_C P_{CO_2}+K_C K_R P^{a+1}_{CO_2}} \quad (1)$$

$$K_C = K^0_C \exp\left(\frac{q_C}{RT}\right) \quad (2)$$

$$K_R = K^0_R \exp\left(\frac{\Delta H_R}{RT}\right) \quad (3)$$

In the SEWGS experimental study by Van Selow et al. [86], the authors have reviewed the adsorption isotherms found in the literature and stated that the adsorption isotherms reported in literature are of limited use for SEWGS modelling, since most isotherms are developed for low CO_2 partial pressures.

However, they do not present a predictive model, describing the adsorption behavior of the CO_2 on the K_2CO_3-promoted HTC material.

The inconsistency observed in the reported isotherms of the CO_2 adsorption over the HTC-based materials is mainly linked to the diversity of the HTC nature, composition, preparation method, promoter type, impregnation degree, pressure and temperature range and wet/dry condition [96, 97].

Until new isotherms are developed, which are consistent with respect to higher partial pressures and adsorption capacities, the isotherms reported in literature have to be used for modelling purposes. The modified non-linear isotherm developed in the work by Lee et al. [57] (Fig. 2-6) is employed for the mathematical modeling of the SEWGS process here, which is reported to give a good fit to the experimental data in the CO_2 partial pressure region of 0-4 bar and at a temperature of 400 °C.

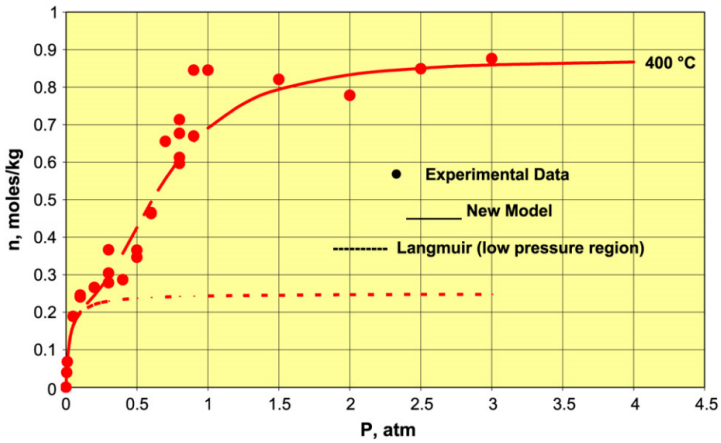

Fig. 2-6. CO_2 chemisorption isotherm on K_2CO_3-promoted HTC at 400 ºC [57]

Linear driving force (LDF) model (equation 4) is widely used to describe the mass transfer mechanism of the CO_2 adsorption on solid adsorbents such as HTC-based materials [49, 50, 53, 56, 57, 59, 76, 78, 80, 86, 92, 94-96, 99-101]. This involves a driving force based on the linear difference between the equilibrium adsorption amount and the actual (volume-averaged) adsorption amount, and a constant of proportionality accounting for the intra-particle diffusional resistance of the adsorbent. It has been found that an LDF model accounting for pore diffusion and a non-linear adsorption isotherm is suitable for describing the adsorption and desorption processes [56].

$$\frac{\partial q_{CO_2}}{\partial t} = K_{LDF}(q^*_{CO_2} - q_{CO_2}) \qquad (4)$$

2.5. Relevant work from literature

An overview of experimental and theoretical studies from literature on the SEWGS process and its integration with the power plant for CO_2 capture is presented in the following.

The CCP, by Air Products and Chemicals, undertook an investigation of a natural gas-based power plant performance, integrated with a SEWGS process for CO_2 capture [78]. First, the PSA-based adsorption process was simulated with assumed adsorbent equilibrium and kinetic parameters to predict the performance of the SEWGS process. The results from the SEWGS process simulation were incorporated into the steady-state simulations of a power plant to determine the potential impact of the SEWGS CO_2 capture process on the overall performance of the power plant. Later, experiments were conducted on different potential CO_2 adsorbent materials, including thermo gravimetric analysis, with the aim of finding the best suited CO_2 adsorbent(s) for the SEWGS application. The simulation work was then refined using the data achieved from the experimental work. The SEWGS process was simulated in Aspen plus, using a "Stoichiometric reactor" block followed by a "Separator" block. It was assumed that the SEWGS as a perfect separator removed all of the CO_2 fed to the reactor. The steady-state simulation of the power plant was carried out using Aspen Plus, by feeding the results from the SEWGS process simulation. One of objectives of the CCP was to consider the applicability of the SEWGS process in Alaskan and Norcap scenarios. The goal for the Norcap scenario was to develop a process for producing power with drastically reduced CO_2 emissions. The goal of the Alaskan scenario was to repower eleven open cycle GTs with hydrogen fuel. Due to the lack of information on the hydrogen-powered turbines, it was assumed that the power of each GT fueled with natural gas remained the same, when fueled with the hydrogen, and so did the temperature from the combustor. The adsorbent material used was a K_2CO_3-promoted HTC. Breakthrough and cyclic tests conducted in packed beds of the adsorbent/HTS catalyst mixture demonstrated the enhancement of the equilibrium WGS reaction and a carbon recovery of over 80% was achieved.

A number of research activities were carried out during the CACHET project on the SEWGS technology and its application for pre-combustion CO_2 capture from NGCC power plants [77, 86, 92, 107]. The SEWGS experiments were carried out using two test rigs [92]. One was a two meter tall reactor vessel and the other included six reactor vessels, each six meter tall. The multiple reactor test rig was built to demonstrate the full cyclic process and concept of the SEWGS and was commissioned in December 2007 [108]. A counter-current steam rinse was employed instead of a co-current CO_2-rinse, which was used in [78]. As stated by authors using the CO_2 rinse, which came from the compressed CO_2 product was costly. Moreover, as the CO_2 was adsorbed on the solid material, extra CO_2 required to be supplied to compensate for the amount of the adsorbed CO_2. Using the counter-current steam for rinsing was suggested in [107]. The counter-current flow pattern helps to maintain a high CO_2 concentration at the feed end and maximize desorption rate during the purge step. The two meter long single reactor vessel was used to conduct the CO_2 breakthrough experiments to determine the CO_2 breakthrough capacity as well as to find the stability of the adsorbent only and the adsorbent/catalyst mixture under the extended cyclic operation condition. The adsorbent material was K_2CO_3-promoted HTC-based material. The reversible adsorption of the CO_2 on the adsorbent was shown at 400 °C, with breakthrough capacities of 1.3-1.4 mmole/g under the realistic condition of the SEWGS process. The stability of the adsorbent was demonstrated for more than 4000 adsorption/desorption cycles and the stability of the mixture of the adsorbent and catalyst was demonstrated for more than 500 cycles. The experiments were yet to continue for further

development/improvement of the adsorbent, reactor and cyclic process to meet the cost objectives for commercialization of the SEWGS technology.

Another research work within the CACHET project was a theoretical study of the SEWGS process concept [77]. The study incorporated eight SEWGS vessels, where each vessel was packed with a mixture of the iron-chrome catalyst and K_2CO_3-promoted HTC-based material. The assumptions used in the simulation of the SEWGS process are summarized in Table 2-1. The feed syngas to the SEWGS vessels was assumed to be the syngas produced from an air-blown autothermal reforming (ATR), at 400 °C and 30 bar. The SEWGS was modeled using an adsorption process simulator [109]. Langmuirian equilibrium and linear driving force kinetics were assumed as the simplified model for the HTC material adsorption/desorption mechanism. Two cases of counter-current steam-rinse and co-current CO_2-rinse were simulated with different feed step durations, rinse and purge flow rates. In the end, optimum operating condition was achieved for each case by minimizing the capture cost. Two constraints of at least 90% carbon capture and 98% purity of the CO_2 product were considered when optimizing the cases for the minimum cost. The results showed that using the counter-current steam-rinse improved the overall efficiency of the power plant in comparison to the previously proposed co-current CO_2-rinse option (about twice as much gas was needed for rinsing the beds with the CO_2 compared with the steam). Also cost reductions of around 20-25% were claimed; by using the SEWGS process versus the amine scrubbing process in the CACHET reference case for pre-combustion CO_2 capture from natural gas (see Table 2-2).

Table 2-1. SEWGS train and vessel design assumed for a 330 MW natural gas-based power plant [77].

Specification	**Value**
Number of trains [-]	4
Number of vessels per train [-]	8
Number of vessels co-currently on feed per train [-]	2
Vessel length [mm]	7377
Vessel diameter [mm]	3658
Mass of adsorbent per vessel [kg]	44465
Mass of catalyst per vessel [kg]	12927

Table 2-2. Comparison of the SEWGS versus CACHET reference case, calculations based on January 2006 prices and for a power output of 330 MW [77].

	Reference Case Amine scrubbing	CO_2-Rinse SEWGS	H_2O-Rinse SEWGS
Fixed capital [million €]	462	409	375
Efficiency [%]	40.9	42.9	44.7
Cost of power [€/MWh]	87	83	77
Cost of CO_2 capture [€/ton CO_2]	82	78	68
Cost of CO_2 avoidance [€/ton CO_2]	118	106	88

During the CACHET project it was concluded that the SEWGS was an appropriate candidate for pre-combustion CO_2 capture from power plants, when the feedstock was natural gas (i.e. NGCC). Still

there were room for improvements of the SEWGS both in terms of the cyclic capacity and chemical/physical stability of the adsorbent pellets [86]. Further investigation of the SEWGS process was therefore assigned for the FP7 project. Due to a rapid increase in the natural gas price, application of the SEWGS technology for pre-combustion from alternative feedstock such as coal (i.e. IGCC) was mainly taken into consideration. Different activities including: development of improved adsorbent materials, SEWGS cycle configuration, process flowsheets for either natural gas or coal-fired power plants integrated with the SEWGS process and economic evaluation of the SEWGS were defined for the FP7 follow-on project [76, 79, 83, 90, 91].

Experimental work was conducted on the new adsorbent material, using the two meter long column for breakthrough experiments [90, 91]. The experimental data collected was used to develop a model for the SEWGS process applicable for both of the natural gas-derived and coal-derived feed syngas [83]. After reforming/gasification, the syngas was passed through a first WGS reactor. The assumed composition of the syngas after the WGS reactor, which was the feed to the SEWGS process, was as in Table 2-3.

Table 2-3. Feed syngas composition to the SEWGS process derived from NG and coal [83]

Syngas to the SEWGS	Natural gas derived [mole %]	Bituminous coal derived [mole %]
CO_2	12	24
CO	5	6
H_2	42	35
H_2O	8	31
Others (e.g.N_2, Ar, CH_4, H_2S)	33	4

The impurities such as H_2S in the feed syngas (higher content in the coal-derived vs. the NG-derived syngas) could potentially have a detrimental effect on the adsorbent stability and long term CO_2 capacity. How to cope with this issue was within the scope of the FP7 project. The cycle time, vessel size, number of trains and cycle configuration (except the number of equalization steps) were fixed and similar to the previous work in the CACHET [77]. The SEWGS performance analysis was carried out by changing the rinse and purge steam flow rates as well as feed pressure, composition and number of the equalization steps to achieve a 95% CO_2 purity and recovery rate. The results indicated that the optimum design for the SEWGS process with minimized steam consumption was achieved when the feed pressure was in the range of 20-30 bar, with the three equalization steps for both the natural gas and coal based syngas. This led to a rinse steam to feed carbon ratio of 0.65-1.00 and purge steam to feed carbon ratio of 1.15-1.55 (i.e. a total steam to feed carbon ratio of 2.15-2.20) for the natural gas based case. For the coal based case, the corresponding values were 0.40-0.65 and 1.25-1.50 (a total steam to carbon ratio of 1.90), respectively. A ratio of the total steam to carbon in the feed of two cases was set as a preliminary goal for the economic success of the SEWGS process.

A performance assessment of a NGCC power plant integrated with the SEWGS process, from a thermodynamic point of view, was carried out theoretically. An in-house computer code called GS was used for the simulation [76]. Three levels of integration between the SEWGS process and

NGCC, from decoupled to tightly integrated power and hydrogen island, were investigated. In the completely decoupled hydrogen and power island scenario, all the steam required for the reforming and SEWGS processes was produced within the hydrogen island. According to the authors statement, the amount of the heat required within the hydrogen island for the steam production, was higher than the available sensible heat in the feed syngas and CO_2-rich product streams. Therefore, the H_2-rich stream required to be cooled down before the combustor to satisfy the steam requirements. This in return, led to a reduction of the overall efficiency and disregarded the advantage of the SEWGS process in maintaining the high temperature of the H_2-rich fuel before it was sent to a GT. On the other hand, the tight integration of the hydrogen and power island allowed utilization of the heat sources in the power island for the heat demands within the hydrogen island. Also, air to the ATR, was taken from the GT air compressor. However, an additional fan was required to compress the air to the pressure at the ATR inlet. In this tight integration option, the heat recovery from the CO_2-rich stream to achieve a temperature of around 30 °C before the compression was still advantageous. The integration between the hydrogen and power island increased the degree of freedom to unitize the HRSG and steam cycle for steam/heat demands by the ATR and SEWGS processes (increased thermal flexibility). However, the operation flexibility of the entire plant was limited. The thermodynamic simulation revealed the efficiency and CO_2 capture ratio of the entire power plant as performance indicators, focusing on the impact of different integration levels on the efficiency penalties. It was found that the tight integration between the power and hydrogen island reduced the efficiency penalty. Also it was shown that the SEWGS process steam usage had strong impact on the plant efficiency penalty, of which the effect of the rinse steam was higher than that of the purge steam (due to higher rinse steam pressure). In addition to the steam usage of the SEWGS process, the H_2-rich fuel temperature at the combustor inlet affected the efficiency. The higher the fuel temperature, the lower the efficiency penalty was. The fuel temperature in the decoupled hydrogen and power island scenario was lower than that of the integrated hydrogen and power island scenario, due to the cooling of the H_2-rich fuel to fulfill the steam demand of the decoupled hydrogen island.

Performance of the NGCC power plant using the SEWGS process from [76] was compared with three reference cases, in terms of the net electric efficiency and CO_2 avoided as well as the second law exergy analysis [81]. The reference cases were NGCC (without CO_2 capture), NGCC with MEA post-combustion and NGCC with MDEA pre-combustion CO_2 capture. The first two reference cases were selected by European Benchmark Task Force (EBTF) and the last case was used because of its similarity to the NGCC with the SEWGS pre-combustion for ease of comparison. A summary of the simulation results achieved for these cases are presented in Table 2-4.

Similar to the work performed in [76], a thermodynamic performance assessment of an IGCC power plant, incorporating the SEWGS process for CO_2 capture was carried out in a follow-on work [80]. Two IGCC reference cases (w/o CO_2 capture) were first introduced for comparison of the results. Two different K_2CO_3-promoted HTC-based materials which were developed within the FP7 project were used (named: adsorbent “alfa” and adsorbent “beta”). The adsorbent “beta”, was similar to the adsorbent “alfa”, but with an improved isotherm shape and adsorption capacity. The adsorbents demonstrated catalytic properties as well as the H_2S adsorption capabilities, besides the CO_2

adsorption. It was therefore assumed that the SEWGS vessels were filled only with the adsorbent pellets and using the WGS catalyst was pointless.

Table 2-4. Comparison of the simulation results for the NGCC, the NGCC with CO_2 capture using three cases of post combustion MEA, pre-combustion MDEA, pre-combustion SEWGS [76, 81]

	NGCC	**NGCC MEA**	**NGCC MDEA**	**NGCC SEWGS**	
				Decoupled hydrogen/power island	Tight integration hydrogen/power island
NO. of GT	2	2	2	2	2
GT [MW]	272.1	272.1	294.5	323.2	276.2
Fuel temperature, [°C]	160	160	300	137.7	350
Steam cycle gross power, [MW]	292.8	215.7	305.1	296	277.8
Net power output, [MW]	829.9	709.7	830.0	806.1	777.9
CO_2 avoided, [%]	-	89.7	91.5	95.3	95.1
SPECCA[1], [$MJ_{LHV}/kgCO_2$]	-	3.3	3.07	5.00	3.08
Net electric efficiency (LHV base), [%]	58.3	49.9	50.3	45.9	50.0

The SEWGS system performed the H_2S separation in addition to the CO_2 separation, but required additional downstream separation of the H_2S and CO_2 [14, 80]. Simulation of the IGCC integrated with SEWGS process for CO_2 capture was carried out using the in-house GS simulator. The results of the thermodynamic performance simulation were indicated in terms of the efficiency and CO_2 capture ratio. Co-adsorption of the H_2S and CO_2 had the benefit of equipment saving and avoidance of thermal swing. Using adsorbent "beta" with the higher cyclic capacity than the adsorbent "alfa", allowed a reduction of the size and number of the SEWGS vessels, while the same CO_2 capture ratio and purity were achieved. The results obtained by using these two adsorbents are presented in Table 2-5.

Table 2-5. Results from the simulation of the IGCC with SEWGS for pre-combustion CO_2 capture [80]

	Efficiency [%]	CO_2 capture ratio [%]	CO_2 purity [%]	NO. of trains	NO. of vessels	SPECCA [$MJ/kgCO_2$]
Adsorbent Alfa	39.2-38.5-37.8	90 -95-98	99	6	9	2.5
Adsorbent beta	38.64	90-95	99	5	9	2

Two different configurations for the integration of the SEWGS process into an IGCC power plant were investigated within the FP7 project [79]. In the first configuration, the so-called sweet SEWGS process was used, where an acid gas removal (AGR) unit was placed upstream of the SEWGS process for sulphur removal. In the second configuration, the so-called sour SEWGS process was

[1] Specific energy consumption for CO_2 avoided

employed, where there was no upstream AGR unit and a simultaneous CO_2 and H_2S separation from the syngas by the SEWGS process was assumed. In the case of the sour SEWGS process, the adsorbent have to be a sulphur tolerant material and capable of adsorbing both the H_2S and CO_2. On the other hand, a downstream CO_2/H_2S separation unit will be required. The H_2S separation method utilized in this mentioned work was based on a catalytic oxidation of the H_2S and conversion to elemental sulphur. Two IGCC reference cases, with and without CO_2 capture process, were introduced as the base case for comparison of the results. The IGCC reference case with the CO_2 capture incorporated a two-stage Selexol process. Heat and material balances were estimated by the GS simulator, to evaluate performance of the power plant. The Selexol and CO_2 compression units were simulated with Aspen Plus. The SEWGS modeling was based on the experimental works carried out during the CACHET and FP7 project. The simulation results showed that the capture cases, in general, had a lower cold gas efficiency (defined as: the ratio of the chemical energy in the syngas and chemical energy in the coal feed) compared to the cases without capture, due to the exothermic WGS reaction. Between the capture cases, the SEWGS cold gas efficiency was the lowest because of the enhanced conversion of the CO by the SEWGS process (conventional capture had about 85% conversion, while the SEWGS had about 99%). The results from the comparison of the different cases are summarized in Table 2-6. Authors concluded that the SEWGS process was capable of reducing the efficiency penalty about 10%, compared to the conventional Selexol process. Also using the SEWGS for the CO_2 capture in power plants could be beneficial with respect to equipment saving, in particular, if the sour SEWGS process was applied.

Table 2-6. Comparison of the results for the IGCC and IGCC with different capture processes [79]

	IGCC	SELEXOL	SWEET SEWGS	SOUR SEWGS
Cold gas efficiency (LHV base) [%]	82.5	74.0	73.6	73.6
Net electric efficiency (LHV base) [%]	47.7	36.5	37.6	38.4
CO_2 avoided [%]	N/A	87.6	98.0	98.0
SPECCA [MJLHV/kgCO_2]	N/A	3.6	2.9	2.6
Net power output [MW]	425.2	383.1	385.9	394.3
GT [MW]	289.9	304.9	311.5	311.7

An overview of the SEWGS process configuration and performance used in the literature is given in Table 2-7.

Table 2-7. A summary of the SEWGS configurations and performance reported in the literature

Ref.	Power plant	CO conversion [%]	CO_2 recovery [%]	CO_2 purity [%]	Ads.	# beds/ # trains	Process cycle								
[78] Thr & Ep.	NGCC	95 assumed	>80	100 assumed	K_2CO_3 promoted HTC-based	7/4	Feed	E1/ R	E2	E3	Bd	P	RE3	RE2	RE1 /RP
Feed syngas (35bar, 350-450 °C): generated in an O_2-blown ATR; SEWGS reactor: packed with catalyst/adsorbent mixture; H_2-rich: produced at essentially feed pressure and higher temperature (~450-550 °C) RE3-RE1: By accepting gas from other vessels, undergoing the pressure equalization (E1-E3) and CO_2 rinse steps; RP: by receiving counter-current product gas E1/R: co-current with part of the CO_2 product; P: counter-current with steam; Bd: counter-current to a pressure of 1.1 atm; E1-E3: co-current														
[92] Exp	NGCC	> 98	>90		K_2CO_3 promoted HTC-based	6/1	Feed		R		D		P		RP
Feed step: CO_2 adsorption and WGS reaction occurrence; Feed syngas: from a ATR at 400 °C; R: counter-current with HP steam; D: counter-current; P: counter-current with LP steam; RP: with N_2 and steam															
[77] Thr.	NGCC	>98	>90 constraint	>98 constraint	K_2CO_3 promoted HTC-based	8/4	Feed	R	E1-E3		D	P	RE3-RE1		RP
Feed syngas (28bar, 400 °C): generated in an air-blown ATR; SEWGS reactor: packed with iron-chrome catalyst and CO_2 adsorbent; Two vessels perform the feed step each time; R: counter current with steam; E1-E3: co-current; D: counter-current; P: counter-current with steam; RE3-RE1: counter-current by accepting gas from other vessels; RP: counter-current with part of the H_2 rich															
[83] Thr.	IGCC NGCC		95	95	K_2CO_3 promoted HTC-based	6-8	Same as Ref. 77								
No. of equalization were changed between 1-3, which corresponds to the NO. of reactors between 6-8															
[76] Thr.	NGCC	99%	96	98%	K_2CO_3 promoted HTC-based	8	Same as Ref. 77								
Feed syngas (30bar, 400 °C); R: counter-current with super-heated steam at 400 °C, 27 bar; D: counter-current down to pressure of CO_2 recovery P: counter-current with super-heated steam at 400 °C, 1 bar; RE3-RE1: co-current by accepting gas from other vessels; RP: counter-current with part of the product gas															
[80] Thr.	IGCC	>98%	90-95-98 (a) and 90-95(b) assumed	99	K_2CO_3 promoted HTC-based	9/5 (b) & 6 (a)	Same as Ref. 77								
Two different cases a, b were investigated by using two types of the K_2CO_3 promoted HTC-based, named adsorbent "alfa" and "beta", respectively. The adsorbent "beta" had improved performance with respect to the CO_2 adsorption capacity and isotherm shape.															

*E1-E3: equalization steps (pressure reduction), RE1-RE3: equalization steps (repressurization); R: rinse; Bd: blow down; D: depressurization; P: purge; RP: repressurization; Thr.: theoretical work; Exp.: experimental work

Chapter 3

3. Methodology

This chapter deals with the inclusion of the SEWGS technology as part of an IGCC power plant for pre-combustion CO_2 capture from a design and modeling perspective. First, the system layout is presented to provide an overview of the system under consideration. The system is then broken up into sub-systems. The SEWGS is the main component of interest, which consists of a number of reactors, undergoing a sequence of steps based on a PSA process. The approach for a detailed dynamic modeling and simulation of the SEWGS, taking into account the multiple-bed operation is presented. The main product of the SEWGS system, H_2-rich, is used as a GT fuel within the IGCC. A schedule for the multi-train SEWGS system is developed to initiate the operation of the trains asynchronously. This is to dampen the H_2-rich stream flow rate fluctuations, associated with the cyclic operation of the SEWGS process, as dictated by the downstream GT. Furthermore, a fuel control system is implemented after the SEWGS and designed to control the H_2-rich fuel stream before entering the GT in terms of the mass flow rate, pressure and composition. The control system is also designed to control the H_2-rich fuel when the GT is operated at part-load. Finally, load-following capabilities of the IGCC integrated with the SEWGS technology at different part-loads is investigated under four different case studies, taking into account the SEWGS dynamic characteristics, obtained from the dynamic simulations. Step/ramp changes of the GT and gasifier, unplanned/planned GT load changes and same/different GT and gasifier load change occurrence time are all addressed through these four cases.

3.1. IGCC integrated with SEWGS process

An IGCC power plant is integrated with a SEWGS technology for pre-combustion CO_2 capture. The process layout of the system is adopted from an IGCC with conventional pre-combustion CO_2 capture technology [68], shown schematically in Fig. 3-1. The feedstock of the power plant is assumed to be Bituminous Douglas Premium coal [68, 110], with the composition given in Table 3-1. A distinction has been made between the Process Island and Power Island, as shown in Fig. 3-1. The Process Island includes the gasification block and the gas treatment block. Key streams are indicated by numbers and information about them is shown in Table 3-2.

Table 3-1. Coal composition [mole%] [68, 110].

Carbon	Nitrogen	Hydrogen	Total sulphur	Ash	Chlorine	Moisture	Oxygen
66.52	1.56	3.78	0.52	14.15	0.009	8.0	5.46

A H_2S removal unit is assumed upstream of the SEWGS process to feed a sulphur free syngas (< 3 ppm) to the SEWGS process. This is due to the H_2S intolerant CO_2 adsorbent material which is assumed in this work.

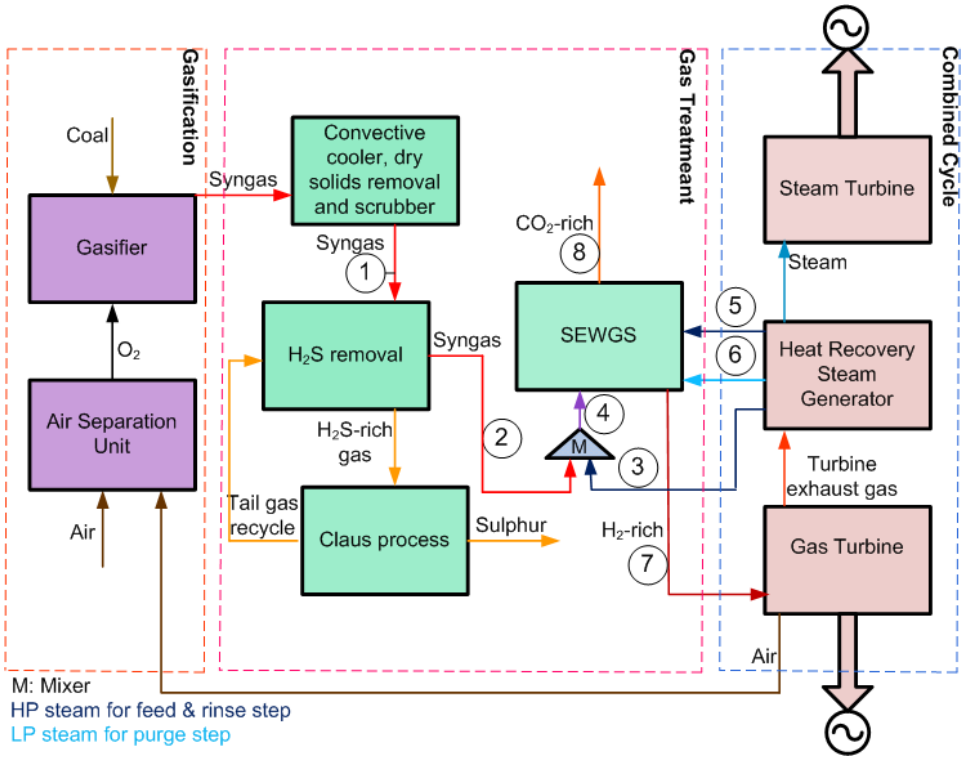

Fig. 3-1. A schematic diagram of an IGCC integrated with the SEWGS technology

Table 3-2. Stream data used in the current simulation work [68].

Stream #	Molar flow	T	P	Composition					
	kmole/s	K	bar	H_2	CO	CO_2	N_2+Ar	H_2S	H_2O
1	4.22	443	35	22.02	49.23	3.45	6.97	0.13	18.13
2	4.21	673	27	22.06	49.33	3.46	6.98	-	18.17
3	3.21	673	27	-	-	-	-	-	100
4	7.42	673	27	12.52	27.99	1.96	3.96	-	53.57
5	0.66	673	27	-	-	-	-	-	100
6	1.32	673	2	-	-	-	-	-	100

A cryogenic type Air Separation Unit (ASU) is used to produce O_2 for the gasifier. Coal is gasified to synthesis gas in an O_2-blown, entrained flow gasifier, operating at 44 bar. The syngas is then cooled and cleaned of particulates by passing through a convective cooler, dry solids removal unit (electrostatic precipitator). H_2S is removed from the syngas to feed a sulphur-free syngas to the sweet

SEWGS process. In the IGCC reference case with conventional CO_2 capture process, the H_2S removal unit is downstream of the WGS reactors, called sour WGS process. The sweet SEWGS process is selected due to the detrimental effect of H_2S on the K_2CO_3-promoted HTC sorbent stability and long term CO_2 adsorption capacity [78].

Syngas to the H_2S removal unit, stream #1, has the same composition and flow rate as the corresponding stream in the reference case. Assuming an efficiency of 100% for the H_2S removal unit, mole fraction and flow rate of the syngas entering the SEWGS system, stream #2, are obtained.

The SEWGS system inlet temperature and pressure as presented in Table 3-2 are selected to be 673 K and 27 bar according to [78], which the selected feed pressure was suggested as the optimal pressure.

Syngas is treated within the SEWGS process for CO_2 capture via the WGS reaction enhanced by the K_2CO_3-promoted HTC CO_2 adsorbent under a multiple bed operation system. It consists of a reaction/adsorption step and a sequence of steps for regeneration of the solid adsorbent. The H_2-rich and CO_2-rich stream, products of the SEWGS system, are shown by stream #7 and #8, respectively**.** The H_2-rich gas (stream #7) is sent to the GT for combustion. The power production section consists of a combined cycle including a GT, steam turbine (ST) and heat recovery steam generator (HRSG). The hot GT exhaust gases are passed through the HRSG for heat recovery and steam generation. Steam is then used to produce power in the ST. Part of the steam produced by the steam cycle is consumed by the SEWGS process as feed, rinse and purge gas, shown by streams #3, #5 and #6, respectively. To control the H_2-rich stream as per GT requirements, a fuel control strategy is included and designed. Fig. 3-2 indicates the block diagram of the IGCC integrated with SEWGS pre-combustion and scope of the mathematical modeling and simulation in this work. The SEWGS upstream components including the gasifier and ASU as well as the gas clean-up unit are not included in the mathematical modeling. However, the load gradient of the gasification process (gasifier and ASU) is incorporated in the calculations to investigate load-following performance of the IGCC integrated with SEWGS at different GT part-loads. In the power island, ST and HRSG are excluded from the numerical calculations. There is no upstream effect from the ST to the GT, while specific load changes of the GT are considered. Also, there is always sufficient steam available from the ST to be fed to the SEWGS system.

The system modeling and simulation approach is as follows:

1. Development of a one-dimensional non-isothermal homogeneous model for axially dispersed plug flow SEWGS reactors and performance simulation of PSA-based SEWGS system with multi-train arrangement (section 3.2.1-3.2.4).
2. Implementation of a scheduled operation strategy for SEWGS trains (section 3.2.5).
3. Development of a fuel control strategy to control the GT fuel (H_2-rich) at full-load and part-load modes of operation (section 3.3).

4. Performance investigation of the IGCC with SEWGS in terms of load-following capability and controllability when incorporating the fuel control system. The dynamics of SEWGS process from step#1 are taken into account (section 3.4).

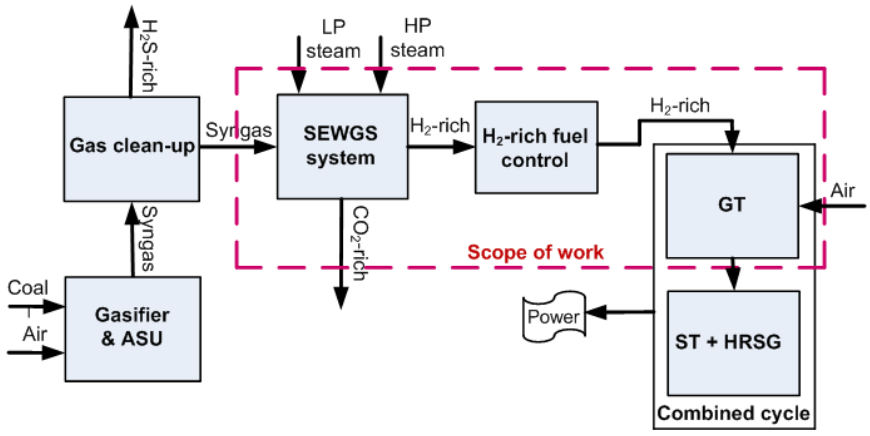

Fig. 3-2. A block diagram of the IGCC integrated with the pre-combustion SEWGS system

3.2. SEWGS system design, modeling and simulation

The SEWGS system consists of a number of reactors in a multi-train arrangement. It is assumed that the behavior of each SEWGS train is the same. This allows for modeling the behavior of one SEWGS train. Each SEWGS train consists of eight reactors operating in parallel based on a PSA process. Each SEWGS reactor undergoes a fixed sequence of PSA processing steps, repeated in a cyclic fashion. Cyclic operation manner of the process means that the system is inherently dynamic and therefore studying dynamic performance of such a system is of great importance, particularly when the process like this is incorporated into even bigger processes like power plants. The modeling approach for the operation of the multi-bed SEWGS train consists of two parts. First, the mathematical model describing the behavior of the system is established. Second, the operation schedule of the PSA-based SEWGS is implemented. The operation schedule includes aspects such as controlling the flow rate of the feed syngas, steam required to be mixed with the feed syngas, transition from one processing step to another for a given bed and switching of the connections between the reactors by interconnecting valves. Furthermore, a strategy to schedule the operation of SEWGS trains is introduced. This is to reduce the H_2-rich product stream fluctuations associated with the cyclic operation of the SEWGS process as per GT requirement.

3.2.1. PSA-based SEWGS process cycle configuration and operation

The PSA-based SEWGS system is subjected to a number of cyclic adsorption/reaction and regeneration steps. The sequence of steps and cycle configuration used in this work is shown in Fig. 3-3 [83]. In addition to the four fundamental PSA process cycle steps, i.e. adsorption, depressurization, purge and pressurization, a rinse step using steam as a rinse gas and three pressure equalization steps are also included in the SEWGS cycle configuration. Such a configuration results in achieving higher cyclic capacity of the adsorbent as well as higher purity and recovery of both the

product gas streams. However, increases the number of beds and consequently additional flow switching valves and piping. Including the rinse step in the SEWGS cycle configuration minimizes the amount of the residual H_2-rich fuel gas in the reactor after the feed step (improved recovery of the H_2-rich product which is used as the GT fuel for power production) and improves the purity of the CO_2-rich stream, recovered during the depressurization and purge step. Pressure swing cycle starts with three pressure reduction steps called pressure equalization (Eq1-Eq3). During each pressure equalization step, the reactor being depressurized is connected to another reactor being pressurized (REq3-REq1). The residual gas in the reactor is subsequently further withdrawn from the reactor to the other connected reactor. Without pressure equalization steps, a larger amount of the rinse steam is required to remove the same amount of the residual gas from the reactor and reach a desired CO_2-rich stream purity and recovery of the products. Using the pressure equalization steps will also be beneficial to utilize and save the energy available in the high pressure feed stream as much as possible. This will reduce the compression energy required to increase the pressure of an already regenerated bed to the feed pressure for starting a new cycle. Using three pressure equalization steps allows ramping down the pressure from the feed pressure (after the rinse step) down to the atmospheric pressure for CO_2 recovery through two different intermediate pressure levels. The number of pressure equalization steps is the governing parameter for the number of adsorption columns.

The SEWGS reactors are interacting with each other in all the cycle steps except during depressurization (D) and purge (P) step. Co-current and counter-current flow patterns in each step are also shown. Steam is used as the rinse and purge gas because it is available at different pressure levels from the combined cycle power plant and can be easily separated from the other gas components. CO_2 is recovered during counter-current depressurization and purge step. During the depressurization step, the pressure is lowered down to the purge step pressure (1 bar) and then the reactor is purged with steam during the purge step to improve the CO_2 recovery. A re-pressurization step is carried out counter-currently by sending part of the H_2-rich product from another reactor being in the feed step. The reactor pressure is hence increased back to the feed pressure (~27 bar) to start a new cycle.

When a PSA-based SEWGS process is applied as a pre-combustion CO_2 capture to an IGCC plant, there should be at least one bed available, to serve the continuously incoming feed gas for the adsorption step, while releasing the second purified product (CO_2) from another saturated bed. An arrangement of eight reactors per train fulfills the requirement of continuous operation of the SEWGS process based on the operation scheme presented in Fig. 3-3. The operation schedule of eight individual SEWGS reactors, operating in parallel and going through the PSA cycle steps is presented in Fig. 3-4.

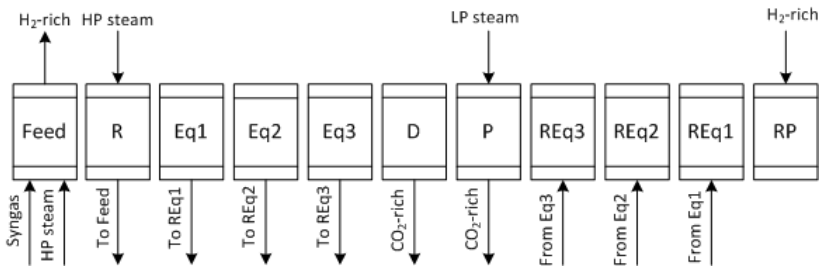

Fig. 3-3. Operation scheme of a SEWGS reactor, Feed (F), rinse (R), three pressure equalization (Eq1-Eq3), depressurization (D), purge (P), three pressure re-equalization (REq3-REq1), re-pressurization (RP)

SEWGS cycle																
System state	1	2	1	2	1	2	1	2	1	2	1	2	1	2	1	2
Cycle state	1	2	3	4	5	6	7	8	9	10	11	12	13	14	15	16
Reactor1	F				R		Eq1	Eq2	Eq3	D	P		REq3	REq2	REq1	RP
Reactor2	REq1	RP	F				R		Eq1	Eq2	Eq3	D	P		REq3	REq2
Reactor3	REq3	REq2	REq1	RP	F				R		Eq1	Eq2	Eq3	D	P	
Reactor4	P		REq3	REq2	REq1	RP	F				R		Eq1	Eq2	Eq3	D
Reactor5	Eq3	D	P		REq3	REq2	REq1	RP	F				R		Eq1	Eq2
Reactor6	Eq1	Eq2	Eq3	D	P		REq3	REq2	REq1	RP	F				R	
Reactor7	R		Eq1	Eq2	Eq3	D	P		REq3	REq2	REq1	RP	F			
Reactor8	F		R		Eq1	Eq2	Eq3	D	P		REq3	REq2	REq1	RP	F	

Fig. 3-4. Operation schedule of a SEWGS train, consisting of eight reactors operating in parallel, with each reactor undergoing a sequence of steps, based on the cycle configuration in Fig. 3-3 [79, 58]

3.2.2. Mathematical model of single SEWGS bed

A dynamic one-dimensional homogeneous model for the SEWGS reactor has been developed. The cylindrical reactor is assumed to be packed with a mixture of catalyst and adsorbent particles (Fig. 3-5). A FeCr-based catalyst was assumed for the high temperature WGS and K_2CO_3-promoted HTC as the CO_2 adsorbent [57, 86, 111].

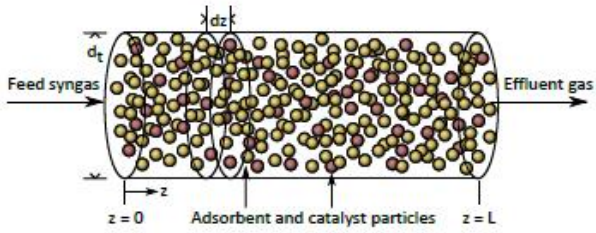

Fig. 3-5. Packed bed SEWGS reactor

Although development of novel K_2CO_3-promoted HTC adsorbents with catalytic properties has been reported in literature recently [93], the K_2CO_3-promoted HTC assumed in this work is taken from [57], for which the adsorption isotherm and kinetic models exist and are reported, but no catalytic properties are considered. This is mainly due to limited data about the adsorption isotherm and

kinetics of the new types of K_2CO_3-promoted HTC adsorbents. The WGS reaction and CO_2 adsorption are assumed to take place in the same unit. In the relevant works in literature, however, a pre-shift reactor is considered upstream of the SEWGS reactor to undertake a bulk of the WGS reaction [76, 80]. In this work the reactor wall temperature is assumed to be kept constant by a cooling jacket around the reactor. The temperature profile in the reactor and magnitudes of the temperature increase due to the exothermic forward WGS reaction and CO_2 adsorption will then be investigated to conclude whether having a pre-shift reactor is inevitable.

The main assumptions used in the reactor model are [57, 111]:

- Axially dispersed plug flow
- Adsorbent only selective for CO_2 and with no catalytic properties
- Ideal gas behavior
- No radial concentration and temperature gradients
- LDF model for mass transfer of CO_2 between the gas phase and adsorbent
- Modified Langmuir isotherm for equilibrium adsorption capacity of CO_2
- Uniform particle size of spherical adsorbent and catalyst
- Equal temperature in gas-phase, adsorbent and catalyst particles
- Non isothermal process

Table 3-3. Mathematical SEWGS reactor model [58]

Components mass balance:	
$\varepsilon_t \frac{\partial c_{CO_2}}{\partial t} = -\frac{\partial \left(u c_{CO_2}\right)}{\partial z} + D_{ax} \frac{\partial}{\partial z}\left(\frac{\partial c_{CO_2}}{\partial z}\right) + \rho_{b,cat}\eta_{CO_2} r - \rho_{b,ads}\frac{\partial q_{CO_2}}{\partial t}$	(1)
$\varepsilon_t \frac{\partial c_i}{\partial t} = -\frac{\partial \left(u c_i\right)}{\partial z} + D_{ax} \frac{\partial}{\partial z}\left(\frac{\partial c_i}{\partial z}\right) + \rho_{b,cat}\eta_i r \qquad i = H_2, CO, H_2O, N_2$	(2)
Total mass balance:	
$\varepsilon_t \frac{\partial c}{\partial t} = -\frac{\partial (uc)}{\partial z} + \rho_{b,cat}\sum(\eta_i) r - \rho_{b,ads}\frac{\partial q_{CO_2}}{\partial t}$	(3)
Energy balance:	
$\left(cC_{p,gas}\varepsilon_t + \rho_{b,cat}C_{p,cat} + \rho_{b,ads}C_{p,ads}\right)\frac{\partial T}{\partial t} = k_z \frac{\partial}{\partial z}\left(\frac{\partial T}{\partial z}\right) - cC_{p,gas}u\frac{\partial T}{\partial z}$ $-\rho_{b,cat}\sum_i (h_i\eta_i) r + \rho_{b,ads}\Delta h_{ads,CO_2}\frac{\partial q_{CO_2}}{\partial t} + \frac{4U}{d_t}\left(T_{wall} - T\right)$	(4)
Momentum balance (Ergun equation): $\frac{dp}{dz} = -150u\frac{\mu\left(\lambda_s\left(1-\varepsilon_b\right)\right)^2}{d_p^2\varepsilon_b^3} - 1.75u\lvert u\rvert\frac{\lambda_s\left(1-\varepsilon_b\right)\rho_{gas}}{d_p^2\varepsilon_b^3}$	(5)

Table 3-4. Additional equations in the SEWGS system modeling

Adsorbent loading based on Linear Driving force Model [57, 111]	
$\frac{\partial q_{CO_2}}{\partial t} = k_{LDF}\left(q^*_{CO_2} - q_{CO_2}\right)$	(6)
Modified Langmuir isotherm [57, 111]	
$q^*_{CO_2}(P_{CO_2}, T) = \frac{mK_C P_{CO_2}\left(1+(a+1)K_R P^a_{CO_2}\right)}{1+K_C P_{CO_2}+K_C K_R P^{a+1}_{CO_2}}$	(7)
$K_C = K^0_C \exp\left(\frac{\Delta H_{ads}}{RT}\right)$	(8)
$K_R = K^0_R exp\left(\frac{\Delta H_R}{RT}\right)$	(9)
Power law model for the WGS reaction rate expression, corrected for pressures up to 30 bar [110]	
$r = \left(p/101325\right)^{0.5-p/(250.101325)}.10^{5.845}\exp\left(\frac{-111000}{RT}\right).$ $\left(\frac{P_{CO}}{1000}\right)^{1.0}\left(\frac{P_{CO_2}}{1000}\right)^{-0.36}\left(\frac{P_{H_2}}{1000}\right)^{-0.09}\left(1-\frac{1}{K_{WGS}}\frac{P_{CO_2}P_{H_2}}{P_{CO}P_{H_2O}}\right)$	(10)
Axial thermal conductivity [58]	
$k_z = (\varepsilon_b + a_{k_z} PrRe_p)k_g$	(11)
Interconnecting valve model	
$\dot{n}_{valve} = x_{valve}.\left(F_c.(\lvert\Delta p\rvert)^{\frac{1}{FlowExponent}}\right)$	(12)

3.2.3. Multi-bed SEWGS train modeling approach

Referring to Fig. 3-4, one SEWGS cycle consists of 16 cycle states that each reactor undergoes. When inspecting all the 16 cycle states and the function of the reactors in each cycle state, a repeating manner in the operation of the SEWGS train of reactors during the entire cycle states is observed. During odd-number cycle states, two reactors in their feed step are producing H_2, while one reactor in its purge step produces CO_2. During even-number cycle states, part of the H_2 being produced by one of the two reactors in the feed step, is sent to another reactor being re-pressurized. CO_2 is also recovered during depressurization and purge steps. Therefore the operation of SEWGS train of eight reactors can be described by only two distinct repeating states referred to as system state 1 and system state 2. The two system states are shown in Fig. 3-6 and Fig. 3-7, respectively.

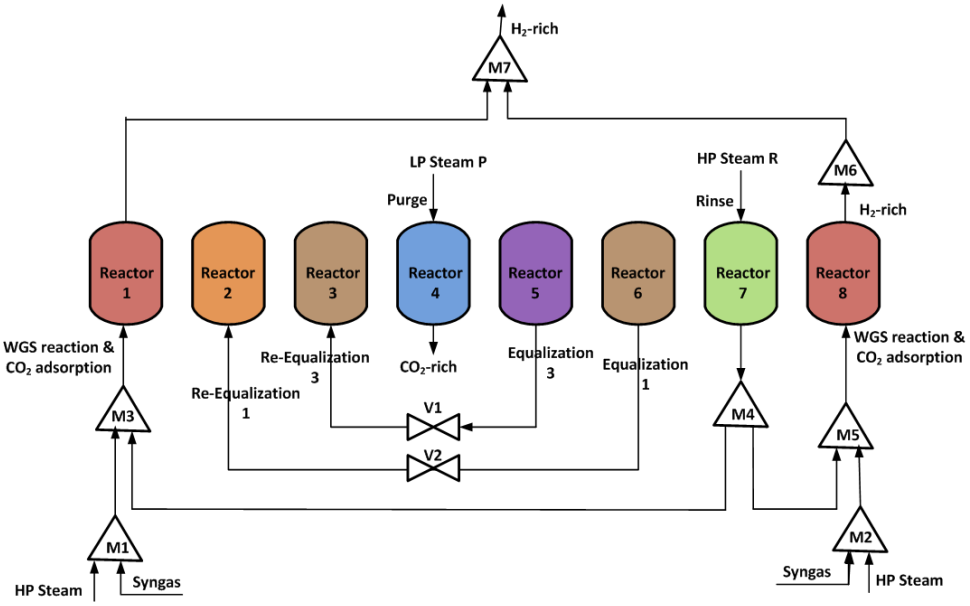

Fig. 3-6. SEWGS train in cycle state one, representing the system state 1, referred to Fig. 3-4

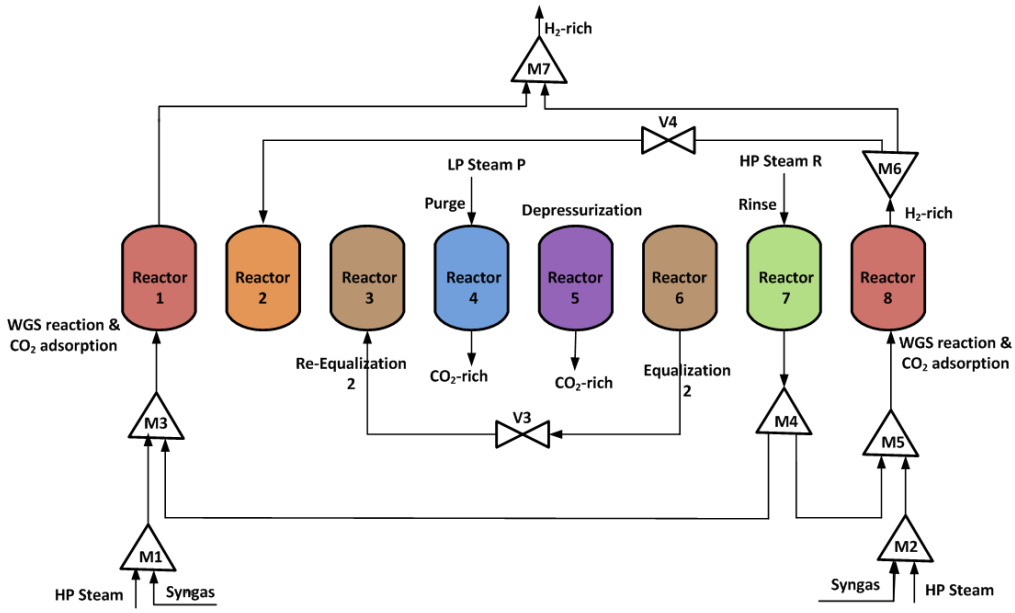

Fig. 3-7. SEWGS train in cycle state two, representing the system state 2, referred to Fig. 3-4

The parallel operation of eight reactors undergoing the 16 cycle states can thus be summarized by two different sets of equations, each one describing one of the two system states. When a SEWGS reactor moves from one cycle state to the next one, the switching between the system states occurs and boundary conditions used in the reactor model are changed accordingly. The boundary conditions for the different PSA cycle steps are based on those proposed by Danckwerts and presented in Tables 3-5 - 3-9 [112].

During pressure equalization steps, the interconnection between the reactors is carried out using valves, represented by equation 12 in Table 3-4. The valves are opened by ramping up the valve opening from zero (closed) to their desired position.
The amount of steam, which is required in the feed step, is always calculated to give the desired amount of steam to carbon (S/C) ratio during the operation of the SEWGS system. The rinse step exhaust gas with high steam content is split and mixed with the feed stream (syngas and steam) to another reactors being in the feed step. The total amount of steam fed to the reactor during the feed step is controlled to keep the S/C ratio constant.

Main assumptions for switches between the system states are:

1) Piping and connection losses are neglected. Stream variables such as flow rate and temperature are remain unchanged when interconnection between the components is made.
2) In the case of interconnection between two reactors at different pressure levels, e.g. interconnection during pressure equalization steps, a pressure-driven flow through an interconnecting valve is established between the reactors.
3) Mass and heat balances are applied for the mixers and splitters.
4) It is assumed that no WGS reaction takes place during the steps Eq1-Eq3, D, P, REq3-REq1.

Table 3-5. Boundary condition for co-current feed step (F) [112]

$z = 0$	$z = L$
$\frac{\partial \overline{c_i}(z=0)}{\partial z} = -\frac{u(z=0)\left(\overline{c}_{i,inlet} - \overline{c_i}(z=0)\right)}{D_{ax}(z=0)}$	$\frac{\partial \overline{c_i}(z=L)}{\partial z} = 0$
$\frac{\partial T(z=0)}{\partial z} = -\frac{\overline{c}(z=0) C_{p,gas}(z=0) u(z=0)\left(T_{inlet} - T(z=0)\right)}{k_z(z=0)}$	$\frac{\partial T(z=L)}{\partial z} = 0$
$u(z=0) = u_{inlet}$	$P(z=L) = P_{outlet}$

Table 3-6. Boundary condition for counter-current rinse step (R) and purge step (P) [112]

$z = 0$	$z = L$
$\frac{\partial \overline{c}_i(z=0)}{\partial z} = 0$	$\frac{\partial \overline{c}_i(z=L)}{\partial z} = -\frac{u(z=L)\left(\overline{c}_{i,outlet} - \overline{c}_i(z=L)\right)}{D_{ax}(z=L)}$
$\frac{\partial T(z=0)}{\partial z} = 0$	$\frac{\partial T(z=L)}{\partial z} = -\frac{\overline{c}(z=L)C_{p,gas}(z=L)u(z=L)(T_{outlet} - T(z=L))}{k_z(z=L)}$
$P(z=0) = P_{inlet}$	$u(z=L) = u_{outlet}$

Table 3-7. Boundary condition for counter-current equalization (Eq1-Eq3) and depressurization (D) steps [112]

$z = 0$	$z = L$
$\frac{\partial \overline{c}_i(z=0)}{\partial z} = 0$	$\frac{\partial \overline{c}_i(z=L)}{\partial z} = 0$
$\frac{\partial T(z=0)}{\partial z} = 0$	$\frac{\partial T(z=L)}{\partial z} = 0$
$P(z=0) = P_{inlet}$	$u(z=L) = u_{outlet} = 0$

Table 3-8. Boundary condition for the co-current re-equalization (REq3-REq1) steps [112]

$z = 0$	$z = L$
$\frac{\partial \overline{c}_i(z=0)}{\partial z} = -\frac{u(z=0)\left(\overline{c}_{i,inlet} - \overline{c}_i(z=0)\right)}{D_{ax}(z=0)}$	$\frac{\partial \overline{c}_i(z=L)}{\partial z} = 0$
$\frac{\partial T(z=0)}{\partial z} = -\frac{\overline{c}(z=0)C_{p,gas}(z=0)u(z=0)(T_{inlet} - T(z=0))}{k_z(z=0)}$	$\frac{\partial T(z=L)}{\partial z} = 0$
$u(z=0) = u_{inlet}$	$u(z=L) = u_{outlet} = 0$

Table 3-9. Boundary condition for the counter-current re-pressurization (RP) step [112]

$z = 0$	$z = L$
$\frac{\partial \overline{c}_i(z=0)}{\partial z} = 0$	$\frac{\partial \overline{c}_i(z=L)}{\partial z} = -\frac{u(z=L)\left(\overline{c}_{i,outlet} - \overline{c}_i(z=L)\right)}{D_{ax}(z=L)}$
$\frac{\partial T(z=0)}{\partial z} = 0$	$\frac{\partial T(z=L)}{\partial z} = -\frac{\overline{c}(z=L)C_{p,gas}(z=L)u(z=L)\left(T_{outlet} - T(z=L)\right)}{k_z(z=L)}$
$u(z=0) = u_{inlet} = 0$	$P(z=L) = P_{outlet}$

System state 1 in Fig. 3-6 is mathematically presented by four independent subsystems as in Table 3-10. The subsystem one includes the reactors #1, #7 and #8 together with the connected streams, splitters and mixers. The boundary conditions for the reactor #1 and #8 are those for the co-current feed step and for the reactor #7, are those for the counter-current rinse step. The stream leaving the reactor #7 from the feed end is split evenly into two streams and mixed with the feed streams to the reactor #1 and reactor #8 in their feed step. Subsystem two includes two reactors (#2, #6) at different pressure levels connected through the valve #2 (V2). Subsystem three is similar to the subsystem two and consists of the reactors #3, #5 with different pressure levels, connected through the valve #1 (V1). Subsystem four only involves the reactor #4 in its purge step.

System state 2 in Fig. 3-7 is also divided into four independent subsystems, presented in Table 3-10. The H_2-rich being produced in the reactor #8 is split. A side H_2-rich stream is passed through the valve #4 (V4) and sent to the reactor #2 until the pressure in the reactor #2 is increased back to the feed pressure. The remaining part is sent to the H_2-rich product sink.

Table 3-10. Subsystems in the system state 1 and system state 2

SEWGS train of eight reactors	**NO. of equations**
System state 1 (Fig. 3-6)	**156**
Subsystem one: Reactor #1, #7, #8; Mixer/Splitter: M1, M2, M3, M4, M5, M6, M7	96
Subsystem two: Reactor #2, #6; Valve: V2	26
Subsystem three: Reactor #3, #5; Valve: V1	26
Subsystem four: Reactor #4	8
System state 2 (Fig. 3-7)	**165**
Subsystem one: Reactor #1, #2, #7, #8; Mixer/Splitter: M1, M2, M3, M4, M5, M6, M7; Valve: V4	113
Subsystem two: Reactor #3, #6; Valve: V3	26
Subsystem three: Reactor #5	18
Subsystem four: Reactor #4	8

The total number of equations describing system state 1 & 2 is shown in Table 3-10. The degrees of freedom of the SEWGS train model, i.e. the number of variables minus the number of equations must be zero throughout the simulation.
The SEWGS reactor model parameters, as well as system parameters are presented in Table 3-11 and Table 3-12, respectively.

The SEWGS system is designed to treat the feed syngas coming from the coal gasifier in the IGCC with a net electric power output of 352. 74 MWe and net electric efficiency of 36.66%. The SEWGS reactor dimensions are taken from [77], in which the SEWGS process is used to treat the syngas generated in a natural gas-fired power plant with 330 MW power output. It is found that ten trains are sufficient to serve the incoming feed syngas to the SEWGS system. In each train, two reactors always operate in their feed step and produce the H_2-rich product gas.
Cycle time is defined as the duration of one SEWG cycle. The time allocated for the feed step is 25% of the cycle time. The duration of the feed step is estimated based on the incoming CO and CO_2 flow rates through the feed syngas stream to the SEWGS system as well as the CO_2 capture capacity of the adsorbent in the reactor. The feed step duration should be near the breakthrough time to ensure that the H_2 product purity is the maximum. After this time the product purity declines and before this time the full adsorbent capacity will not be employed.

Table 3-11. SEWGS reactor model parameters [56, 77, 78, 86, 111-113]

Parameter	Value	Unit
L	7.4	m
d_t	3.66	m
d_p	4.8×10^{-3}	m
D_{ax}	5.0×10^{-4}	m^2/s
$C_{p,cat.}$	850	$J/(kg_{cat}\,K)$
$C_{p,ads.}$	850	$J/(kg_{ads}\,K)$
ΔH_R	42133	J/mole
$\Delta H_{ads.}$	21004	J/mole
k_g	0.09	J/(mole K)
k_{LDF}	0.05	1/s
T_{wall}	673	K
U	22.4	$W/(m^2\,K)$
ε_b	0.63	m^3 gas in bed/m^3 reactor
ε_t	0.74	m^3 gas /m^3 reactor
μ	2.87×10^{-5}	Pa s
m	0.25	mole/kg
K_C^0	8.66×10^{-6}	1/Pa
K_R^0	4.1×10^{-16}	$1/Pa^{2.5}$
η_i	±1	-
λ_s	1.0	-
a	2.5	-
a_{k_z}	0.5	-
$\rho_{b,\,ads}$	573.5	kg ads./m^3 reactor
$\rho_{b,\,cat}$	166.7	kg cat./ m^3 reactor
u_0	0.075	m/s

Table 3-12. SEWGS system model parameters

Parameter	Value	Unit
Cycle time	695	s
F_c	1×10^{-3}	mole/(s Pa)
T_{Feed}	673	K
$\dot{n}_{Feed}$	210.5	mole/s
S/C	1.91	-

3.2.4. Numerical simulation of the PSA-based SEWGS process

The multi-bed PSA-based SEWGS process mathematical model was implemented in gPROMS, an equation-oriented modeling tool for process simulation, optimization and parameter estimation for steady state and dynamic processes [114]. Switching between the system of equations from one cycle state to those describing the next cycle state is carried out in gPROMS. In any given cycle state, the stream variables which are not used in the equations defining the system state behavior, are assigned arbitrary dummy values. The simulation is defined to start at t=0 seconds, at which the SEWGS system of eight reactors is at the beginning of cycle state one, shown in Fig. 3-4. The operating schedule should then give a procedure to simulate the system for a time period corresponding to the duration of cycle state one (1/16 of the total cycle time). After this time, the system of equations must be switched to describe the behavior in cycle state two. Then simulation of the next time period for the cycle state two (1/16 of the total cycle time) is carried out. This pattern continues until all the 16 cycle states, representing one complete cycle, are simulated. Equations describing the behavior of the SEWGS system over the cycle time are described by partial differential algebraic equations. The axial direction is discretized to 600 elements, using the centered finite difference method (CFDM) of second order. The resulting system of equations is integrated over time by employing DASOLV solver [115]. The time step size is automatically adjusted to maintain the error of integration within the specified tolerance. Multiflash physical property package is used for the calculation of physical properties.

3.2.5. Scheduled operation strategy for SEWGS trains

The simulation of one SEWGS train is carried out and results for the operation of multi-train SEWGS system are obtained. The flow rate of H_2-rich and CO_2-rich product stream, achieved from the simulation of the SEWGS train, is multiplied by the number of trains (ten) to yield the total production rate out of the SEWGS system of ten trains. The H_2-rich stream flow rate is found to undergo a periodic fluctuation of around ±33%, due to using part of the H_2-rich product stream during the re-pressurization step. This is not desired when the SEWGS system is part of a power plant for pre-combustion CO_2 capture and H_2-rich product is used as the GT fuel. The GT requires a smooth fuel heat input (flow rate, composition) at any given load of operation, it is essential to dampen the H_2-rich product flow rate fluctuations as much as necessary. A schedule for the multi-train SEWGS system is developed to initiate the operation of the trains asynchronously and evaluate its impact on improving the H_2-rich product fluctuation. Two different configurations are tested for

the operation of the SEWGS system, as shown in Fig. 3-8. The first configuration divides the system of ten SEWGS trains into five sets of double trains and operates each of the five "double-train" sets one after other with a time lag in between (Fig. 3-8, left). However, the two trains in each "double-train" set operate in parallel. The second configuration allocates two sets of pentuple trains. The two "pentuple-train" sets operate with a time lag between them, while the five trains in each "pentuple-train" set operate simultaneously (Fig. 3-8, right). The time lag between the operations of two "pentuple-train" sets was optimized to be about 10 s, which gives the smoothest H_2 production profile. By using this configuration, fluctuations are reduced to ~±14%, compared to ~±33% in the basic case (ten trains operating in parallel). On the other hand, the minimized fluctuation of the H_2-rich product by using this operation strategy, is achieved at the expense of a decreased overall H_2-rich production rate of around 5.5% on average, which is a disadvantage of such a strategy. By optimizing the time lags, the minimum achievable fluctuation with the five double-train sets was found to be ~±11%. It is compared with the fluctuation of ~±33% in the basic case. The time lags for the operation of five "double-train" sets are about 0s, 9s, 11s, 15s and 18s. Both trains in each set operate in parallel. In contrast, the net H_2-rich stream production rate by using this configuration is decreased about 6.2%.

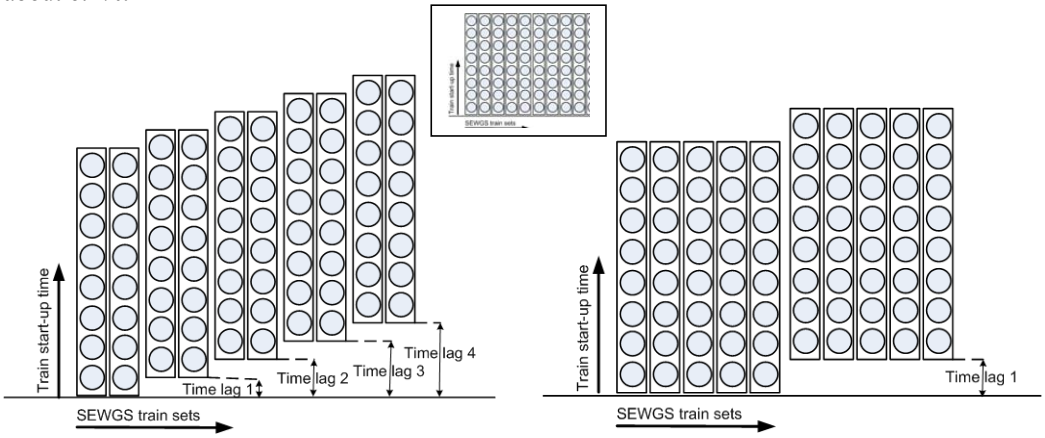

Fig. 3-8. Five double-train sets operate asynchronously with time lags in between (left); Two "pentuple-train" sets operate asynchronously with a time lag between them (right); Basic case: simultaneous operation of the ten SEWGS trains (middle top)

3.3. GT fuel control structure

A closed-loop control strategy including a buffer tank followed by a fuel control valve, between the SEWGS system and the GT is implemented to smooth out the fluctuations in the H_2-rich fuel resulted from the cyclic operation of the PSA-based SEWGS system. The control system is designed to undertake the control of fluctuating H_2-rich fuel stream with respect to mass flow rate as well as pressure and composition before entering the GT. The control system is also designed to control the GT fuel at part-load operations of the IGCC, where the GT fuel mass flow rate is changed following the GT load change. This enables investigation of the load-following capabilities and controllability

of the IGCC integrated with the SEWGS technology at different part-load levels. The logic considered in designing such a control strategy is explained below:

1) The H_2-rich stream mass flow rate is required to be controlled before entering the GT. This is carried out by changing the fuel control valve stem position to correct the mass flow rate and minimize the difference between the desired and measured mass flow rate. Also, to ensure a forward flow of the H_2-rich stream towards the GT at any time of operation, the buffer tank pressure needs to be checked during the operation to be within the SEWGS system and the GT pressures. The buffer tank pressure is measured at the exit of the tank and checked with the desired range. If it is out of the desired range, it is controlled by the feed syngas valve before the SEWGS system (changing the load of the SEWGS system). A pressure relief valve is also assumed for the emergency cases of too high tank pressure. The H_2-rich stream composition is dampened after it leaves the buffer tank.

2) Considering the control objectives explained above, the components of the proposed control strategy are arranged as shown in Fig. 3-9 and explained in the following subsections.

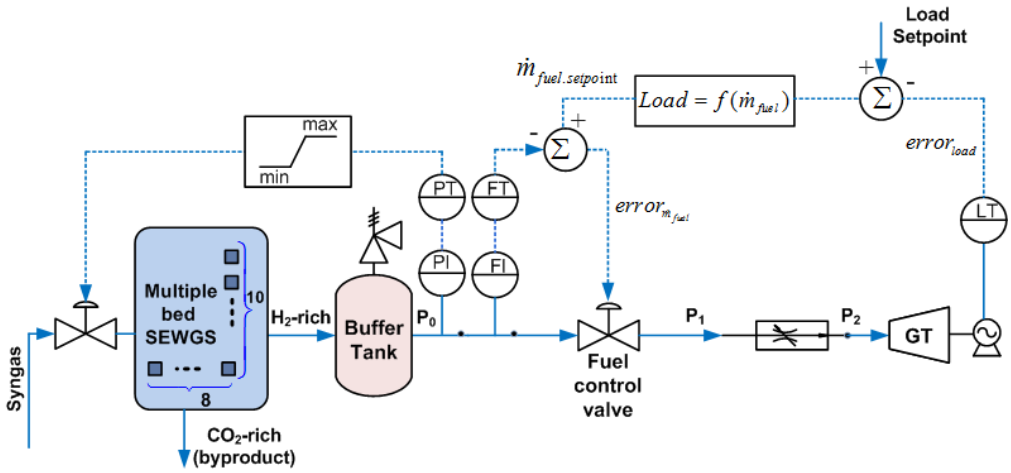

Fig. 3-9. H_2-rich fuel control system

3.3.1. Buffer tank

The H_2-rich stream coming from the SEWGS system has almost constant temperature and pressure (~500ºC, ~27 bar), but the mass flow rate and composition fluctuate over time (~±14% and ~±10%). A buffer tank suppresses a large portion of the H_2-rich mass flow rate fluctuations. It also facilitates mixing of the H_2-rich fuel composition. The H_2-rich stream that leaves the buffer tank has significantly reduced fluctuations and smoothened composition. On the other hand, pressure of this stream is not constant any more due to the pressure build-up associated with the mass flow rate fluctuation of the tank inlet stream, from the SEWGS system. Further control of the buffer tank outlet

stream in terms of pressure and mass flow rate is accomplished by a fuel control valve downstream of the tank (Fig. 3-9).

The buffer tank is a vertical cylindrical vessel. It is designed for the full-load condition of the GT. The assumptions used in the modeling of the tank are:

1) Isothermal process
2) Ideal gas behavior
3) Continuous mixing tank

The material balance around the tank is written:

$$\frac{V_{tank}}{RT}\frac{d(Mw.P_0)}{dt} = \dot{m}_{in,tank} - \dot{m}_{out,tank} \qquad (13)$$

$\dot{m}_{in,tank}$, the buffer tank inlet mass flow rate, is achieved by the simulation of the SEWGS system. R, T and, V_{tank} are the gas constant, temperature and volume of the tank, respectively, Mw is the molecular weight of the gas in the tank and P_0 is the buffer tank pressure.

3.3.2. Fuel control valve

A control valve right after the buffer tank further controls mass flow rate and pressure of the H_2-rich fuel to the GT. The valve upstream pressure is the buffer tank pressure, which is fluctuating. The fuel mass flow rate through the valve, $\dot{m}_{valve}$, is controlled by changing the valve stem position, x_{valve} to correct the deviations of the mass flow rate from its set-point (desired value) and minimize the difference between the desired and measured mass flow rate (error). The set-point for the fuel mass flow rate is determined by the desired GT load. The valve downstream pressure, P_1, is estimated by assuming a choked turbine (refer to section 3.3.3).

The control valve main equation is presented by equation (14). C_v is the valve flow coefficient, defined as the volume flow in cubic meters per second of water at a temperature of between 5° C and 40°C with a pressure drop across the valve of 1 bar, which represents the flow capacity of the valve. At any time of operation, $\dot{m}_{valve}$ and P_1 , are dictated by the GT requirements. Considering the oscillatory nature of P_0, x_{valve} may change rapidly to maintain the desired value of the fuel mass flow rate. Dotted lines in Fig. 3-9 represent the transmission lines that carry the measurement signals from measuring devices to transmitters and controllers.

$$\dot{M}_{valve} = \rho_{gas} C_v x_{valve} \sqrt{P_0 - P_1} \qquad (14)$$

$$\dot{m}_{valve} = \dot{m}_{out,tank} \qquad (15)$$

The controller type utilized in this work is a Proportional Integral (PI) controller [116]. Transfer function of the PI controller is given by equation (16):

$$\frac{OUT(s)}{E(s)} = K_P\left(\frac{1}{1+\tau_I S}\right) \qquad (16)$$

$$E(S) = \dot{m}_{valve} - \dot{m}_{fuel,setpoint} \qquad (17)$$

$$OUT(s) = \Delta x_{valve} \qquad (18)$$

Controller parameters, K_P and τ_I, are proportional and integral gains, respectively. E(s) is the deviation of the fuel mass flow rate from the set-point value. OUT(s) is the change in valve stem position.

Ziegler-Nichols method is used for tuning of the PI controller [117]. The Controller gains were obtained by step responses [118]. From a control theory point of view, the main role of the proportional term in the controller is to establish the stability of the system and improving the transient response, while the most important term, the integrator term makes the steady-state errors vary within negligible values.

Following the closed loop Ziegler-Nichols rule, the controller parameters are found as in Table 3-13, which satisfy a fast dynamic response and acceptable performance characteristics.

Table 3-13. PI controller parameters after tuning

K_p	0.232×10^{-3}
K_i	0.16×10^{-4}

3.3.3. GT performance characteristics

The characteristics of turbines are seldom published by manufacturers. Normally, the only publicly available data for GT performance are for the design point. Therefore, to estimate performance of GTs, models are employed. Such models depend on a point of operation to be known, which is typically the design point. In performance calculation of GTs, the turbine is commonly considered as choked and the so-called choked nozzle equation is used to describe the turbine inlet conditions [119]. Performance at low load conditions is exempted from this rule. Choked condition is referred to a condition which occurs when any further increase in pressure difference over the turbine does not increase the volumetric flow rate. The equation as presented in equation (19) relates turbine inlet pressure, turbine inlet mass flow rate, turbine inlet temperature (TIT) and turbine inlet molecular weight at an actual operating point to those of another operating point [120].

$$\frac{P_{in}}{P_{in,design}} = \frac{\dot{m}}{\dot{m}_{design}} \sqrt{\frac{T_{in}.Mw_{design}}{T_{in,design}.Mw}} \qquad (19)$$

The type of the GT considered is a large scale “F-class”, 50 Hz GT [68, 110]. Main operating parameters and performance of these kinds of turbines are given in Table 3-14. The variable-load operation of the GT is controlled by the fuel flow management. The GT fuel mass flow rate at different loads is estimated using the GTPRO software from Thermoflow [121]. The relation between the load of the GT and fuel mass flow rate is almost linear. The TIT varies according to energy balance of the combustor. The pressure ratio of the GT is varying according to the choked nozzle equation, meaning that turbine inlet pressure depends on TIT, turbine inlet flow rate and turbine inlet molecular weight. Change of the air flow rate using variable guide vanes in the compressor was not considered, but could be considered in future work.

Table 3-14. F-class, 50 Hz, large scale gas turbines, average operating parameters [110]

Pressure ratio: 18.1
Net efficiency= 38.5%
Nominal power output = 279 MW
Natural gas pressure at the combustor inlet: 2.31 MPa (5 bar above the compressor outlet pressure
Specific work (defined as gas turbine output divided by the compressor intake mass flow rate) = 420 kJ/kg
Turbine Outlet Temperature (TOT) = 603 °C

Using a H_2-rich instead of natural gas as the GT fuel, demands some modifications on the design and hardware of a natural gas-based GT, including the combustion system and fuel nozzles. For the purpose of this work the impacts of changing the GT fuel from natural gas to H_2-rich on the design of the GT are neglected. Because the change in transient performance is only slightly influenced by the design and operational modifications, that are necessary with a H_2-rich fuel.

3.3.4. Numerical simulation

The mathematical model of the designed PI-based closed-loop control strategy, including the buffer tank, fuel control valve and the GT were implemented in a common programming platform, Matlab/Simulink®. The outlet of the SEWGS system is interfaced into Matlab/Simulink® to simulate the behavior of the IGCC integrated with the SEWGS technology for CO_2 capture at full-load and different part-load operations. Simulation of the GT in GTPRO, provided required input data such as the fuel mass flow rate variation per load change and TIT to simulate the entire system in Matlab/Simulink®. When the GT load is changed, the feed syngas to the SEWGS system is changed in a way to produce the H_2-rich fuel corresponding to the GT load. Simulation of the SEWGS system at different flow rates of syngas is carried out in gPROMS. The results from the simulations are extracted in excel. In the Simulink, the relevant excel spreadsheets are called, where the SEWGS results are needed as inputs in the calculations, for any particular GT load.

3.4. Approach for investigating load-following capability/controllability of the IGCC with SEWGS

Performance assessment of the IGCC with SEWGS technology at full-load condition is carried out in terms of the designed control system functionality and smooth operation achievability. An IGCC plant generally shows a lower flexibility than the combined cycle or the PC power plants, due to the inertia related to the process units such as gasification, syngas treatment/conditioning and ASU to generate and prepare the fuel at the conditions required by the GT. The process components within the IGCC plant have different response time to the load changes. The GT as a turbo machinery unit operation is a component with fast dynamics. On the other hand, gasification and gas treatment including the SEWGS CO_2 capture process are operating as chemical plants with relatively slow dynamics. This may cause problems for the smooth operation and control of the entire IGCC when a GT load change occurs. The question to be answered is how the process units, mainly the gasification

and SEWGS, impact the flexibility of the IGCC at part-load? Simulation of the SEWGS process based on the developed mathematical model at different inlet conditions provides understanding about the dynamic characteristic of this system. For the gasification process, the typical gasification load gradient of 3% is assumed in this work [122].

Part-load performance simulations enable to investigate the capability of the control system to control the GT fuel at different part loads. Also, load-following performance of the IGCC taking into account the limited load gradient of the gasifier and SEWGS units compared to the GT is addressed. The improved operation flexibility of the GT as a result of including an intermediate buffer tank before the GT is also evaluated.

To investigate part-load operations, four different case studies introducing various load change strategies for the GT and gasifier are evaluated, as shown schematically in Fig. 3-10. In the first case, the GT load changes (stepwise), without making any change in the upstream components (gasification, SEWGS). This is to investigate improved operation flexibilities of the GT when introducing an intermediate buffer tank between the SEWGS system and the GT. The capability of the introduced control strategy to respond to the GT load changes is revealed as well. In the second case, the GT load changes to a level that corresponding changes in the upstream components (gasification, SEWGS) are also required. It is assumed that the upstream components respond instantaneously to the GT load changes. This is to examine the feasibility of the operation of the IGCC integrated with the SEWGS technology at part-loads in the absence of the time delays associated with the transient response of the components to the load changes. The third case takes into account the transient response of the GT upstream components. This case is studied to observe how the slowness of the GT upstream components impacts the operation of the entire IGCC with CO_2 capture, when the GT load is changed. Finally, in the fourth case, the investigation is about the part-load conditions, where priorly planned GT and gasification load changes are applied. This is in contrast with the second and third cases, where the GT load changes are unplanned events (disturbances) and the gasification load change occurs once the disturbance is imposed on the GT load. In the fourth case, the gasifier load change does not necessarily take place at the same time with the GT load change. It can be initiated prior to the planned GT load change occurrence time. Due to the different load gradients of the gasifier, SEWGS and GT, this case can further improve load following performance of the IGCC integrated with the SEWGS technology.

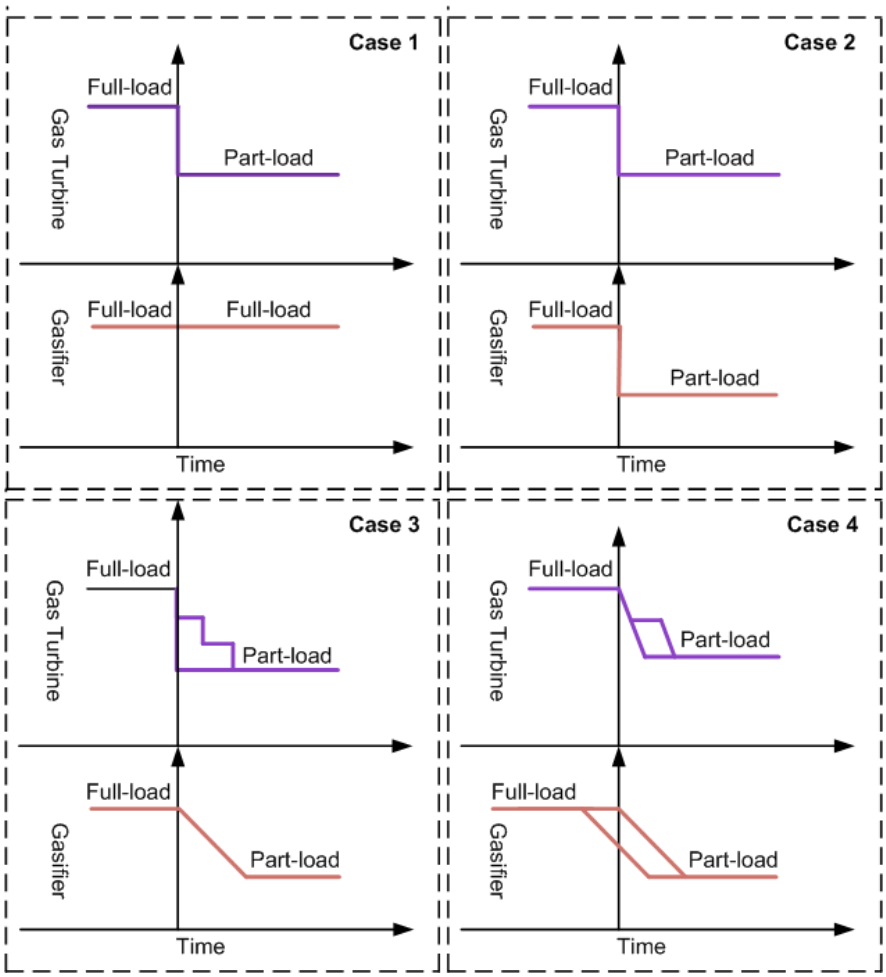

Fig. 3-10. Four case studies for part-load operation

Chapter 4

4. Conclusions and Recommendations for future work

4.1. Conclusions

4.1.1. The SEWGS system

The Sorption Enhanced Water Gas Shift (SEWGS) system is a pre-combustion CO_2 capture process to remove carbon content of feed syngas coming from a coal gasifier in an Integrated Gasification Combined Cycle (IGCC) [68]. The operating conditions of the system are similar with those of the IGCC power plant. The objective is to produce a H_2-rich fuel for a Gas Turbine (GT) within the IGCC power plant, as well as sufficient performance of the SEWGS system in terms of the CO_2 recovery rate and purity. The SEWGS system operates based on a Pressure Swing Adsorption (PSA) process, consisting of eleven steps. The PSA processing steps are feed, rinse, three pressure equalization, depressurization, purge and repressurization steps. During the feed step, the Water Gas Shift (WGS) reaction and CO_2 adsorption take place simultaneously. High pressure steam is used during the feed step, to be mixed with feed syngas, as well as during the rinse step to counter-currently withdraw residual gases left in the reactor after the feed step and recycle them as feed to another reactor. Low pressure steam is used during the purge step to increase recovery of the adsorbed CO_2. The SEWGS system is a multi-train system, where each train consists of eight reactors working in parallel and going through the PSA cycle steps. The reactors are packed with a mixture of the WGS reaction catalyst and CO_2 adsorbent. A K_2CO_3-promoted HTC is selected and assumed as the CO_2 adsorbent material in this work.

Dynamic performance simulations of the SEWGS, based on the developed mathematical model, and the results on operating characteristics of the process are presented and discussed in papers 1 and 2 (Appendix). The main conclusions are:

- The SEWGS system performance shows the equilibrium WGS reaction is shifted towards higher conversions of CO into CO_2 and H_2-rich fuel gas is produced. Also, CO_2 is captured and taken out of the system in a separate stream containing mostly CO_2 and steam. The performance of the system is characterized by CO_2 recovery and CO_2 purity as well as the H_2 purity. The designed SEWGS system gives a CO_2 recovery rate of 95%, with around 99% purity of the recovered CO_2. The H_2-rich product purity achieved is around 81%. It is seen that using rinse and purge steam improves the performance of the system towards higher purity and recovery rates.

- Using three successive pressure equalization steps (after the rinse step is completed at feed pressure), allows for partial reduction of the pressure in the reactor through three steps of pressure equalization from 27 bar down to about 20 bar, 14 bar and 7 bar in sequence. Each pressure reduction step is carried out by connecting the reactor to another reactor with a lower pressure level. When the pressure difference between the two reactors is balanced, the next pressure reduction step starts. The last pressure reduction level from about 7 bar down to 1 bar is related to the depressurization step. Finally, the pressure reaches its minimum level of 1 bar

at the start of purge step. During the three pressure reduction steps, CO_2 desorption starts to take place and adsorbent loading drops moderately. The major part of the CO_2 desorption, however, takes place during the depressurization and purge step, where a sharp desorption front is detected. The recovered CO_2 is discharged from the feed end of the reactor during these two steps.

- The amount of steam used for the rinse step is not required to be as large as being able to withdraw the residual gases from the reactor entirely. Further removal of the residual gases takes place counter-currently from the feed end of the reactor during the three pressure equalization steps. After the third pressure equalization step, the residual gases are mainly transferred to the other connected reactors. The purity of the CO_2 stream, to be released in the gas phase is therefore increased. This is one benefit of adding the pressure equalization steps in reducing the rinse steam consumption. Moreover, kinetics of the adsorbent have a great impact on the amount of the purge steam required. There is still uncertainty about the adsorption and desorption kinetics of K_2CO_3-promoted HTC adsorbents [113]. But it is evident that with decreasing the desorption coefficient, the purge steam requirements will increase.

- Changing the flow rate of the rinse and purge steam affects the performance of the system in terms of the CO_2 purity and recovery. However, the H_2-rich product purity is less sensitive to changes in flow rate of rinse and purge steam.

- Identifying dynamic characteristic of the integrated SEWGS system in responding to load changes is of great importance for part-load operation of the power plant. Simulations of the SEWGS system at different loads of the feed syngas are carried out. To maintain the CO_2 recovery and purity of the design case the target performance, duration of the feed step and thus the cycle time should be varied, in addition to changing the rinse and purge steam flow rates.

- The temperature at the entry zone of the reactor is about 200 °C higher than the feed temperature of 400 °C because of the slightly exothermic WGS reaction and CO_2 adsorption during the feed step. Moving forward along the reactor, a temperature reduction is observed and close to the exit of the reactor, the temperature is almost equal to the feed temperature. Formation of the hot spots in the beginning of the reactor might not be in favor of the catalyst and CO_2 adsorbent material. The maximum temperature rise in the reactor when using a shifted syngas as the feed to the reactor (assuming a pre-shift reactor upstream of the SEWGS process), was calculated. Doing so, the maximum temperature rise in the reactor was found to be about 30 °C. In this case, however, less mass of catalyst in the reactor is required or the catalyst can be eliminated, depending on the CO content in the shifted syngas or catalytic properties of the adsorbent.

- The H_2-rich product stream flow rate was found to undergo periodic fluctuations of around ±33%, associated with using part of the H_2-rich stream for repressurization step. Due to the requirements of the GT to have a smooth fuel heat input at any given load of operation, it is essential to dampen the H_2-rich product flow rate fluctuations to an acceptable level. The approach of scheduled SEWGS trains operation, by incorporating time lags between the operations of trains is successful in achieving partly dampened H_2-rich product flow rate

fluctuations. Using two different operation schemes, the fluctuations of the H_2-rich stream flow rate are decreased from ±33% to ~±14% and ~±11% in the first and second case, respectively. However, the minimized fluctuation, is achieved at the expense of a decrease in the overall H_2-rich production rate of about 5.5% and 6.2% on average, respectively.

- SEWGS process performance changes at different flow rates of the feed syngas, when the cycle time is kept unchanged. For instance, at 80% load of the syngas, the CO_2 recovery was decreased on average about 4.5%, compared to the design case. CO_2 purity, on the other hand, decreased about 2%.

4.1.2. IGCC integrated with the SEWGS system

Full-load and part-load performance assessment of the IGCC power plant incorporating the SEWGS pre-combustion CO_2 capture technology were investigated. The control strategy consisting of a buffer tank followed by a control valve is implemented to control the H_2-rich fuel, with respect to mass flow rate as well as pressure and composition, complying with the requirements of the GT. The dynamics of the SEWGS achieved from the previous step (4.1.1) is used in part-load performance investigations of the IGCC integrated with the SEWGS. The results obtained from the full-load and different part-load simulations are presented and discussed in papers 3 and 4 (Appendix).

The main conclusions from this part are:

- Simulation of the IGCC with SEWGS at full-load reveals the designed fuel control strategy performs properly and the fuel mass flow rate approaches the set-point after steady-state is reached. The flow rate fluctuation is dampened from ~±14% to 1-2%. Moreover, the buffer tank pressure variations fall within the acceptable range, ensuring sufficient flow rate and pressure of the H_2-rich fuel to the GT. Also the oscillating fuel composition from the SEWGS system (~±10%) is smoothened sufficiently at the exit of the buffer tank.

- The SEWGS system possesses the slowest transient dynamics compared to the gasifier. When a load change is imposed to the GT, operation of the entire IGCC plant is dictated by the rate of change of the SEWGS system. This is revealed from the simulation of the SEWGS at different loads of the feed syngas and compared with the typical load gradient of the gasifier used in this work.

- Using the intermediate buffer tank between the SEWGS and GT, as part of the fuel control system, improves the operation flexibility of the GT. The length of the time that the GT can operate at part-load without the need to make any change in the upstream components is an indicator of the improved operation flexibility of the GT at part-load condition. Also, when different disturbances in the GT load are applied, the fuel control system functions properly and provides the corresponding GT fuel flow rate after a new steady-state is reached.

- Different part-load operation strategies such as priorly planned GT load and gasifier load change occurrence time (vs. sudden GT load change) can be considered to minimize the flow rate imbalances during the transient state of the IGCC plant, as a result of different transient dynamics of the gasifier, SEWGS and the GT. Depending on the time allowed between the gasifier and the GT load change occurrence, it is possible to achieve a smooth operation of the

IGCC with the SEWGS, while mass flow rate is also controlled properly. It was found that the CO_2 capture process together with the gasification process can follow different GT load changes, when the part-load operation schedule of the gasifier and GT is planned. Also, the multiple-ramp plus waiting time strategy for the GT load change appears as an effective strategy to maintain the smooth operation of the plant when the GT load is changed either unplanned (disturbance) or planned.

4.2. Recommendations for future work

- One important step in designing a SEWGS PSA-based process is to choose an adsorbent material. A wide range of potential adsorbent materials and various possibilities of combining different materials to improve their adsorption characteristics demand a large number of experimental work. This is a key step as the adsorbent significantly affects the performance of the process in terms of carbon capture efficiency, cycle time, size and number of vessels. K_2CO_3-promoted HTC materials have been recognized as the most suitable CO_2 adsorbents in many of the relevant works in literature for the SEWGS application. However, they are still not fully characterized. Also, the effect of presence of steam and different steam partial pressures on CO_2 capture capacity, selectivity and mechanism has not been fully addressed yet. Different preparation methods and combinations of the HTC-based materials may result in different properties with respect to CO_2 adsorption. Further experimental work is therefore required on development of adsorbent materials and characterizing their performance under the condition of the SEWGS process to make sure adsorbent data, isotherm and kinetic models used for the design of the SEWGS are representing real properties of these adsorbents. Moreover, newly development HTC-based materials, with the capability of H_2S adsorption along with the CO_2, may provide the opportunity to employ sour SEWGS process and perform a combined H_2S/CO_2 removal in the SEWGS system.

- Recent literature reports on development of novel HTC-based materials with catalytic properties. This should be investigated in future. Use of such adsorbents may decrease the amount of the catalyst required. This will affect the design of the SEWGS system. Moreover, a pre-shift reactor, before the SEWGS process can be considered. This option will reduce the catalyst required for the SEWGS process. It will therefore, reduce the size of the SEWGS reactors. Also, it ensures that the temperature rise in the reactor will be within the thermal stability of the adsorbent and catalyst.

- Developing a heterogeneous reactor model to predict the behavior of the solid phase, i.e. adsorbent and catalyst. This will help for instance to investigate temperature variation inside the adsorbent and catalyst and see if this is within their thermal stability range.

- It will be worthwhile to optimize the SEWGS process. A large number of parameters and variables are involved in the design and modeling of the SEWGS process including but not limited to; feed gas condition (temperature, pressure, composition, flow rate), regeneration pressure, rinse and purge steam flow rate, steam to carbon ratio in the feed syngas, number of equalization steps, cycle operation scheme, cycle time, reactor size and number of reactors. Different combination of them may result in different performance of the system. Therefore, finding an optimum configuration of the system, which fulfills the objectives such as CO_2 capture ratio and purity are very important. However, the computational time required to evaluate each option is significant.

- An option of using (off-line) H_2-rich storage tank can be investigated. This allows for the GT upstream components such as gasification and SEWGS capture process to operate at full load (design point), while changing the GT load for variable power demands from the combined cycle. In this case, there would not be any concern about the load-following capability of the GT upstream components (compared to the relatively fast ramp rates of the GT). The stored H_2-rich can be used to generate electricity at peak times or in other industrial applications.

- Changes in the GT air flow rate, by using inlet guide vanes can be considered, when the GT load and consequently the fuel flow rate is changed. Also the effect of burning a H_2-rich fuel on the GT design should be investigated.

- Including the steam cycle in the computational model to further investigate the impact of steam consumption by the SEWGS process on the power penalty of the steam cycle. Also thermal integration between the IGCC and SEWGS process can be investigated.

- Further studies on reliability as well as cost estimations, when dealing with a complex system such as IGCC with SEWGS power production plant.

References

[1] Gale, J., Bradshaw, J., Chen, Z., Garg, A., Gomez, D., Rogner, H. H., Simbeck, D., Williams, R., 2005. IPCC Special Report on Carbon dioxide Capture and Storage, Cambridge.

[2] Figueroa, J. D., Fout, T., Plasynski, S., McIlvried, H., Srivastava, R. D., 2007. Advances in CO_2 capture technology-The U.S. Department of Energy's Carbon Sequestration Program. International Journal of Greenhouse Gas Control 1, 37–46.

[3] World Energy Outlook, 2011. http://www.worldenergyoutlook.org/.

[4] Chu, S., Majumdar, A., 2012. Opportunities and challenges for a sustainable energy future. Nature 488, 294–303.

[5] Pires, J. C. M., Martins, F. G., Alvim-Ferraz, M. C. M., Simões, M., 2011. Recent developments on carbon capture and storage: An overview. Chem. Eng. Res. Des. 89, 1446–1460.

[6] Kohl, A., Nielsen, R., 2005. Gas Purification, 5th ed. Gulf Publishing Company, Houston.

[7] Samanta, A., Zhao, A., Shimizu, G. K. H., Sarkar, P., Gupta, R., 2012. Post-Combustion CO2 Capture Using Solid Sorbents: A Review. Ind. Eng. Chem. Res. 51, 1438–1463.

[8] Kanniche, M., Gros-Bonnivard, R., Jaud, Ph., Valle-Marcos, J., Amann, J. M., Bouallou, Ch., 2010. Pre-combustion, post-combustion and oxy-combustion in thermal power plant for CO2 capture. Applied Thermal Engineering 30, 53–62.

[9] Metz, B., Davidson, O., de Coninck, H., Loos, M., Meyer, L., 2005. IPCC, Special report on carbon capture and storage. Working group III of the Intergovernmental Panel on Climate Change, Cambridge, UK.

[10] Lackner, K.S., Brennan, S., 2009. Envisioning carbon capture and storage: expanded possibilities due to air capture, leakage insurance, and C-14 monitoring. Clim. Change 96, 357–378.

[11] Lee, Zh. H., Lee, K. T., Bhatia, S., Mohamed, A. R., 2012. Post-combustion carbon dioxide capture: Evolution towards utilization of Nanomaterials. Renewable and Sustainable Energy Reviews 16, 2599–2609.

[12] Padurean, A., Cormos, C. C., Agachi, P. S., 2012. Pre-combustion carbon dioxide capture by gas–liquid absorption for Integrated Gasification Combined Cycle power plants. International Journal of Greenhouse Gas Control 7, 1–11.

[13] Aydin, G., Karakurt, I., Aydiner, K., 2010. Evaluation of geologic storage options of CO_2: Applicability, cost, storage capacity and safety. Energy Policy 38, 5072–5080.

[14] Dave, A. D., Rezvani, S., Huang, Y., McIlveen-Wright, D., Hewitt, N., 2012. Integration and performance assessment of hydrogen fired combined cycle power plant with PSA process for CO_2 capture in pre-combustion IGCC power plant. Proceedings of the ASME Gas Turbine India Conference, Mumbai, Maharashtra, India.

[15] Chue, K. T., Kim, J. N., Yoo, Y. J., Cho, S. H., Yang, R. T., 1995. Comparison of activated carbon and zeolite 13X for CO_2 recovery from flue gas by pressure swing adsorption. Ind. Eng. Chem. Res. 34, 591–598.

[16] Wang, Q., Luo, J., Zhong Z., Borgna, A., 2011. CO_2 capture by solid adsorbents and their applications: current status and new trends. Energy Environ. Sci. 4, 42–55.

[17] Yang, H., Xu, Zh., Fan, M., Gupta, R., Slimane, R. B., Bland, A. E., Wright, I., 2008. Progress in carbon dioxide separation and capture: A review. Journal of Environmental Sciences 20, 14–27.

[18] Leung, D. Y. C., Caramanna, G., Maroto-Valer, M. M., 2014. An overview of current status of carbon dioxide capture and storage technologies, Renewable and Sustainable Energy Reviews 39, 426–443.

[19] Ghougassiana, P. G., Lopez, J. A. P., Manousiouthakis, V. I., Smirniotis, P., 2014. CO_2 capturing from power plant flue gases: Energetic comparison of amine absorption with MgO based, heat integrated, pressure–temperature-swing adsorption, International Journal of Greenhouse Gas Control 22, 256–271.

[20] Kenarsari, S. D., Yang, D., Jiang, G., Zhang, S., Wang, J., Russell, A. G., Wei Q., Fan, M., 2013. Review of recent advances in carbon dioxide separation and capture. RSC Adv., 3, 22739–22773.

[21] Field, R. P., Brasington, R., 2011. Baseline Flowsheet Model for IGCC with Carbon Capture. Ind. Eng. Chem. Res. 50, 11306–11312.

[22] Feron, P. H. M., Hendriks, C.A., 2005. CO_2 Capture Process Principles and Costs. Oil & Gas Science and Technology – Rev. IFP, 60, 451-459.

[23] García, S., Gil, M.V., Martín, C.F., Pis, J.J., Rubiera, F., Pevida, C., 2011. Breakthrough adsorption study of a commercial activated carbon for Pre-combustion CO_2 capture. Chemical Engineering Journal 171, 549–556.

[24] Ebner, A. D., Ritter, J. A., 2009. State-of-the-Art Adsorption and Membrane Separation Processes for Carbon Dioxide Production from Carbon Dioxide Emitting Industries. Separation Science and Technology 44, 1273–1421.

[25] Choi, S., Drese, J.H., Jones, C.W., 2009. Adsorbent materials for carbon dioxide capture from large anthropogenic point sources. ChemSusChem 2, 796–854.

[26] Casas, N., Schell, J., Blom, R., Mazzotti, M., 2013. MOF and UiO-67/MCM-41 adsorbents for pre-combustion CO2 capture by PSA: Breakthrough experiments and process design. Separation and Purification Technology 112, 34–48.

[27] Schell, J., Casas, N., Blom, R., Spjelkavik, I., Andersen, A., Hafizovic Cavka, J., Mazzotti, M., 2012. MCM-41, MOF and UiO-67/MCM-41 adsorbents for pre-combustion CO2 capture by PSA: adsorption equilibria. Adsorption 18, 213–227.

[28] Cormos, C. C., 2012. Integrated assessment of IGCC power generation technology with carbon capture and storage (CCS). Energy 42, 434-445.

[29] Higman, C., Van Der Burgt, M., 2008. Gasification. 2nd ed. Burlington: Gulf Professional Publishing, Elsevier Science.

[30] Cormos, C. C., 2009. Assessment of hydrogen and electricity co-production schemes based on gasification process with carbon capture and storage. Int J Hydrogen Energy 34, 6065-6077.

[31] Wall, T. F., 2007. Combustion processes for carbon capture. Proceedings of the Combustion Institute 31, 31–47.

[32] Damen, K., van Troost, M., Faaij, A., Turkenburg, W., 2006. A comparison of electricity and hydrogen production systems with CO2 capture and storage. Part A: Review and selection of promising conversion and capture technologies. Progress in Energy and Combustion Science 32, 215–246.

[33] Eide L.I., Bailey, D.W., 2005. Precombustion Decarbonisation Processes. Oil & Gas Science and Technology – Rev. IFP, 60, 475-484.

[34] Potential for improvement in gasification combined cycle power generation with CO_2 capture. International Energy Agency (IEA), Greenhouse Gas R&D Programme (GHG); 2003. Report PH4/19.

[35] Kanniche, M., Bouallou, Ch., 2007. CO_2 capture study in advanced integrated gasification combined cycle. Applied Thermal Engineering 27, 2693–2702.

[36] Cormos, C. C., Starr, F., Tzimas, E., 2010.Use of lower grade coals in IGCC plants with carbon capture for the co-production of hydrogen and electricity. International journal of hydrogen energy 35, 556–567.

[37] Liu, Z., Green, W. H., 2014. Analysis of Adsorbent-Based Warm CO2 Capture Technology for Integrated Gasification Combined Cycle (IGCC) Power Plants. Ind. Eng. Chem. Res. 53, 11145−11158.

[38] Webley, Paul A., 2014. Adsorption technology for CO_2 separation and capture: a perspective. Adsorption 20, 225–231.

[39] Boot-Handford, M. E., Abanades, J. C., Anthony, E. J., Blunt, M. J., et al., 2014. Carbon capture and storage update. Energy Environ. Sci. 7, 130–189.

[40] Martín, C.F., Plaza, M.G., García, S., Pis, J.J., Rubiera, F., Pevida, C., 2011. Microporous phenol formaldehyde resin based adsorbents for pre-combustion CO2 capture. Fuel 90, 2064–2072.

[41] Chen, Zh., Deng, Sh., Wei, H., Wang, B., Huang, J., Yu, G., 2013. Activated carbons and amine-modified materials for carbon dioxide capture — a review. Front. Environ. Sci. Eng. 7, 326–340.

[42] Ko, D., Siriwardane, R., T. Biegler, L., 2003. Optimization of a Pressure-Swing Adsorption Process Using Zeolite 13X for CO_2 Sequestration", Ind. Eng. Chem. Res. 42, 339-348.

[43] Brandani, F., M. Ruthven, D., 2004. The Effect of Water on the Adsorption of CO2 and C3H8 on Type X Zeolites. Ind. Eng. Chem. Res. 43, 8339-8344.

[44] Inui, T., Okugawa, Y., Yasuda, M., 1988. Relationship between Properties of Various Zeolites and Their CO_2-Adsorption Behaviors in Pressure Swing Adsorption Operation. Ind. Eng. Chem. Res. 27, 1103-1109.

[45] Zhao, Ch., Chen, X., Zhao, Ch., 2010. Study on CO_2 capture using dry potassium-based sorbents through orthogonal test method. International Journal of Greenhouse Gas Control 4, 655–658.

[46] Yi, C.K., Jo, S. h., Seo, Y., Lee, J.B., Ryu, C.K., 2007. Continuous operation of the potassium-based dry sorbent CO_2 capture process with two fluidized-bed reactors. International Journal of Greenhouse Gas Control 1, 31–36.

[47] Cavani, F., Trifirb, F., Vaccari, A., 1991. Hydrotalcite-type Anionic clays: preparation, properties and applications. Catalysis Today 11, 173-301.

[48] Ram Reddy, M. K., Xu, Z. P., Lu, G. Q. (Max) and Diniz da Costa, J. C. 2008. Effect of SOx Adsorption on Layered Double Hydroxides for CO_2 Capture. Ind. Eng. Chem. Res. 47, 7357–7360.

[49] Oliveira, E. L. G., Grande, C. A., Rodrigues, A. E., 2008. CO_2 sorption on hydrotalcite and alkali-modified (K and Cs) hydrotalcites at high temperatures. Separation and Purification Technology 62, 137–147.

[50] Walspurger, S., Boels, L., Cobden, P.D., Elzinga, G.D., Haije, W.G., Van Den Brink, R.W., 2008. The crucial role of the K+-aluminium oxide interaction in K+-promoted alumina- and hydrotalcite-based materials for CO_2 sorption at high temperatures. ChemSusChem 1, 643.

[51] Florin, N. H., Harris, A. T., 2009. Reactivity of CaO derived from nano-sized CaCO3 particles through multiple CO2 capture-and-release cycles. Chemical Engineering Science 64, 187–191.

[52] Lu, H., Khan, A., Pratsinis, S. E., Smirniotis, P. G., 2009. Flame-Made Durable Doped-CaO Nanosorbents for CO2 Capture. Energy & Fuels 23, 1093–1100.

[53] Halabi, M.H., de Croon, M.H.J.M., van der Schaaf, J., et al., 2012. High capacity potassium-promoted hydrotalcite for CO_2 capture in H_2 production. international journal of hydrogen energy 37, 4516- 4525.

[54] Sun, P., Lim, C. J., Grace, J. R., 2008. Cyclic CO_2 Capture by Limestone Derived Sorbent During Prolonged Calcination/Carbonation Cycling. AIChE J 54, 1668-1677

[55] Grasa, G.S., Abanades, J.C., 2006. CO_2 capture capacity of CaO in long series of carbonation/calcination cycles. Ind Eng Chem Res 45, 8846-8851.

[56] Ding, Y., Alpay, E., 2000. Equilibria and kinetics of CO_2 adsorption on hydrotalcite adsorbent. Chemical Engineering Science 55, 3461–3474.

[57] Lee, K.B., Verdooren, A., Caram, H.S., and Sircar, S., 2007. Chemisorption of carbon dioxide on potassium carbonate-promoted hydrotalcite. Journal of colloid and interface science 308, 30–39.

[58] Ding, Y., and Alpay, E., 2000. Adsorption-enhanced steam methane reforming. Chemical Engineering Science 55, 3929-3940.

[59] Waldron, W. E., Hufton, J. R., Sircar, S., 2001. Production of hydrogen by cyclic sorption enhanced reaction process. AIChE Journal 47, 1477–1479.

[60] Xiu, G., Li, P., and Rodrigues, A.E., 2002. Sorption-enhanced reaction process with reactive regeneration. Chemical engineering science, 57, 3893–3908.

[61] Skarstrom C. W, 1960. Method and Apparatus for Fractionating Gaseous Mixtures by Adsorption. U S Patent 2,944,627 to Exxon Research and Engineering, July 12.

[62] Schell, J., Casas, N., Mazzotti, M., 2009. Pre-combustion CO_2 capture for IGCC plants by an adsorption process. Energy Procedia 1, 655–660.

[63] Casas, N., Schell, J., Joss, L., Mazzotti, M., 2013. A parametric study of a PSA process for pre-combustion CO2 capture. Separation and Purification Technology 104, 183–192.

[64] Park, J. H., Kim, J. N., Cho, S. H., 2000. Performance analysis of four-bed H2 PSA process using layered beds. AIChE Journal, 46, 790-802.

[65] Schell, J., Casas, N., Marx, D., Mazzotti, M., 2013. Pre-combustion CO_2 Capture by Pressure Swing Adsorption (PSA): Comparison of Laboratory PSA Experiments and Simulations. Ind. Eng. Chem. Res. 52, 8311−8322.

[66] Diagne, D., Goto, M., Hirose, T., 1994. New PSA process with intermediate feed inlet position operated with dual refluxes: application to carbon dioxide removal and enrichment. J. Chem. Eng. Jpn. 27, 85-89.

[67] Van Dijk, H.A.J., Walspurger, S., Cobden, P.D., van den Brink, R.W., de Vos, F.G., 2011. Testing of hydrotalcite-based sorbents for CO2 and H2S capture for use in sorption enhanced water gas shift. International Journal of Greenhouse Gas Control 5, 505-511.

[68] Franco, F., Anantharaman, R., Bolland, O., Booth, N., van Dorst, E., Ekstrom, C., Sanchez, E., Macchi, E., Manzolini, G., Prins, M., Pfeffer, A., Rezvani, S., Robinson, L., Zahra, A.M., 2010.

Common framework and test cases for transparent and comparable techno-economic evaluations of CO_2 capture technologies - the work of the European Benchmarking Task Force. Proceedings of GHGT-10, Amsterdam, NL.

[69] Hufton, J.R., Mayorga, S., Sircar, S., 1999. Sorption-enhanced reaction process for hydrogen production. Separations 45, 248–256.

[70] Carvill, B.T., Hufton, J.R., Anand, M., Sircar, S., 1996. Sorption-enhanced reaction process. AIChE J., 42, 2765–2772.

[71] Hufton, J.R., Mayorga, S., Sircar, S., 1999. Sorption-enhanced reaction process for hydrogen production. AIChE J., 45, 248–256.

[72] Sircar, S., Hufton, J.R., Nataraj, S., 2000. Process and apparatus for the production of hydrogen by steam reforming of hydrocarbon. U.S. Patent, NO. 6103143.

[73] Barelli, L., Bidini, G., Gallorini, F., Servili, S., 2008. Hydrogen production through sorption-enhanced steam methane reforming and membrane technology: A review. Energy 33, 554–570.

[74] Reijers, H.T.J., Valster-Schiermeier, S.E.A., Cobden, P. D., van den Brink, R. W., 2006. Hydrotalcite as CO_2 Sorbent for Sorption-Enhanced Steam Reforming of Methane. Ind. Eng. Chem. Res. 45, 2522-2530.

[75] Solieman, A.A.A., Dijkstra, J.W., Haije, W.G., Cobden, P.D., van den Brink, R.W., 2009. Calcium oxide for CO2 capture: Operational window and efficiency penalty in sorption-enhanced steam methane reforming. International Journal of Greenhouse Gas Control 3, 393–400.

[76] Manzolini, G., Macchi, E., Binotti, M., Gazzani, M., 2011. Integration of SEWGS for carbon capture in natural gas combined cycle. Part A: Thermodynamic performances. International Journal of Greenhouse Gas Control 5, 200–213.

[77] Wright, A., White, V., et.al., 2009. Reduction in the cost of pre-combustion CO_2 capture through advancements in sorption-enhanced water-gas-shift. Energy Procedia 1, 707–714.

[78] Allam, R.J., Chiang, R., Hufton, J.R., Middleton, P., Weist, E., White, V., 2005. Development of sorption enhanced water gas shift process. In: Thomas, D., Benson, S. (Eds.), Carbon Dioxide Capture for Storage in Deep Geologic Formations. 1, 227–256.

[79] Gazzani, M., Macchi, E., Manzolini, G., 2011. CAESAR: SEWGS integration into an IGCC plant. Energy Procedia 4, 1096–1103.

[80] Gazzani, M., Macchi, E., Manzolini, G., 2013. CO2 capture in integrated gasification combined cycle with SEWGS – Part A: Thermodynamic performances. Fuel 105, 206–219.

[81] Manzolini, G., Macchi, E., Gazzani, M., 2013. CO_2 capture in natural gas combined cycle with SEWGS. Part B: Economic assessment. International Journal of Greenhouse Gas Control 12, 502–509.

[82] Choi, Y., Stenger, H.G., 2003. Water gas shift reaction kinetics and reactor modeling for fuel cell grade hydrogen. J. Power Sources 124, 432–439.

[83] Wright, A.D., White, V., Hufton, J.R., Quinn, R., Cobden, P.D., van Selow, E.R., 2011. CAESAR: Development of a SEWGS model for IGCC. Energy Procedia 4, 1147–1154.

[84] Caesar FP7 Project, 2008. http://caesar.ecn.nl.

[85] Carbon Capture Project, http://www.co2captureproject.org/ccp2 capture.html.

[86] van Selow, E. R., Cobden, P. D., et.al., 2009. Carbon Capture by Sorption-Enhanced Water-Gas Shift Reaction Process using Hydrotalcite-Based Material. Ind. Eng. Chem. Res. 48, 4184–4193.

[87] Beavis, R., 2011. The EU FP6 Project CACHET - Final Results. Energy Procedia 4, 1074–1081.

[88] Decarbit FP7 Project, 2008. http://www.sintef.no/Projectweb/DECARBit/.

[89] Cesar FP7 Project, 2008, http://www.co2cesar.eu/.

[90] Bakken, E., Cobden, P. D., Henriksen, P. P., Håkonsen, S. F., Spjelkavik, A. I., Stange, M., et al., 2010. Development of CO_2 sorbents for the SEWGS process using high throughput techniques. Proc. GHGT-10, Amsterdam.

[91] Van Selow, E. R., Cobden, P. D., Wright, A. D., Van Den Brink, R. W., Jansen, D., 2010. Improved sorbent for the sorption-enhanced water-gas shift process. Proc. GHGT-10, Amsterdam.

[92] E.R. van Selow, P.D. Cobden, R.W. van den Brink, J.R. Hufton, A. Wright, 2009. Performance of sorption-enhanced water-gas shift as a pre-combustion CO2 capture technology. Energy Procedia 1, 689-696.

[93] Jansen, D., van Selow, E.R., Cobden, P.D., et.al., 2013. SEWGS technology is now ready for scale-up. Energy Procedia 37, 2265– 2273.

[94] Ebner, A. D., Reynolds, S. P., Ritter, J. A., 2007. Nonequilibrium Kinetic Model That Describes the Reversible Adsorption and Desorption Behavior of CO2 in a K-Promoted Hydrotalcite-like Compound. Ind. Eng. Chem. Res. 46, 1737-1744.

[95] Marono, M., Torreiro, Y., Gutierrez, L., 2013. Influence of steam partial pressures in the CO_2 capture capacity of K-doped hydrotalcite-based sorbents for their application to SEWGS processes. International Journal of Greenhouse Gas Control 14, 183–192.

[96] Hutson, N.D., Attwood, B.C., 2008. High temperature adsorption of CO_2 on various hydrotalcite-like compounds. Adsorption 14, 781-789.

[97] Leon, M., Diaz, E., et al., 2010. Adsorption of CO_2 on Hydrotalcite-Derived Mixed Oxides: Sorption Mechanisms and Consequences for Adsorption Irreversibility. Ind. Eng. Chem. Res. 49, 3663–3671.

[98] Ram Reddy, M. K., Xu, Z. P., Lu, G. Q (Max), Diniz da Costa, J. C., 2008. Influence of Water on High-Temperature CO_2 Capture Using Layered Double Hydroxide Derivatives", Ind. Eng. Chem. Res. 47, 2630-2635.

[99] Pavel, O.D., Birjega, R., Angelescu, E., Zavoianu, R., Florea, M., Mitran, G., 2010. Modifications of the Catalytic Activity for Cyanoethylation Induced by the Memory Effect of Mg/Al-Type Modified Hydrotalcites. Revista de Chimie 61, 395–399.

[100] Rives, V., 2001. Layered Double Hydroxides: Present and Future. Nova Science, NewYork.

[101] Stephenson, H., Bradshaw, H., 2006. Hydrotalcites. MEL Chemicals, Clifton Junction, Swinton.

[102] Ficicilar, B., Dogu, T., 2006. Breakthrough analysis for CO_2 removal by activated hydrotalcite and soda ash. Catalysis Today 115, 274–278.

[103] Walspurger, S., Cobden, P.D., et al., 2010. High CO_2 storage capacity in alkali-promoted hydrotalcite based material: in situ detection of reversible formation of magnesium carbonate. Chemistry – A European Journal 16, 12694–12700.

[104] Van Dijka, H.A.J., Walspurger, S., Cobden, P.D., et al., 2011. Testing of hydrotalcite-based sorbents for CO_2 and H_2S capture for use in sorption enhanced water gas shift", International Journal of Greenhouse Gas Control 5, 505–511.

[105] Reijers, H.T.J., Boon, J., Elzinga, G.D., et al., 2009. Modeling study of the sorption-enhanced reaction process for CO_2 capture. I. Model development and validation. Ind Eng Chem. Res 48, 6966-6974.

[106] Lee, K. B., Beaver, M. G., Caram, H. S., Sircar, S. 2007. Reversible Chemisorption of Carbon Dioxide: Simultaneous Production of Fuel-Cell Grade H_2 and Compressed CO_2 from Synthesis Gas. Adsorption 13, 385–397.

[107] Ying, D.H.S., Nataraj, S., Hufton, J.R., Xu, J., Allam, R.A., Dulley, S.J., 2008. Simultaneous shift-reactive and adsorptive process to produce hydrogen. U.S. Patent NO. 7354562.

[108] White, V., 2008. Sorption-Enhanced Water Gas Shift. Update CaCHET 2nd public workshop, Lyon.

[109] Kumar, R., Fox, V.G., Hartzog, D.G., Larson, R.E., Chen, Y. C., Houghton P. A., Naheiri, T., 1994. A versatile process simulator for adsorptive separations. Chem Eng Sci, 49, 3115-3125.

[110] Franco, F., Anantharaman, R., Bolland, O., Booth, N., van Dorst, E., Ekstorm, C., Sanchez, E., Macchi, E., Manzoloni, G., Nikolic, D., Pfeffer, A., Prins, M., Rezvani, S., Robinson, L., 2011. Enabling advanced pre-combustion capture techniques and plants. Technical report, Alstom UK.

[111] Jang, H.M., Lee, K.B., Caram, H.S., Sircar, S., 2012. High-purity hydrogen production through sorption enhanced water gas shift reaction using K2CO3-promoted hydrotalcite. Chemical Engineering Science 73, 431–438.

[112] Danckwerts, P.V., 1953. Continuous flow systems: Distribution of residence times. Chemical Engineering Science 21, 1–13.

[113] Lee, K.B., Beaver, M.G., et al., 2008. Reversible chemisorbents for carbon dioxide and their potential applications. Industrial & Engineering Chemistry Research 47, 8048–8062.

[114] gPROMS, PSE Enterprise, 2007, www.psenterprise.com.

[115] Jarvis, R.B., Pantelides, C.C., 1992. DASOLV-A Differential-Algebraic Equation Solver. Centre for Process Systems Engineering, Imperial College, London.

[116] Luyben, M.L., Luyben, W., 1997. Essentials of Process Control. McGraw-Hill.

[117] Astrom K. J., Hagglund, T., 1995. PID controllers: Theory, Design and Tuning. Instruments Society of America.

[118] Ogata, K. 2010. Modern Control Engineering, fifth ed. Prentice Hall.

[119] Bolland, O., 2010. Thermal Power Generation, Department of Energy and Process Engineering, NTNU.

[120] Ulfsnes, R.E., Bolland, O., Jordal, K., 2003. Modeling and simulation of transient performance of the semiclosed O_2/CO_2 gas turbine cycle for CO_2 capture. Proceedings of ASME Turbo Expo, 16-19.

[121] GTPro, ThermoFlow, 2011. User's Manual. Release 21.

[122] Syngas from Waste: Emerging Technologies, By Luis Puigjaner,Springer.

Appendix

Papers

Paper 1

Available online at www.sciencedirect.com

SciVerse ScienceDirect

Energy Procedia 37 (2013) 2293– 2302

Energy Procedia

GHGT-11

Simulation of the cyclic operation of a PSA-based SEWGS process for hydrogen production with CO_2 capture

Bita Najmi[a]*, Olav Bolland[a], Snorre Foss Westman[a]

[a]*Energy and Process Engineering Department, Norwegian University of Science and Technology, Trondheim, Norway*

Abstract

A dynamic one-dimensional homogeneous model for multiple bed Sorption Enhanced Water Gas Shift (SEWGS) system has been developed in this work. The SEWGS system under consideration is based on a Pressure Swing Adsorption (PSA) process which operates in a cyclic manner. During the reaction/adsorption step, CO_2 produced by Water Gas Shift (WGS) reaction is simultaneously adsorbed on a highly CO_2-selective solid adsorbent and removed from the gas phase, enhancing the WGS reaction toward higher reaction conversion and hydrogen production. The periodic adsorption and desorption of CO_2 is induced by a pressure swing cycle, and the cyclic capacity can be amplified by purging with steam. Simulation results enable tracking the operation of the system over sequence of steps. As it is expected, high levels of CO conversion and CO_2 capture ratio are achieved by enhancing the equilibrium reaction of WGS with adsorbents. Moreover there is no need to reheat the hydrogen product before it enters the gas turbine due to operability of SEWGS system at high temperature of approximately 400°C. Hydrogen production undergoes repeating fluctuations over cycle time which is associated with using part of the H_2 product for repressurization step.

Selection and/or peer-review under responsibility of GHGT

Keywords: Sorption Enhanced Water Gas Shift; SEWGS; Pressure Swing Adsorption; PSA; dynamic modelling and simulation

Nomenclature

ε_t	Total void fraction of reactor bed (total gas volume/reactor volume) (m^3 gas/m^3 reactor)
c_i	Gas-phase concentration of component i in gas mixture (mol i/m^3 gas)
u	Superficial gas velocity (m/s)
D_{ax}	Molecular diffusion coefficient (m^2/s)
y_i	Gas-phase gas molar fraction of component i [-]

**E-mail address:* bita.najmi@ntnu.no

1876-6102
Selection and/or peer-review under responsibility of GHGT
doi:10.1016/j.egypro.2013.06.110

$\rho_{b,cat}$	Catalyst bulk density in reactor bed (kg catalyst/m^3 reactor)
$\rho_{b,ads}$	Adsorbent bulk density in reactor bed (kg adsorbent/m^3 reactor)
$C_{p,gas}$	Gas-phase molar specific heat capacity at constant pressure (J/ (mol gas.K))
$C_{p,cat}$	Catalyst specific heat capacity at constant pressure (J/ (kg catalyst.K))
q_{CO_2}	Adsorbent loading of CO_2 (mol CO_2 adsorbed/kg adsorbent)
$q^*_{CO_2}$	Equilibrium adsorbent loading of CO_2 (mol CO_2 adsorbed/kg adsorbent)
k_{LDF}	LDF mass transfer coefficient (1/s)
η_i	Catalyst efficiency for component i (-)
c	Total gas-phase concentration (mol gas/m^3 gas)
r	Reaction rate of forward WGS reaction (mol/kg catalyst.s))
$C_{p,ads}$	Adsorbent specific heat capacity at constant pressure (J/ (kg adsorbent K))
k_z	Effective axial, thermal conductivity (W/ (m^2K)
$\Delta h_{ads,CO_2}$	Isosteric heat of adsorption of CO_2 (J/mol CO_2 adsorbed)
h_i	Enthalpy of component i at temperature T (J/mol i)
T_{wall}	Temperature of reactor wall (K)
T	Temperature (K)
U	Overall bed-to-wall heat transfer coefficient (W/ (m^2K))
d_t	Internal diameter of reactor (m)
μ	Gas-phase dynamic viscosity (Pa. s)
λ_s	Shape factor of the catalyst and adsorbent particles [-]
ε_b	Void fraction of reactor bed (inter particle gas volume/reactor volume)(m^3 gas in bed/m^3 reactor)
d_p	Catalyst and adsorbent particle diameter (m)
ρ_{gas}	Gas-phase density (kg gas/m^3)
SEWGS	Sorption Enhanced Water Gas Shift
PSA	Pressure Swing Adsorption
IGCC	Integrated Gasification Combined Cycle
F	Feed step
R	Rinse step
RP	Repressurization step
D	Depressurization step
P	Purge step
Eq, REq	Pressure equalization and re-equalization steps
M	Mixer
V	Valve

1. Introduction

Solid sorbents for pre-combustion CO_2 capture as high temperature operating technologies has attracted significant attentions lately. One of the newly developed concepts using solid sorbents for pre-combustion CO2 capture is so called Sorption Enhanced Water Gas Shift (SEWGS) system. It incorporates both Water Gas Shift (WGS) reaction and CO_2 adsorption in a single unit and eliminates any further downstream CO_2 capture process. A single SEWGS reactor is in fact a batch unit operation, however by using several SEWGS reactors operating in parallel, one or more being fed syngas and capturing CO_2; while the other CO_2-saturated reactors are being regenerated based on PSA process. The total SEWGS system is able to operate in a semi-continuous process. It means that the effluent gas from SEWGS contains a H_2-rich product stream which is fed continuously to gas turbine and a CO_2-rich stream which is transferred for compression and storage. In the present work, a multiple bed SEWGS system operating based on a PSA process has been considered. A mathematical model describing the system is developed and the simulation results are discussed.

2. PSA-based SEWGS system

The SEWGS system configuration used in the present work is based on a work by Wright et.al. [1]. As it is shown in Fig.1, it consists of a sequence of steps. The first step is a feed step (step F) in which WGS reaction and CO_2 adsorption take place at high temperature and pressure. It is followed by a rinse step (step R) to remove some of the residual H_2 by passing high-pressure steam through the reactor. According to the concept of a PSA process, the desorption of CO_2 is carried out by lowering the pressure in the reactor down to atmospheric pressure in a series of steps called equalizations (steps Eq1, Eq2, Eq3).

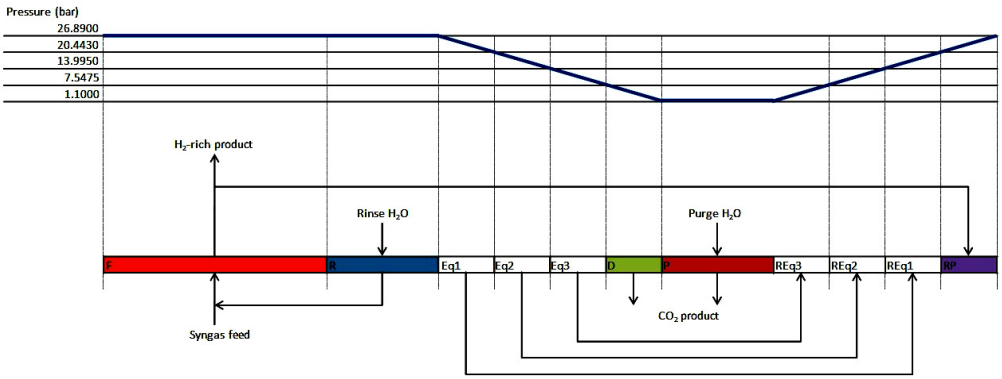

Fig.1. SEWGS cycle operation schedule; countercurrent high pressure steam for Rinse step and low pressure steam for purge step

This is done by connecting the reactor to another reactor whose pressure is to be increased after the CO_2 has been removed which is called REqualization. The purpose of this connection is to lower the energy consumption associated with increasing the pressure in the reactor [1]. Then there is a final depressurization (step D) to approximately atmospheric pressure, and followed by a purge step (step P) where a low-pressure steam is passed through the reactor to desorb CO_2 and regenerate the adsorbent. Then repressurization steps are initiated (steps REq3, REq2, REq1) in equalization with other reactor

which is to be depressurized [1]. Finally some of the effluent gas from other reactors which contains close to no CO_2 is used to bring the reactor pressure up to the feed step pressure. This is the final repressurization step (RP) and the reactor condition is prepared for accepting feed gas and starting a new cycle. The main reason for using high pressure steam for rinse step and low pressure steam for purge step, is to enable a high degree of integration of SEWGS system into an IGCC power plant, where both high pressure and low pressure steam is available from the steam cycle; However, there should be always a limit for steam consumption by SEWGS system to avoid significant efficiency drop for steam turbine and make the SEWGS system a competitive technology with other pre-combustion CO_2 capture technologies.[1].

To be able to integrate the SEWGS system into an IGCC power plant, the operating condition of the system should be compatible with those of power plants. Calculations for the current SEWGS system were made based on European Benchmarking Task Force (EBTF) [2].

3. SEWGS system design and modeling approach

The SEWGS system considered in this work consists of 10 trains; each train incorporates 8 individual reactors working in parallel. The mathematical model for dynamic simulation of the entire SEWGS system is achieved by developing mass, energy and momentum balance equations for individual reactors in the system. Appropriate initial and boundary conditions for all the steps taking place in sequence are determined. Syngas as one of the feed streams to the system is defined to be the syngas from the gasifier used in the reference case [2]. Each reactor vessel is packed with a mixture of high-temperature FeCr-based WGS catalyst pellets and K_2CO_3-promoted Hydrotalcite CO_2 adsorbent which has been found to be suitable for adsorption of CO_2 at high temperatures such as 400°C and proper for using in SEWGS reactors [3, 4]. WGS reaction kinetic model proposed by Hla et al. [5] and modified Langmuir isotherm for the equilibrium adsorption capacity of CO_2 as proposed by Lee et al. [6] was used in this work. Fig.2 defines the system border for one SEWGS train, with the relevant streams going in and out of the train. The stream "CO_2 Product 1" comes from the reactor in the purge step, while the stream "CO_2 Product 2" is from the reactor in the depressurization step. Moreover "Feed 1" and "Feed 2" refer to syngas stream which enters each of the two vessels working in the feed step at the same time according to cycle operation schedule presented in Fig.1. "HP steam 1" and "HP steam 2" are high pressure steam which is added to the "Feed 1" and "Feed 2" respectively. "HP steam R" is the high pressure steam used for the Rinse step and "LP steam P" is a low "pressure steam used in the Purge step. "H_2 product" represents the H_2-rich stream.

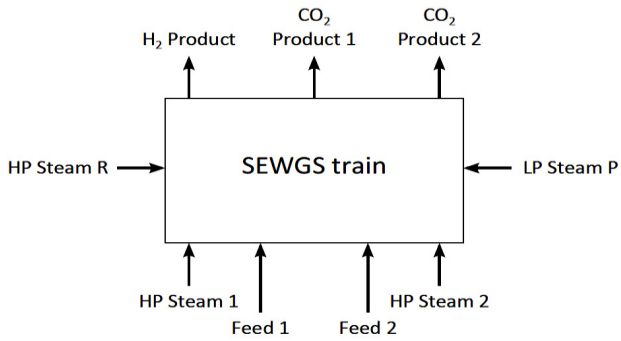

Fig.2. SEWGS system flow diagram

According to the cycle operating schedule shown in Fig.1, system of 8 reactors in each train can be in 16 different states which are referred to as cycle state 1 through 16. However among these 16 cycle states, There are only 2 fundamentally different states that the system switches between, referred to as system states. Fig.3 shows the flow directions and interconnections between the vessels for two different system states 1 and 2.

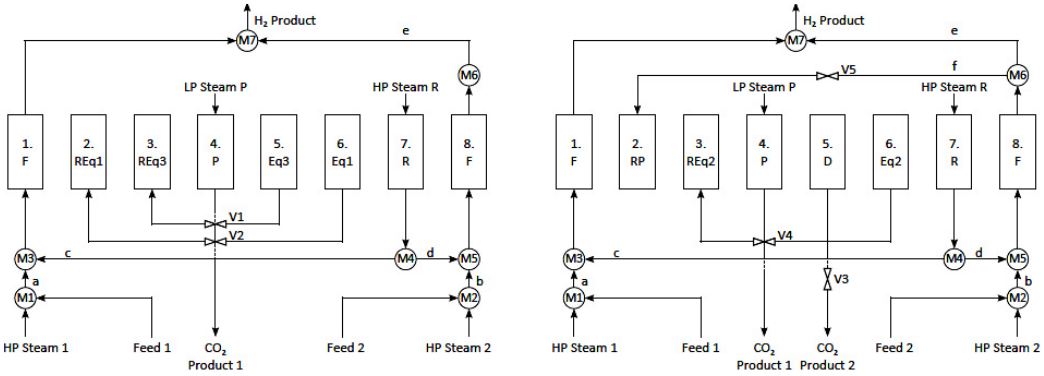

Fig.3. System state 1(left), 2(right), external streams referred to Fig.2

3.1. Components mass balance

The components mass balance in the reactor in the axial domain $z \in [0, L]$ can be formulated as follows, adapted from [7, 8], assuming that each reactor vessel comprises the following five components: CO_2, H_2, CO, H_2O and N_2

$$\varepsilon_t \frac{\partial c_{CO_2}}{\partial t} = -\frac{\partial (u c_{CO_2})}{\partial z} + \frac{\partial}{\partial z}\left(c D_{ax} \frac{\partial y_{CO_2}}{\partial z} \right) + \rho_{b,cat} \eta_{CO_2} r - \rho_{b,ads} \frac{\partial q_{CO_2}}{\partial t}$$

$$\varepsilon_t \frac{\partial c_i}{\partial t} = -\frac{\partial (u c_i)}{\partial z} + \frac{\partial}{\partial z}\left(c D_{ax} \frac{\partial y_i}{\partial z} \right) + \rho_{b,cat} \eta_i r \qquad i = H_2, CO, H_2O, N_2$$

3.2. Total mass balance

The total mass balance in the axial domain $z \in [0, L]$ can be formulated as follows [9]

$$\varepsilon_t \frac{\partial c}{\partial t} = -\frac{\partial (u c)}{\partial z} + \rho_{b,cat} \sum \eta_i \, r - \rho_{b,ads} \frac{\partial q_{CO_2}}{\partial t}$$

3.3. Energy balance

The energy balance in the axial domain $z \in [0, L]$ can be formulated as follows [7, 10]

$$c C_{p,gas} \varepsilon_t + \rho_{b,cat} C_{p,cat} + \rho_{b,ads} C_{p,ads} \frac{\partial T}{\partial t} = \frac{\partial}{\partial z}\left(k_z \frac{\partial T}{\partial z} \right) - c C_{p,gas} u \frac{\partial T}{\partial z}$$

$$-\rho_{b,cat} \sum_i h_i \eta_i \, r + \rho_{b,ads} \Delta h_{ads,CO_2} \frac{\partial q_{CO_2}}{\partial t} + \frac{4U}{d_t} (T_{wall} - T)$$

3.4. Momentum balance

For the momentum balance, the Ergun equation, which describes pressure drop in a packed bed column, is used for the whole axial domain $z \in [0, L]$ this can be formulated as

$$\frac{\partial p}{\partial z} = -150u\frac{\mu\ \lambda_s\ (1-\varepsilon_b)^2}{d_p^2\varepsilon_b^3} - 1.75u|u|\frac{\lambda_s\ (1-\varepsilon_b)\ \rho_{gas}}{d_p^2\varepsilon_b^3}$$

3.5. Adsorption kinetics

Linear Driving Force (LDF) model for adsorbent loading has been used to account for mass transfer limitations in the adsorbent. The adsorption rate of CO_2 in the whole axial domain $z \in [0, L]$ can be formulated as follows: [6, 7]

$$\frac{\partial q_{CO_2}}{\partial t} = k_{LDF}\ \left(q^*_{CO_2} - q_{CO_2}\right)$$

Boundary conditions for concurrent feed flow are presented in table 1. They are based on the boundary conditions proposed by Danckwerts [11]

Table1. Boundary conditions for the concurrent feed step (F)

$z = 0$	$z = L$
$\frac{\partial c_i\ (z=0)}{\partial z} = -\frac{u\ (z=0)\ (c_{i,inlet} - c_i\ (z=0))}{D_{ax}\ (z=0)}$	$\frac{\partial c_i\ (z=L)}{\partial z} = 0$
$\frac{\partial T\ (z=0)}{\partial z} = -\frac{c\ (z=0)\ C_{p,gas}\ (z=0)\ u\ (z=0)\ (T_{inlet} - T\ (z=0))}{k_z\ (z=0)}$	$\frac{\partial T\ (z=L)}{\partial z} = 0$
$u\ (z=0) = u_{inlet}$	$p\ (z=L) = p_{outlet}$
$p\ (z=0) = p_{inlet}$	$c_i\ (z=L) = c_{i,outlet}$
	$T\ (z=L) = T_{outlet}$
	$u\ (z=L) = u_{outlet}$

4. **Results and discussion**

The mathematical model developed for the system was implemented in gPROMS, process modelling software developed by Process Systems Interprise Ltd., and the operating schedule for running the system based on the defined cycle configuration in Fig.1 was utilized. One of the main objectives of the SEWGS system in addition to CO_2 capture is to convert feed syngas into product stream consisting of combustible H_2 which should be sent to Power Island for power production. Table 2 shows the average mole fractions in H_2 product stream, referred to Fig.2. According to this table the H_2 purity in the H_2 product stream is approximately 81% on dry basis. Average mole fractions in the H_2 rich stream in the reference case has been shown in table 3 for comparison. The H_2 purity in the reference case is approximately 90% on dry basis. It shows that the SEWGS system with current design and configuration produces a H_2 rich stream with less purity than the reference case. The impurities are mostly steam and N_2. CO and CO_2 contents are well below than that of the reference case. The average temperature and pressure of the H_2 product stream from the simulation results is approximately 400°C and 27 bar respectively.

Table2. Average mole fractions in H2 product Stream referred to Fig.2

Mol-% CO2	0.184
Mol-% H2	51.4
Mol-% CO	0.0281
Mol-% H2O	36.4
Mol-% N2	12.0

Table3. Average mole fractions in H2 rich stream, IGCC reference case [2]

Mol-% CO2	3.20
Mol-% H2	85.64
Mol-% CO	2.66
Mol-% H2O	0.05
Mol-% N2	8.41

As it is seen in Fig.2, the other streams coming out of the SEWGS system are CO_2 product 1 and 2. It is of interest to calculate the CO_2 capture ratio for the SEWGS system under consideration. It can be expressed by the amount going out through the CO_2 product streams divided by the total amount of CO_2 and CO that have gone into the system over the simulation time. Based on the simulation results the capture ratio is calculated approximately 94%. This capture ratio is comparable to results from SEWGS modeling and experimental studies in the literature, such as the previously mentioned study by Wright et al. [1], which states a capture ratio of 95 %. In another work by Wright et al. [12]; a capture ratio of 92.3 % is calculated.

Moreover simulation results show that in the beginning of the reactor, where the reaction rate is high, a temperature increase of approximately 200K takes place. It has been shown in Fig.4. The reason is that compared to previous works there is no WGS reactor upstream of the SEWGS system for bulk conversion of CO to CO_2 which is slightly exothermic reaction and develops heat. With this high temperature spike the catalysts in that region may be destroyed. The maximum operating temperature reported for the FeCr-based catalyst is around773 K [13] and for K-HTC is around 800 K [14]. One of the options to avoid the hot spots is to place a WGS WGS reactor upstream of the SEWGS system as it has been observed in the literature [1, 12]; However it has not been considered whether it is economically advantageous or not. Further investigation in this regard is required.

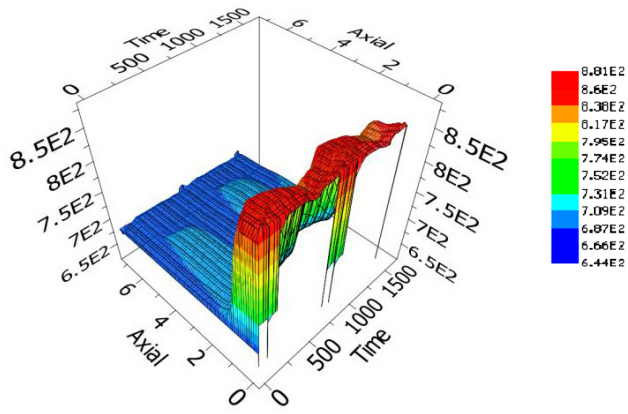

Fig.4. Temperature profile T (K) in reactor 1, as a function of time t (s) and axial position z (m)

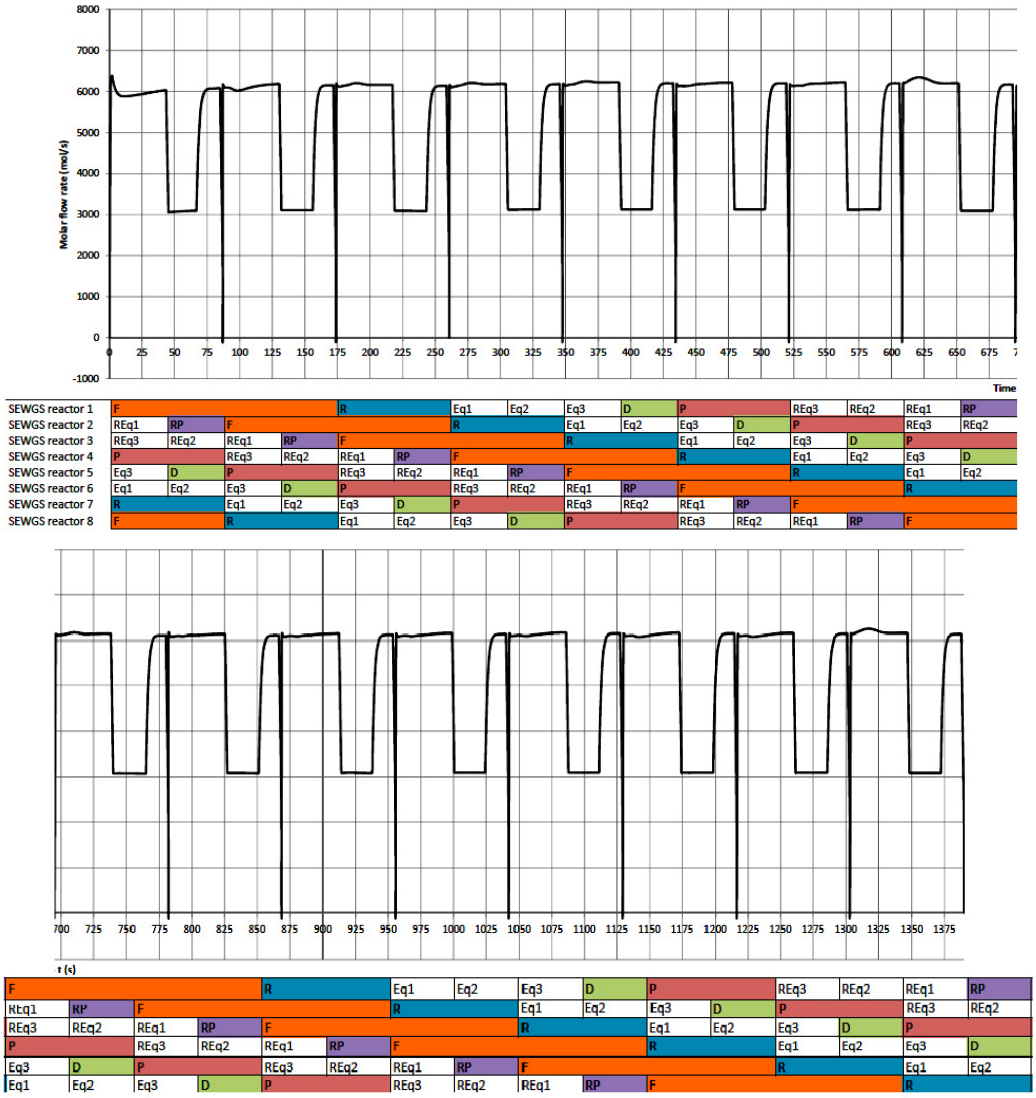

Fig. 5.Total flowrate (mol/s) of H2 product stream, referred to Fig.2

Fig.5 shows the total flowrate of H_2 product stream which leaves the SEWGS system. As it can be seen from the figure there are fluctuations in the production over the time which is described according to the operation of different cycle states shown in Fig.3. Two reactors in each train are operating in the feed step at the same time and producing hydrogen. When system state 2 occurs, part of the hydrogen product as it is shown in Fig.3 is used to repressurise the vessel up to feed step pressure and reduction in hydrogen product flowrate happens until the pressure in the repressurized vessel reaches the feed pressure.

Typically the amount of maximum allowed fluctuation in hydrogen production rate is determined by gas turbine fuel load and pressure constraints. Further work on this matter is yet to be completed and if it is required, any possible solution for product fluctuation will be considered.

Fig.6 shows the behavior of reactor one as an example of an individual reactor in the system at key points in time. The top left graph shows the mole fractions in the reactor at the end of step F. As it can be seen from the figure CO2 front has travelled along the reactor and due to the conversion of CO to CO_2, there is almost no CO left in the reactor at the outlet. Hydrogen is produced during step F. The top right graph shows the mole fractions at the end of step R. it is visible that steam has been sent to the reactor and pushed out some of the residual gas in the reactor. But it doesn't continue until all of the residuals are blown out of the reactor. The remaining components in the gas phase will be further sent out of the reactor during Equalization steps and transferred to other reactors. It can be seen from bottom left graph which shows the mole fractions at the end of step Eq3. Finally the mole fractions at the end of step P are shown in the bottom right graph. Purge steam is coming into the reactor counter-currently and drives out desorbed CO_2.

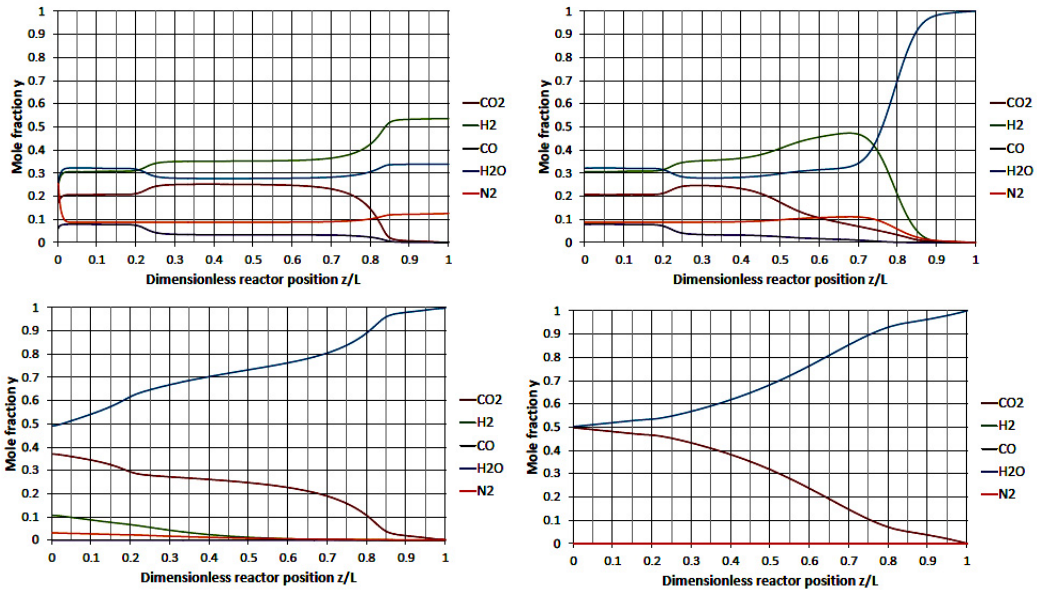

Fig.6. Mole fractions along the reactor one at the end of step F (top left); end of step R (top right); end of step Eq3 (bottom left); end of step P (bottom right)

5. **Conclusion**

The results obtained from the simulation of the SEWGS system confirm the physical mechanism and qualitative trend expected for a SEWGS system. The system operates as it is intended, fulfilling its primary objective of converting carbon-rich syngas into a hydrogen-rich combustible gas mixture. The secondary objective is also achieved, capturing CO_2 and bringing this out of the system in a gas stream containing mostly CO_2 and steam. However, significant variations were observed in hydrogen product flow rate. It is desirable to have as much close to constant production of hydrogen as possible, in particular when the hydrogen product is being fed to a gas turbine which is designed to handle a limited

range of pressure variations. One possibility to lower H_2 production fluctuations is to run different trains at different times in a way to achieve a smooth production rate out of the entire system. Other possibilities can be changing cycle configuration or using feed gas for repressurization which all need to be further investigated. Moreover, with no upstream WGS reactor, hot spots were made due to the WGS exothermic reaction. It proves the need for a WGS reactor, upstream the SEWGS system, if it is economically advantageous as well or any other solution which avoid formation of temperature spikes.

6. References

[1] A.D. Wright, V. White, J.R. Hufton, R. Quinn, P.D. Cobden, and E.R. Van Selow. CAESAR: Development of a SEWGS model for IGCC. Energy Procedia, 4:1147–1154, 2011

[2]European Benchmarking Task Force (EBTF) "Common Framework Definition document" (Franco et al., 2009). The reference IGCC case with CO2 capture using cryogenic ASU is taken to be the case presented in the EBTF "Test cases and preliminary benchmarking results from the three projects" (Franco et al., 2009).

[3]P.D. Cobden, P. van Beurden, H.T.J. Reijers, G.D. Elzinga, S.C.A. Kluiters, J.W. Dijkstra, D. Jansen, and R.W. Van Den Brink. Sorption-enhanced hydrogen production for pre-combustion CO2 capture:Thermodynamic analysis and experimental results. International Journal of Greenhouse Gas Control, 1(2):170–179, 2007.

[4] J.R. Hufton, R.J. Allam, R. Chiang, P. Middleton, E.L. Weist, and V. White. Development of a process for CO2 capture from gas turbines using a sorption enhanced water gas shift reactor system.
In Proceedings of 7th International Conference on Greenhouse Gas Control Technologies, volume 1, pages 253–262, 2005

[5]S.S. Hla, D. Park, G.J. Du_y, J.H. Edwards, D.G. Roberts, A. Ilyushechkin, L.D. Morpeth, and T. Nguyen. Kinetics of high temperature water-gas shift reaction over two iron-based commercial catalysts using simulated coal-derived syngases. Chemical Engineering Journal, 146(1):148–154, 2009.

[6] K.B. Lee, A. Verdooren, H.S. Caram, and S. Sircar. Chemisorption of carbon dioxide on potassiumcarbonate-promoted hydrotalcite. Journal of colloid and interface science, 308(1):30–39, 2007

[7] Y. Ding and E. Alpay. Adsorption-enhanced steam-methane reforming. Chemical Engineering Science, 55(18):3929–3940, 2000

[8] A.M. Ribeiro, C.A. Grande, F.V.S. Lopes, J.M. Loureiro, and A.E. Rodrigues. A parametric study of layered bed PSA for hydrogen purification. Chemical Engineering Science, 63(21):5258–5273, 2008

[9] H.T.J. Reijers, J. Boon, G.D. Elzinga, P.D. Cobden, W.G. Haije, and R.W. van den Brink. Modeling study of the sorption-enhanced reaction process for CO2 capture. I. model development and validation. Industrial & Engineering Chemistry Research, 48(15):6966–6974, 2009.

[10] Y. Ding and E. Alpay. Equilibria and kinetics of CO2 adsorption on hydrotalcite adsorbent. Chemical Engineering Science, 55(17):3461–3474, 2000.

[11] P.V. Danckwerts. Continuous flow systems: Distribution of residence times. Chemical Engineering Science, 2(1):1–13, 1953.

[12] A. Wright, V. White, J. Hufton, E. Selow, and P. Hinderink. Reduction in the cost of pre-combustion CO2 capture through advancements in sorption-enhanced water-gas-shift. Energy Procedia, 1(1):707–714, 2009.

[13] O. Bolland. Power generation: CO2 capture and storage. 2011.

[14] S. Choi, J.H. Drese, and C.W. Jones. Adsorbent materials for carbon dioxide capture from large anthropogenic point sources. ChemSusChem, 2(9):796–854, 2009.

Paper 2

Is not included due to copyright

Paper 3

International Journal of Greenhouse Gas Control 35 (2015) 30–46

Contents lists available at ScienceDirect

International Journal of Greenhouse Gas Control

journal homepage: www.elsevier.com/locate/ijggc

Load-following performance of IGCC with integrated CO_2 capture using SEWGS pre-combustion technology

Bita Najmi[a], Olav Bolland[a,*], Konrad Eichhorn Colombo[b]

[a] Energy and Process Engineering Department, Norwegian University of Science and Technology, 7491 Trondheim, Norway
[b] TDW Offshore Services, 4033 Stavanger, Norway

ARTICLE INFO

Article history:
Received 6 August 2014
Received in revised form 27 January 2015
Accepted 28 January 2015
Available online 16 February 2015

Keywords:
IGCC
SEWGS
CO_2 capture
Full-load
Part-load
Buffer tank

ABSTRACT

The performance assessment of an Integrated Gasification Combined Cycle (IGCC) integrated with the Sorption Enhanced Water Gas Shift (SEWGS) technology for pre-combustion CO_2 capture at full-load and part-load modes of operation is investigated. Syngas from a coal gasifier is sent to the SEWGS system after going through solids and H_2S removal units. A H_2-rich stream is produced by the SEWGS system and used in a gas turbine (GT) for combustion. A control strategy including a buffer tank followed by a control valve, between the SEWGS system and the GT is implemented to smooth out the fluctuations in the H_2-rich fuel flow rate, resulted from the cyclic operation of the PSA-based SEWGS system. Simulation of the IGCC integrated with the SEWGS system is first performed at full-load operation of the GT. For evaluating part-load performances, four different cases, introducing various load change strategies for the GT and gasifier are studied. Step/ramp changes of the GT and gasifier, unplanned/planned GT load changes and same/different GT and gasifier load change occurrence time are all addressed through these four cases. Simulation results indicate that the designed control strategy is able to minimize the H_2-rich fuel flow rate fluctuations and dampen the fuel composition variations, while keeping the buffer tank pressure within the desired range. Dynamic characteristics of the SEWGS system are revealed and compared with those of the gasifier and the GT. Using the buffer tank between the SEWGS and the GT, improves part-load operation flexibility of the GT. Smooth operation and load following capability of the IGCC integrated with the SEWGS system are achievable, depending on the GT part-load level and load change strategy, taking into account the limited load gradient of the gasifier and the SEWGS units compared to the GT.

1. Introduction

Power generation plants are one of the largest sectors contributing to CO_2 emissions and global warming. On the other hand, increasing demand for electricity requests more use of coal-fueled power plants, as coal, in particular in developing countries, is abundant and inexpensive compared to natural gas. Coal-fired power plants have approximately twice as high CO_2 emissions than natural gas-fired power plants. Therefore CO_2 capture from such plants is of great importance to make significant reductions in CO_2 emissions (Lawal et al., 2009; Gazzani et al., 2013a).

One of the routes for CO_2 capture from power plants is to remove carbon content of the fuel before combustion takes place, known as pre-combustion CO_2 capture. A novel pre-combustion CO_2 capture technology, called Sorption Enhanced Water Gas Shift (SEWGS) combines both the water gas shift (WGS) reaction and CO_2 capture in one single unit, at elevated temperatures (Manzolini et al., 2011). CO_2 adsorption on a solid material shifts the equilibrium of the WGS reaction toward higher conversions of CO into CO_2. In contrast, conventional pre-combustion CO_2 capture technologies typically consist of two stages of high and low temperature WGS reactors followed by a CO_2 capture unit. The most common pre-combustion CO_2 capture process is based on physical absorption at low temperature, i.e. a SELEXOL-based process. Also there are intermediate cooling and reheating stages in such methods to prepare the fuel as per gas turbine (GT) requirement (Harrison, 2008; Allam et al., 2005).

SEWGS technology can lower the efficiency penalty of power plants with Carbon Capture and Storage (CCS) technologies by combining the WGS reaction and CO_2 capture steps, as well as eliminating the need for cooling and re-heating of syngas streams, as is done in conventional processes. Also higher H_2 recovery rates can be achieved, due to the higher conversion of CO into CO_2 by the SEWGS technology compared to the conventional CO_2 capture

* Corresponding author. Tel.: +47 73591604; fax: +47 73598390.
E-mail address: olav.bolland@ntnu.no (O. Bolland).

http://dx.doi.org/10.1016/j.ijggc.2015.01.015
1750-5836/

Nomenclature

Symbols

$\dot{m}_{in,tank}$	mass flow rate to the buffer tank ($kg\,s^{-1}$)
$\dot{m}_{out,tank}$	mass flow rate out of the tank ($kg\,s^{-1}$)
$\dot{m}_{valve}$	mass flow rate through the fuel control valve ($kg\,s^{-1}$)
C_v	flow coefficient ($m^3\,s^{-1}\,bar^{-1/2}$)
Mw	molecular weight ($kg\,kmol^{-1}$)
ρ	density ($kg\,m^{-3}$)
P_0	buffer tank pressure (bar)
P_1	downstream fuel control valve pressure (bar)
R	gas constant ($L\,bar\,K^{-1}\,mol^{-1}$)
T	temperature in the tank (K)
V_{tank}	buffer tank volume (m^3)
x_{valve}	valve opening

Abbreviations

ASU	air separation unit
CCS	carbon capture and storage
FI	flow indicator
FT	flow transmitter
GT	gas turbine
HP	high pressure
HRSG	heat recovery steam generator
IGCC	integrated gasification combined cycle
LP	low pressure
NGCC	natural gas combined cycle
PI	proportional integral
PI	pressure indicator
PSA	pressure swing adsorption
PT	pressure transmitter
SEWGS	Sorption Enhanced Water Gas Shift
ST	steam turbine
TIT	turbine inlet temperature
TOT	turbine outlet temperature
WGS	water gas shift

processes (Manzolini et al., 2011). A H_2-rich and a CO_2-rich stream are the main and by-products of this process, respectively. The H_2-rich stream is used in a GT for combustion. The CO_2 rich stream is further processed and compressed for underground storage (Liu et al., 2011; Nikolic et al., 2008).

A key to the success of implementing the SEWGS technology for pre-combustion CO_2 capture is to select a proper CO_2 adsorbent material that efficiently adsorbs and desorbs CO_2 during Pressure Swing Adsorption (PSA) cycles (operating condition: pressures between ~30 and ~1 bar, temperatures in the range of ~350–550 °C) (Manzolini et al., 2011). Some important properties of an ideal CO_2 adsorbent material are as follows: (1) sufficient CO_2 adsorption isotherm and kinetics, (2) adequate mechanical strength over a series of process cycles, (3) tolerant to the impurities in the gas, (4) being able to be formed into pellets and (5) low cost (Harrison, 2008; Singh et al., 2009; Siriwardane et al., 2007).

Several screening research studies have been conducted with the aim of identifying well-suited CO_2 adsorbent materials (Allam et al., 2005; Siriwardane et al., 2007; Reijers et al., 2006; Stevens et al., 2010; Choi et al., 2009; Martunus et al., 2011; Yong et al., 2002). A screening study was carried out on a number of candidate adsorbent materials including commercial sodium oxides (CL750), K_2CO_3-promoted hydrotalcites, lead oxide adsorbents (PbO), and double salt adsorbents (DS), to distinguish the most suitable adsorbent material for SEWGS application within the power plants for pre-combustion CO_2 capture. The K_2CO_3-promoted hydrotalcite was found as the best suited material that can effectively adsorb and desorb CO_2 in PSA cycles at operating conditions of the SEWGS process. PbO and CL750 were rejected due to their lower adsorption capacity at high temperature than K_2CO_3-promoted hydrotalcites. Double salt materials showed very unusual adsorbent isotherms and it was a big challenge to make pellets of these materials (Allam et al., 2005; Reijers et al., 2006; Martunus et al., 2011).

In an Integrated Gasification Combined Cycle (IGCC) power plant with integrated SEWGS technology, the H_2-rich stream from the SEWGS enters the GT for combustion. It is thus desirable from the GT efficiency point of view to keep the temperature of the H_2-rich fuel gas stream as high as possible. This limits the selection of the adsorbent materials for the SEWGS process to those that can endure under high temperatures. However, the WGS reaction is slightly exothermic and is consequently promoted at low temperature (Stevens et al., 2010). Hence, there is a trade-off between the need for lower temperatures in favor of the WGS reaction and higher temperatures for the effluent gas entering the GT. The ideal temperature range was reported to be between 250 and 450 °C (Singh et al., 2009).

For many years, CaO adsorbents have been frequently investigated for CO_2 capture. But they demand high temperatures for regeneration and their CO_2 capture capabilities suffer from rapid degradation in multi-cycle use (Reijers et al., 2006; Choi et al., 2009). High temperatures associated with regeneration of CaO adsorbents could pose a problem with respect to the reactor vessel, where heat-resistant alloys could be required (Reijers et al., 2006). To improve properties of CaO materials for SEWGS application, novel CaO-based materials have been considered as CO_2 adsorbents. A NaOH-promoted CaO was developed in an experimental work for use in SEWGS reactors within IGCC plants (Siriwardane et al., 2007; Stevens et al., 2010). When CaO is promoted with NaOH, the CO_2 adsorption capacity is also improved. Furthermore, the regeneration temperature is significantly reduced.

Taking into account the main characteristics of an ideal CO_2 adsorbent, zeolite 13x, K_2CO_3-promoted hydrotalcite and double salt adsorbents, were considered as well-suited candidate materials to be used in a SEWGS system integrated with an IGCC plant (Singh et al., 2009). Zeolite 13x can be used at temperatures up to 200 °C. Beyond that, the adsorption capacity of zeolites decreases rapidly. Double salt adsorbents showed a relatively high CO_2 capture capacity and selectivity. However, the presence of water vapor lowers the CO_2 capture capacity and it is still a challenge to produce pellets of these materials (Reijers et al., 2006). On the other hand, K_2CO_3-promoted hydrotalcite showed a good performance at a temperature of 350 °C in the presence of water, which is needed for the WGS reaction. The presence of H_2S might have an adverse effect on the K_2CO_3-promoted hydrotalcite performance and therefore a H_2S removal unit before a SEWGS reactor is recommended. The undesirable effect of H_2S on the hydrotalcite adsorbent materials stability and long-term CO_2 capacity was also discussed in another work (Allam et al., 2005). An experimental research work on the CO_2 capture capacity and behavior of a K_2CO_3-promoted hydrotalcite in the presence of the H_2S, on the other hand, showed that the adsorbent was capable of co-adsorption of the H_2S along with the CO_2. In this case, additional desulphurization unit may be required for separation of the CO_2 and H_2S which needs further investigations in terms of the efficiency penalty. Moreover, sorbents with different contents of the K_2CO_3 may demonstrate different characteristics with respect to H_2S adsorption (Van Dijk et al., 2011).

In many works, K_2CO_3-promoted hydrotalcite-based adsorbents have been found as the most promising CO_2 adsorbent materials for SEWGS applications (Manzolini et al., 2011; Allam et al., 2005; Jang et al., 2012; Halabi et al., 2012; Van Selow et al., 2011; Wright et al., 2011; Bakken et al., 2011; Van Selow et al., 2009;

Reijers et al., 2009; Lu et al., 2013). Usability of these materials at temperature of ~800 °C as the CO_2 adsorbent has been reported as well (Choi et al., 2009). A K_2CO_3-promoted hydrotalcite material is therefore assumed as the CO_2 adsorbent in this work.

A SEWGS reactor is packed with a mixture of WGS catalyst and CO_2 adsorbent material. Regeneration of the adsorbent is typically carried out by a PSA process through a number of steps in sequence. This is therefore an inherently dynamic process. Multistep regeneration of the adsorbent demands a multiple bed SEWGS system in which the operation of a single reactor is a batch process, but the total system is able to operate as a semi-continuous process.

Few research works have been published on the performance of the SEWGS process and its impact on the operation of the power plants. An experimental study, launched within the CO_2 Capture Project (CCP), on selection of the most suitable CO_2 adsorbent material among a number of potential CO_2 adsorbents (Allam et al., 2005). The work was followed by a steady-state simulation of a natural gas-based power plant integrated with the SEWGS process for pre-combustion CO_2 capture. A study on the SEWGS steady-state performance for power plant application was initiated within the CAESAR project (Caesar FP7, 2008). The SEWGS system was a multiple reactor operating based on a PSA process. It was shown that the steam consumption and the cost were reduced by using the SEWGS technology for CO_2 capture compared to the conventional pre-combustion CO_2 capture technologies using solvent-based processes (Wright et al., 2009, 2011). Another steady-state performance assessment of both natural gas combined cycle (NGCC) and IGCC power plant with the SEWGS process from a thermodynamic point of view was performed through a follow-on simulation work within the CAESAR project (Gazzani et al., 2013a; Manzolini et al., 2011). The Thermodynamic simulation revealed the efficiency and CO_2 capture ratio of the entire power plant as performance indicators and focused on the impact of different integration levels between the hydrogen and power island on the efficiency penalties. It was found that the tight integration between the power and hydrogen island was thermodynamically superior and reduced the efficiency penalty. Also it was shown that the SEWGS process steam usage had strong impact on the plant efficiency penalty. In addition, the SEWGS working conditions were optimized in terms of the CO_2 purity and carbon capture ratio and economic assessments were carried out (Gazzani et al., 2013b; Manzolini et al., 2013). Also the impacts of the adsorbent cyclic capacity on the number of SEWGS vessels and energy consumption of the CO_2 capture process were investigated. The power plant layout considered was a NGCC with tight integration between the power and hydrogen island (Manzolini et al., 2011). The CO_2 purity of 99% was indicated as the optimal value. An experimental/theoretical analysis was performed on the application of the SEWGS process in IGCC power plant for pre-combustion CO_2 capture (Jansen et al., 2013). A newly developed K_2-CO_3 promoted hydrotalcite adsorbent with catalytic properties was used. Effects of the new adsorbent on reducing the energy consumption of the SEWGS process and costs were predicted and compared with conventional pre-combustion technologies in IGCC plants.

On a system level, there are not works investigating the performance of the PSA-based SEWGS process and its impact on the performance of an IGCC at transient and part-load conditions, when integrated with the SEWGS-based pre-combustion CO_2 capture process. In this paper operation of an IGCC power plant with CO_2 capture using the SEWGS technology (see Fig. 1) at full-load and part-load modes of operation is investigated. A detailed dynamic model of the SEWGS system, previously developed, is used as a base model (Najmi et al., 2013). A H_2-rich stream coming from the SEWGS is used as a GT fuel. A closed-loop control strategy is designed to smooth out fluctuations in the H_2-rich stream flow rate, associated with the cyclic operation of the PSA-based SEWGS process before it is sent to the GT. A buffer tank, which is part of the control system, undertakes the main function of dampening out most of the fluctuations. A control valve right after the buffer tank further controls the fuel mass flow rate and pressure. First, full-load operation is simulated. Part-load performance is then investigated in four different cases, which introduce different load change strategies applied to the components of the IGCC with the SEWGS technology. Step/ramp changes of the GT and gasifier, unplanned/planned load changes of the GT and same/different GT and gasifier load change occurrence time are addressed through these four cases. Operability and controllability of the IGCC with the SEWGS technology in each case are discussed. Load-following performance of the entire plant considering the limited load gradient of the gasifier and the SEWGS units compared to the GT is investigated. Also the improved operation flexibility of the GT as a result of including an intermediate buffer tank before the GT is evaluated.

2. System description

A schematic diagram of an IGCC with SEWGS technology is shown in Fig. 1. It is based on an IGCC reference case with conventional pre-combustion CO_2 capture technology (Franco et al., 2010). The feedstock of the power plant is assumed to be bituminous Douglas Premium coal, with the composition given in Table 1. A distinction has been made between Process Island and Power Island as shown in Fig. 1. Process Island includes the gasification block and the gas treatment block. Key streams have been indicated by numbers and information about them is shown in Table 2.

A cryogenic type Air Separation Unit (ASU) is used to produce O_2 for the gasifier. Part of the N_2 produced in the ASU is used for lock hoppers and filters. Coal is gasified to synthesis gas in an O_2-blown, entrained flow gasifier, operating at 44 bar. The syngas is then cooled and cleaned of particulates by passing through a convective cooler, dry solids removal unit (electrostatic precipitator). H_2S is removed from the syngas using a physical solvent (SELEXOL) to feed a sulphur-free syngas to the sweet SEWGS process. In the IGCC reference case with conventional CO_2 capture process the H_2S removal unit is situated downstream of the WGS reactors, which is called sour WGS process. The reason for selecting the sweet SEWGS process is due to the detrimental effect of H_2S on the K_2CO_3-promoted hydrotalcite sorbent stability and long term CO_2 adsorption capacity (Allam et al., 2005). Syngas to the H_2S removal unit, stream #1, has the same composition and flow rate as the corresponding stream in the reference case. Assuming an efficiency of 100% for the H_2S removal unit, mole fraction and flow rate of the syngas entering the SEWGS system, stream #2, are obtained.

The SEWGS system inlet temperature and pressure as presented in Table 2 are selected to be 673 K and 27 bar according to Allam et al. (2005), which the selected feed pressure was suggested as the optimal pressure.

Syngas is treated within the SEWGS process for CO_2 capture via the WGS reaction enhanced by the K_2CO_3-promoted hydrotalcite CO_2 adsorbent under a multiple bed operation system. It consists of a reaction/adsorption step and a sequence of PSA processing steps for regeneration of the solid adsorbent at a temperature of about 723 K. The H_2-rich and CO_2-rich stream, products of the SEWGS system, are shown by stream #7 and #8, respectively. The H_2-rich (stream #7) is sent to the GT for combustion. To control the H_2-rich stream flow rate and pressure as per GT requirements, a control strategy is introduced before the GT. The power production section consists of a typical combined cycle including a GT, steam turbine (ST) and heat recovery steam generator (HRSG). The hot GT exhaust gases are passed through the HRSG for heat recovery and steam generation. Steam is then used to produce power in the ST. Part of the steam produced by the steam cycle is consumed by the SEWGS

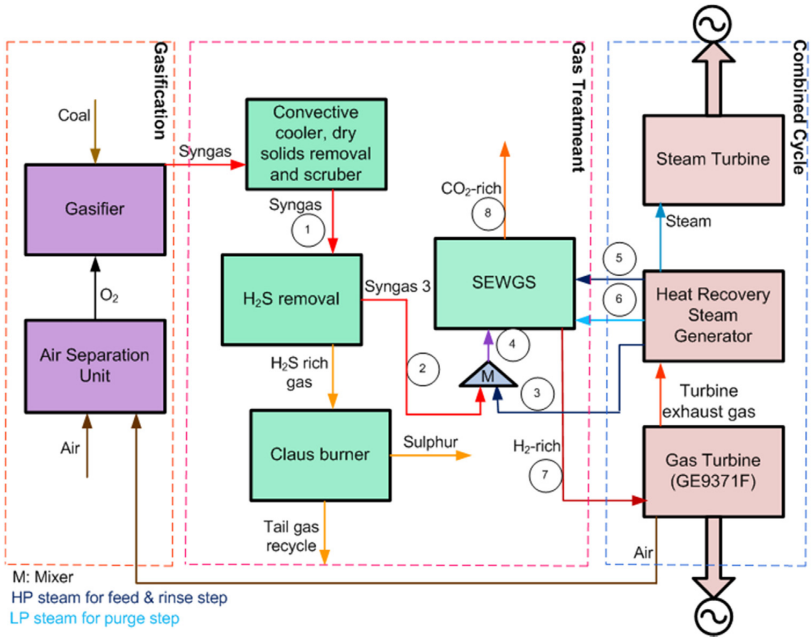

Fig. 1. A schematic diagram of an IGCC integrated with the SEWGS technology.

process as feed, rinse and purge gas, shown by streams #3, #5 and #6, respectively.

2.1. GT fuel control structure

Simulating the operation of the SEWGS system, it was found that the H_2-rich stream flow has quite large fluctuations, which do not meet requirements of the GT to have a smooth fuel heat input at any given load of operation (Najmi et al., 2013). Therefore it is essential to utilize a control strategy to suppress the fuel flow rate fluctuations as much as possible before the GT. The logic considered in designing such a control strategy is explained as follows:

(1) The H_2-rich stream mass flow rate is required to be controlled before entering the GT. This is carried out by changing the fuel control valve stem position to correct the mass flow rate and minimize the difference between the desired and measured mass flow rate. Also, to ensure a forward flow of the H_2-rich stream toward the GT at any time of operation, the buffer tank pressure needs to be checked during the operation to be within the SEWGS system and the GT pressures. The buffer tank pressure is measured at the exit of the tank and checked with the given range. If it is out of the desired range, it is controlled by the feed syngas valve before the SEWGS system. A pressure relief valve is also installed for the emergency cases of too high tank pressure. The H_2-rich stream composition is dampened after it leaves the buffer tank.

(2) Considering the control objectives explained above, the components of the proposed control strategy are arranged as shown in Fig. 2 and explained in the following subsections.

2.1.1. Buffer tank

The H_2-rich stream coming from the SEWGS system has almost constant temperature and pressure (~500 °C, ~27 bar), but the mass flow rate fluctuates over time (~±14%) (Najmi et al., 2013). A buffer tank suppresses a large portion of the H_2-rich mass flow rate

Table 1
Coal composition (mol%) (Franco et al., 2010, 2011).

Carbon	Nitrogen	Hydrogen	Total sulphur	Ash	Chlorine	Moisture	Oxygen
66.520	1.560	3.780	0.520	14.150	0.009	8.000	5.46

Table 2
Stream data used in the current simulation work, adopted from the IGCC reference case with CO_2 capture (Franco et al., 2010).

Stream #	Molar flow (kmol/s)	T (K)	P (bar)	Composition					
				H_2	CO	CO_2	N_2 + Ar	H_2S	H_2O
1	4.22	443	35	22.02	49.23	3.45	6.97	0.13	18.13
2	4.21	673	27	22.06	49.33	3.46	6.98	–	18.17
3	3.21	673	27	–	–	–	–	–	100.00
4	7.42	673	27	12.52	27.99	1.96	3.96	-	53.57
5	0.66	673	27	–	–	–	–	–	100.00
6	1.32	673	2	–	–	–	–	–	100.00

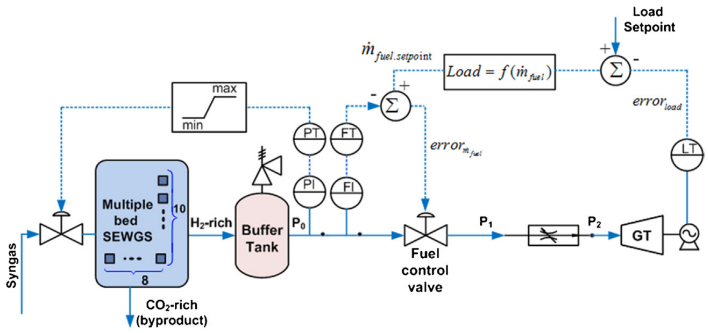

Fig. 2. H_2-rich fuel control system.

fluctuations. It is also used for fuel storage. The H_2-rich stream that leaves the buffer tank has significantly reduced fluctuations and also more dampened composition. On the other hand, pressure of this stream is not constant any more due to the pressure build-up associated with the mass flow rate fluctuation of the tank inlet stream, from the SEWGS system. Further control of the buffer tank outlet stream in terms of pressure and mass flow rate is accomplished by a fuel control valve downstream of the tank (Fig. 2).

The buffer tank used in this work is a vertical cylindrical vessel. It is designed for the full-load condition of the GT. The following assumptions are made in the modeling of the tank:

(1) isothermal process condition,
(2) ideal gas behavior, and
(3) continuous mixing tank.

Considering the above assumptions the material balance around the tank is written:

$$\frac{V_{tank}}{RT}\frac{d(Mw \cdot P_0)}{dt} = \dot{m}_{in,tank} - \dot{m}_{out,tank} \quad (1)$$

$\dot{m}_{in,tank}$, the buffer tank inlet mass flow rate, is achieved by the simulation of the SEWGS system. R, T and, V_{tank} are the gas constant, temperature and volume of the tank, respectively, Mw is the molecular weight of the gas in the tank and P_0 is the buffer tank pressure.

2.1.2. Fuel control valve

A control valve right after the buffer tank further controls mass flow rate and pressure of the H_2-rich fuel to the GT. The valve upstream pressure is the buffer tank pressure, which is fluctuating. The fuel mass flow rate through the valve, $\dot{m}_{valve}$, is controlled by changing the valve stem position, x_{valve} to correct the deviations of the mass flow rate from its set-point (desired value) and minimize the difference between the desired and measured mass flow rate (error). The set-point for the fuel mass flow rate is determined by the desired GT load. The valve downstream pressure, P_1, is estimated by assuming a choked turbine (refer to Section 2.2).

The control valve main equation is presented by Eq. (2). C_v is the valve flow coefficient, defined as the volume flow in cubic meters per second of water at a temperature of between 5 and 40 °C with a pressure drop across the valve of 1 bar, which represents the flow capacity of the valve. At any time of operation, $\dot{m}_{valve}$ and P_1, are dictated by the GT requirements. Considering the oscillatory nature of P_0, x_{valve} may change rapidly to maintain the desired value of the fuel mass flow rate. Dotted lines in Fig. 2 represent the transmission lines that carry the measurement signals from measuring devices to transmitters and controllers.

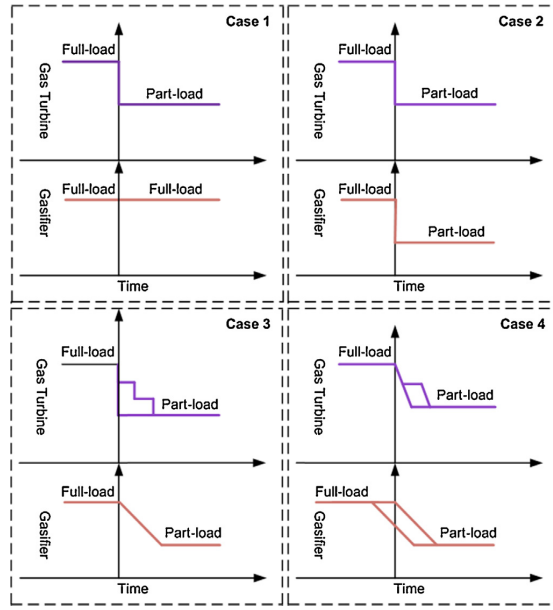

Fig. 3. Four case studies for part-load operation.

$$\dot{M}_{valve} = \rho C_v x_{valve}\sqrt{P_0 - P_1} \quad (2)$$

$$\dot{m}_{valve} = \dot{m}_{out,tank} \quad (3)$$

The controller type utilized in this work is a proportional integral (PI) controller. This type of controllers has shown a well-proved record in process industry (Luyben and Luyben, 1997). A PI controller transfer function is given by Eq. (4):

$$\frac{OUT(s)}{E(s)} = K_P\left(\frac{1}{1+\tau_I S}\right) \quad (4)$$

$$E(S) = \dot{m}_{valve} - \dot{m}_{fuel,setpoint} \quad (5)$$

$$OUT(s) = \Delta x_{valve} \quad (6)$$

Controller parameters, K_P and τ_I, are proportional and integral gains, respectively. $E(s)$ is the deviation of the fuel mass flow rate from the set-point value. $OUT(s)$ is the change in valve stem position.

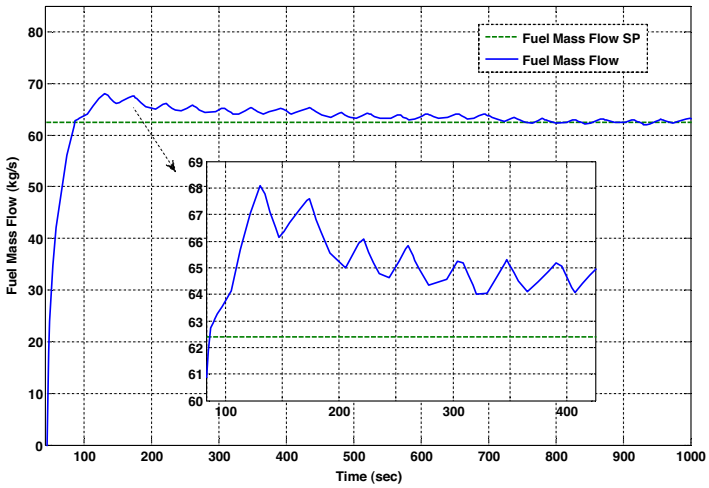

Fig. 4. GT fuel mass flow rate profile, after the buffer tank, full-load operation.

Table 3
PI controller parameters after tuning.

K_p	0.232×10^{-3}
K_i	0.16×10^{-4}

Ziegler–Nichols method is used for tuning of the PI controller (Astrom and Hagglund, 1995). The controller gains were obtained by step responses (Ogata, 2010). (From a control theory point of view, the main role of the proportional term in the controller is to establish the stability of the system and improving the transient response, while the most important term, the integrator term makes the steady-state errors vary within negligible values.)

Following the closed loop Ziegler–Nichols rule, the controller parameters are found as in Table 3, which satisfy a fast dynamic response and acceptable performance characteristics.

2.2. GT performance characteristics

The characteristics of turbines are seldom published by manufacturers. Normally, the only publicly available data for GT performance are for the design point. Therefore, to estimate performance of GTs, models are employed. Such models depend on a point of operation to be known, which is typically the design point. In performance calculation of GTs, the turbine is commonly considered as choked and the so-called choked nozzle equation is used to describe the turbine inlet conditions. Performance at low load condition is exempted from this rule. Choked condition is referred to a condition which occurs when any further increase in pressure difference over the turbine does not increase the volumetric flow rate. The equation as presented in Eq. (7) relates turbine inlet pressure, turbine inlet mass flow rate, turbine inlet temperature (TIT) and turbine inlet molecular weight at an actual operating point to those of another operating point (Ulfsnes et al., 2003). The equation is derived based on the equation of continuity, Bernoulli conservation equation and assuming an isentropic change of state between the stagnation and actual static condition for sonic flow.

$$\frac{P_{\text{in}}}{P_{\text{in, design}}} = \frac{\dot{m}}{\dot{m}_{\text{design}}} \sqrt{\frac{T_{\text{in}} \cdot Mw_{\text{design}}}{T_{\text{in,design}} \cdot Mw}} \tag{7}$$

The type of the GT considered is based on the IGCC reference case, which is a large scale “F-class”, 50 Hz GT. Main operating parameters and performance of these kinds of turbines are given in Table 4. The variable-load operation of the GT is controlled by the fuel flow management. The GT fuel mass flow rate at different loads is estimated using the GTPRO software from Thermoflow (GTPro and ThermoFlow, 2011). The relation between the load of the GT and fuel mass flow rate is almost linear. The TIT varies according to energy balance of the combustor. The pressure ratio of the GT is varying according to the choked nozzle equation, meaning that turbine inlet pressure depends on TIT, turbine inlet flow rate and turbine inlet molecular weight. Change of the air flow rate using variable guide vanes in the compressor was not considered, but could be considered in future work.

Table 4
F-class, 50 Hz, large-scale gas turbines, average operating parameters (Franco et al., 2011).

Pressure ratio: 18.1
Net efficiency = 38.5%
Nominal power output = 279 MW
Natural gas pressure at the combustor inlet: 2.31 MPa (5 bar above the compressor outlet pressure
Specific work (defined as gas turbine output divided by the compressor intake mass flow rate) = 420 kJ/kg
Turbine outlet temperature (TOT) = 603 °C

Using a H_2-rich instead of natural gas as the GT fuel, demands some modifications on the design and hardware of a natural gas-based GT, including the combustion system and fuel nozzles. For the purpose of this work, the impacts of changing the GT fuel from natural gas to H_2-rich on the design of the GT are neglected. The reason for this is that change in transient performance is only slightly influenced by the design and operational modifications that are necessary with a H_2-rich fuel.

2.3. Numerical simulation

The set of partial differential algebraic equations describing the operation of the multi-bed PSA-based SEWGS process, available from the SEWGS modeling and simulation in the previous work (Najmi et al., 2013), was implemented in gPROMS (an equation-oriented modeling tool for process simulation, optimization and parameter estimation for steady-state and dynamic processes) (gPROMS, 2007). Multiflash physical property package incorporating Soave Redlich Kwong equation of state was used for calculation

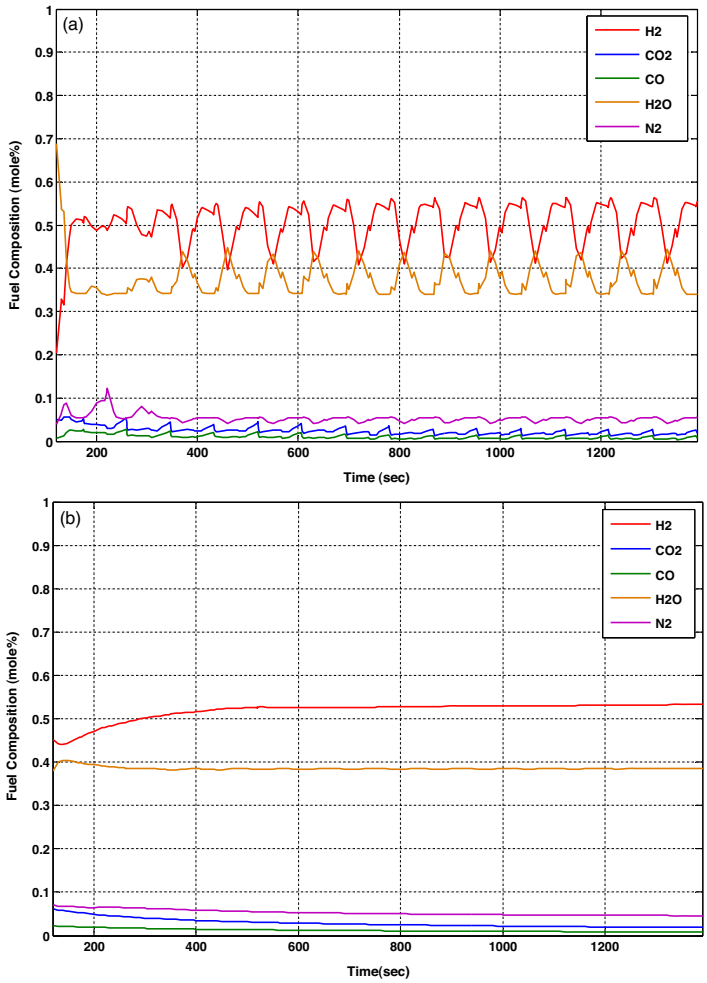

Fig. 5. (a) GT fuel composition, before the buffer tank. (b) GT fuel composition, after the buffer tank.

of physical properties. The centered finite difference method (CFDM) of second order was used to discretize the axial domain. The resulting system of equations was integrated over time by employing DASOLV solver (Jarvis and Pantelides, 1992). The time step size is automatically adjusted to maintain the error of integration within the specified tolerance. The mathematical model of the designed PI-based closed-loop control strategy including the buffer tank, fuel control valve and the GT, which consists of a set of non-linear algebraic and ordinary differential equations were implemented in a common programming platform, Matlab/Simulink®. The outlet of the SEWGS system is interfaced into Matlab/Simulink® to simulate the behavior of the IGCC integrated with the SEWGS process for CO_2 capture at full-load and part-load operations. Simulation of the GT in GTPRO, provided required input data such as the fuel mass flow rate variation per load change and TIT to simulate the entire system in Matlab/Simulink®.

3. Results

The results for full-load and part-load operation of the IGCC with the SEWGS pre-combustion technology are presented. To investigate part-load operations, four case studies are evaluated as shown schematically in Fig. 3. In the first case, the GT load changes (stepwise), without making any change in the upstream components (gasification, SEWGS). This is to investigate improved operation flexibilities of the GT when introducing an intermediate buffer tank between the SEWGS system and the GT. The capability of the current control strategy to respond to the GT load changes is revealed as well.

In the second case, the GT load changes to a level that corresponding changes in the upstream components (gasification, SEWGS) are also required. It is assumed that the upstream components respond instantaneously to the GT load changes. This is to examine the feasibility of the operation of the IGCC integrated with the SEWGS technology at part-loads in the absence of the time delays associated with the transient response of the components to the load changes. The third case takes into account the transient response of the GT upstream components. This case is studied to observe how the slowness of the GT upstream components impacts on the operation of the entire IGCC with CO_2 capture, when the GT load is changed. Finally, in the fourth case, the investigation is about the part-load conditions, where priorly planned GT and

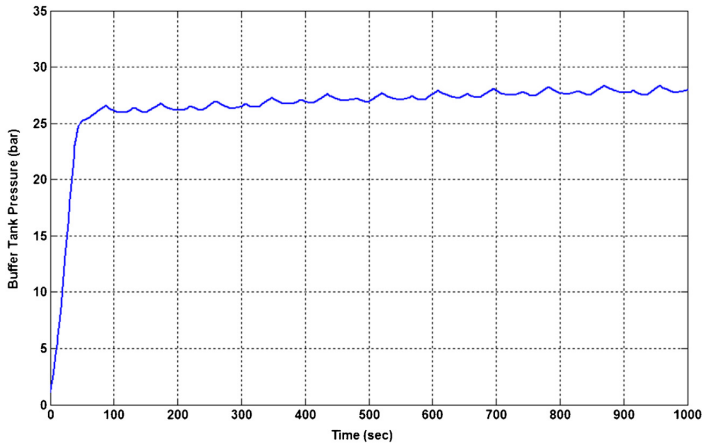

Fig. 6. Buffer tank pressure profile, full-load operation.

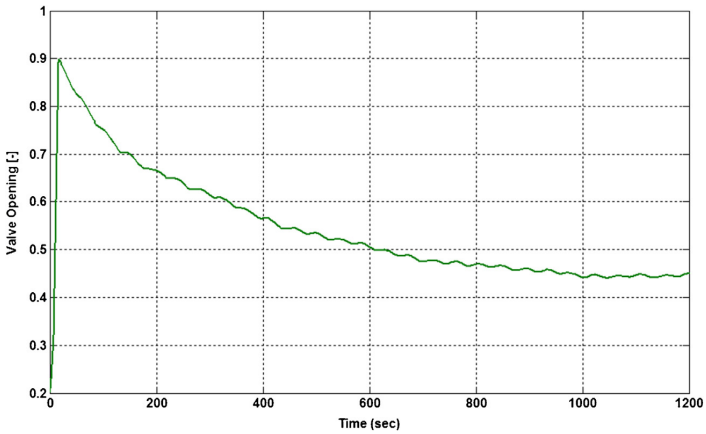

Fig. 7. Fuel control valve opening variation, full-load operation.

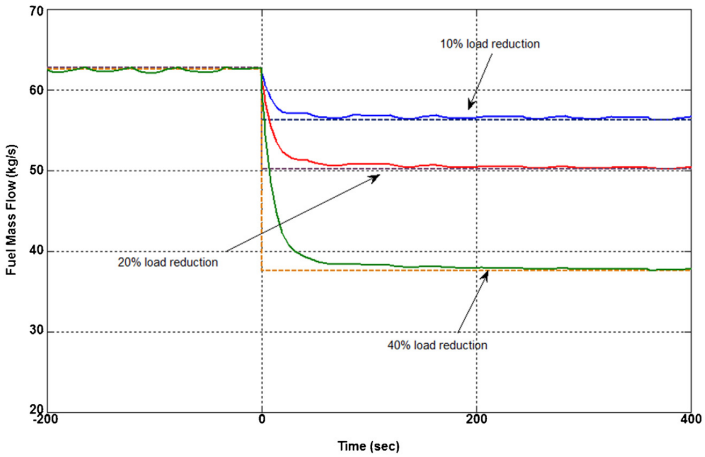

Fig. 8. Fuel mass flow rate profile, 10%, 20%, 40% GT load reduction (stepwise) at time = 0 s, constant GT upstream components.

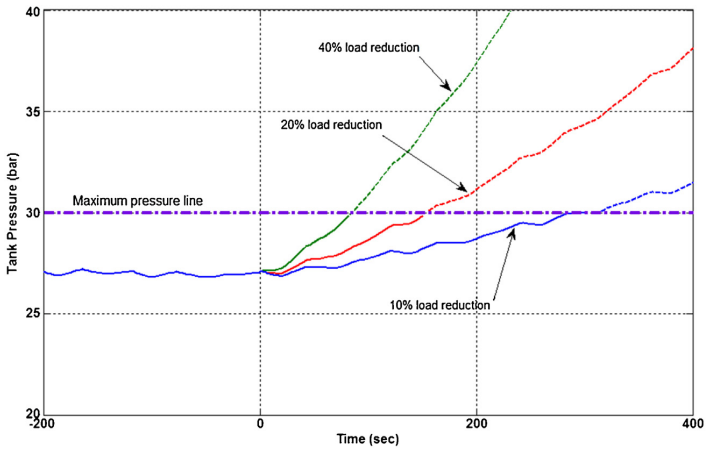

Fig. 9. Buffer tank pressure profile, 10%, 20%, 40% GT load reduction (stepwise) at time = 0 s, constant GT upstream components.

gasification load changes are applied. This is in contrast with the second and third cases, where the GT load changes are unplanned events (disturbances) and the gasification load change occurs once the disturbance is imposed on the GT load. In the fourth case, the gasifier load change does not necessarily take place at the same time with the GT load change. It can be initiated prior to the planned GT load change time. Due to the different load gradients of the gasifier, SEWGS and GT, this case can further improve load following performance of the IGCC integrated with the SEWGS technology.

To address each individual above-mentioned case, different GT part-load levels are employed. This is due to the different operation strategy of various cases. The GT part-load levels applied to one case may not provide fruitful results, when they are used for another case.

3.1. Full-load operation

Results obtained for the full-load operation of the GT are presented in this section. Simulation starts at an arbitrary point of operation, far from the full-load condition. The fuel mass flow rate is regulated by the control system to approach its set-point of 62.4 kg s^{-1}, corresponding to the GT full-load. Fig. 4 shows how the control strategy demonstrated in Fig. 2 controls the H_2-rich fuel mass flow rate. There is a transient state for about 600 s (10 min), before the steady-state operation mode is achieved. Thereafter, the fuel mass flow rate follows the set-point well, with oscillations of around 1–2%.

In addition to the fuel mass flow rate, the fuel composition is also of a great importance for the operation of the GT as variations may change the heating value of the fuel. Fig. 5a and b shows the H_2-rich fuel composition profile before and after the buffer tank at full-load operation of the GT. As it is observed from Fig. 5a, the composition of the H_2-rich fuel leaving the SEWGS system, which mainly consists of hydrogen and steam, fluctuates over time. The buffer tank between the SEWGS unit and the GT facilitates mixing of the H_2-rich fuel composition and damps out the fluctuations in the composition of the fuel as shown in Fig. 5b.

Furthermore, pressure variations within the buffer tank are illustrated in Fig. 6. The H_2-rich stream entering the buffer tank from the SEWGS system has an oscillating mass flow rate and

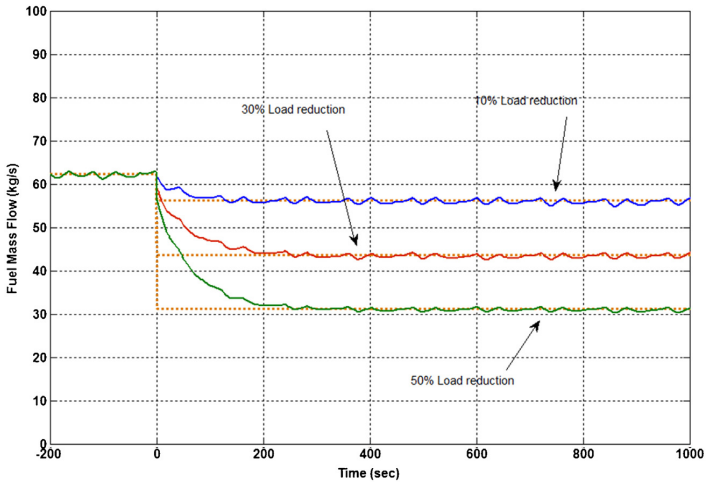

Fig. 10. Fuel mass flow rate profile at three different stepwise GT load reductions, instantaneous change of the GT upstream components.

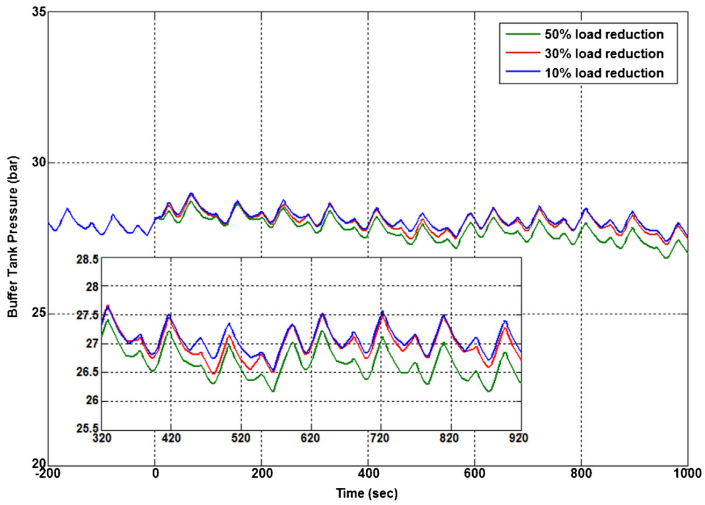

Fig. 11. Buffer tank pressure profile at three different stepwise GT load reductions, instantaneous change of the GT upstream components.

constant pressure about 27 bar as described (Najmi et al., 2013). The outlet flow rate of the buffer tank is set constant, due to the GT requirements. This results in fluctuating pressure in the buffer tank. To ensure a right direction of the flow toward the GT, pressure in the tank should always fall within the pressure of the upstream and downstream components, i.e. the SEWGS outlet pressure and the GT inlet pressure. Under the designed control strategy, controller parameters were tuned to maintain the pressure variations in the buffer tank within the acceptable range, while controlling the fuel mass flow rate leaving the buffer tank.

Fig. 7 shows the change of the fuel control valve stem position (opening) with time. The valve opening is inversely proportional to the square root of the pressure drop across the valve, when the fuel mass flow rate through the valve is set constant (Eq. (2)). The fluctuating pressure upstream of the control valve, but the constant downstream pressure is fulfilled with rapid changes of the valve opening to maintain the constant mass flow rate across the valve.

3.2. Part-load operation results

The results for the four cases considered for part-load operation strategies are presented in this section. It is assumed that the entire plant is operating at steady-state, before a GT load change takes place. The results are expressed in terms of two important plant variables, GT fuel mass flow rate and buffer tank pressure profile and acceptability of the results are evaluated. Performing dynamic simulations at different part-load, transient response time of the gasifier and SEWGS units to load changes are also compared and load following capability of the IGCC with CO_2 capture using the SEWGS technology is addressed.

3.2.1. First case: constant load of the GT upstream components

In this case, sudden changes are imposed to the GT load, while the load of the GT upstream components is kept constant. This manipulates the set-point value of the fuel mass flow rate. The measured fuel mass flow rate is compared against the new

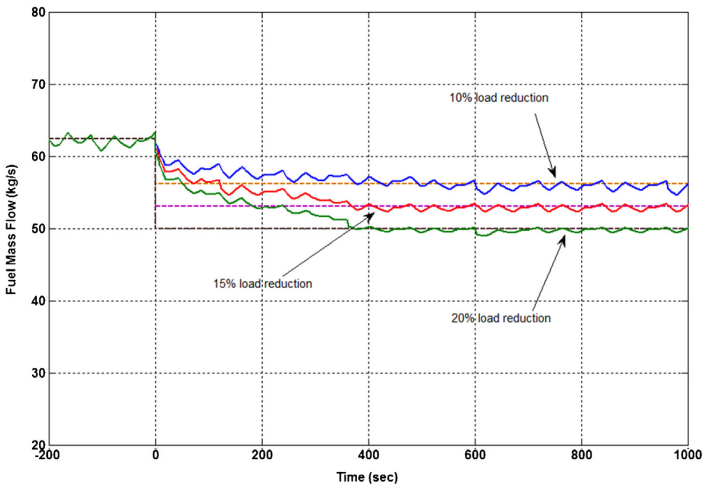

Fig. 12. Fuel mass flow rate profile, three different GT load reductions (stepwise), including the GT upstream components transient response time.

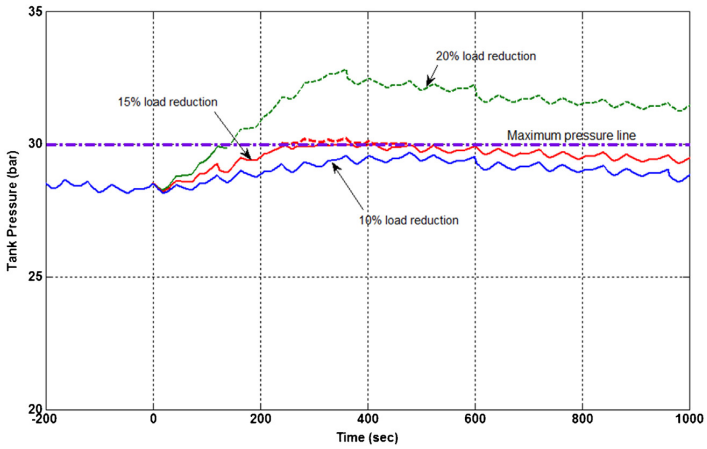

Fig. 13. Buffer tank pressure, three different GT load reductions (stepwise), including the GT upstream components transient response time.

set-point value and the fuel control valve manipulates the fuel flow rate to match its new set-point value as quick and accurate as possible. While the fuel mass flow rate is controlled properly, the buffer tank pressure determines if any change to the GT upstream components is necessary. As long as the pressure in the buffer tank stays within the acceptable range, the tank inlet flow can be kept constant when a change in the GT load takes place. In this case there would be no concern about load following capability of the GT upstream components.

10%, 20% and 40% stepwise load changes are given to the GT in sequence. The results for all three cases are shown in Figs. 8 and 9 in terms of the fuel mass flow rate and buffer tank pressure profile. As shown in Fig. 8, the higher the GT load reduction, the more smooth the GT fuel mass flow rate profile is.

When the GT load is reduced, the fuel mass flow rate leaving the buffer tank is reduced correspondingly. On the other hand, the inlet stream to the tank is kept constant, meaning that the gasification process is operated without any change. This, as shown in Fig. 9, results in a constantly pressure build-up in the tank. Setting the high tank pressure limit at 30 bar, it takes about 280, 160, 85 s for the buffer tank pressure to reach this limit when the GT load reduction of 10%, 20% and 40% are applied, respectively. The length of the time that the GT can operate at part-load without the need to make any change in the upstream components is an indicator of the improved operation flexibility of the GT at part-load condition. This temporary operation flexibility is achieved as a result of having the intermediate buffer tank before the GT. The less the GT load is reduced, the more the length of the flexible operation time is extended. The maximum pressure limit is indicated by the maximum pressure line in Fig. 9. The dashed pressure lines which are higher than the maximum pressure limit represent unrealistic conditions. However, they are shown to facilitate assessment and identification of the transients, i.e. transient response time of the components (SEWGS and gasifier) and the buffer tank pressure trend until a new steady state is achieved.

3.2.2. *Second case: instantaneous load change of the GT upstream components*

This case is a starting point to investigate load following performance of an IGCC integrated with the SEWGS process. It is assumed that once a disturbance in the GT load occurs, the resulting change will be transferred immediately through the entire system and the upstream components respond to the GT load changes with no delay. Fig. 10 shows the fuel mass flow rate when 10%, 30% and 50% stepwise change in the GT load is imposed at an arbitrary operating point (time = 0 s). Following the GT load change, the corresponding changes in the GT upstream components and as a consequence in the buffer tank inlet stream take place (with no delay).

The transient mass flow rate behavior is a consequence of the PI controller response time. For the three different GT load reductions of 10%, 30% and 50%, the length of the time required by the controller to reach a new steady-state condition is shown (Fig. 10). It is expected that as the load goes down, the transient behavior of the controller before a new steady-state lasts longer. For instance for the 50% GT load reduction, this time is around ~250 s, while ~180 s is for that of 30% GT load reduction.

Pressure changes in the buffer tank for this case are shown in Fig. 11. The figure shows that for all three levels of the GT load reduction, pressure in the tank falls within the acceptable range and the forward flow of the H_2-rich fuel to the GT is ensured.

3.2.3. *Third case: including transient response of the GT upstream components*

In a real operating process, when a disturbance is imposed to the process at one end, it will not be transferred to the other end immediately, but with some delay. The main source of the delay is related to the response time of the sub-processes and depending on the dynamics of the process, response time varies from a process component to another process component.

In this case, when a sudden load change (stepwise) is imposed to the GT, it triggers corresponding changes in the upstream components (gasification, SEWGS). The main source of the time delay upstream of the GT is caused mainly by the slow dynamics of the SEWGS and the gasifier compared to the GT. A gasification process load gradient in an IGCC power plant is typically around 3–5% load/min (Domenichini et al., 2013). The SEWGS system response time to the load changes is revealed by dynamic simulation of the system.

Figs. 12 and 13 show the condition where the GT undergoes three different step changes of 10%, 15% and 20% in the load. Following the GT load change, the gasification and SEWGS system loads are changed. A gasification load gradient of 3% is assumed to take into account the gasification response time to the load changes. As shown in Fig. 12, the control strategy of the GT fuel functions similar to the previously demonstrated cases and controls the fuel mass flow rate to approach each new set-point value shown as dotted lines.

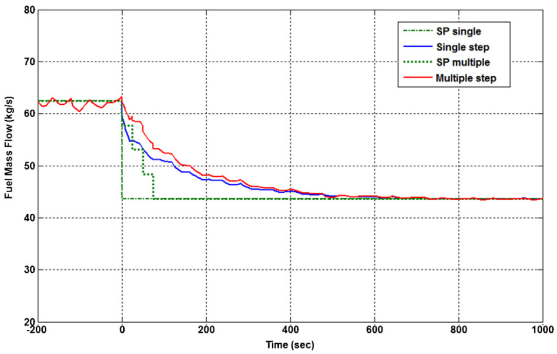

Fig. 14. Fuel mass flow rate profile, 30% step change in the GT load via a single step of 30% and four small steps of 7.5%, with 15 s waiting time between the steps.

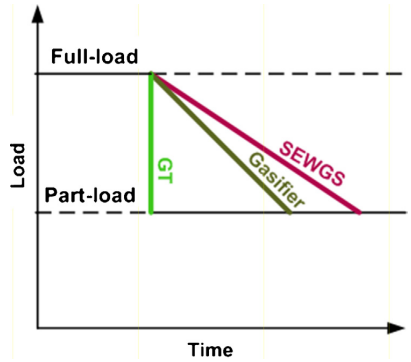

Fig. 16. Comparison of the GT, gasifier and SEWGS load gradients.

On the other hand, as indicated in Fig. 13, once a step reduction in the GT load is occurred, the buffer tank pressure starts increasing and after some time exceeds its maximum value, set at 30 bar. (~280 s and ~160 s for 15% and 20% load reduction, respectively). The pressure increase continues until the gasifer and the SEWGS transient response time is passed and the buffer tank inlet and outlet streams are balanced again. The buffer tank pressure then follows a slightly decreasing pattern toward stabilization. Pressure lines above the maximum pressure limit (indicated by dashed lines) cannot be achieved realistically.

Investigating part-load operations in the third case, demonstrates that some part-load operations (GT load reduction of more than 10%) will lead to undesirably high tank pressures which result in backflow and safety problems. This is mainly due to the slow dynamics of the SEWGS and gasification processes compared to the relatively fast dynamics of the GT. With increasing the load reduction percentage, i.e. 30% load reduction, the tank pressure will exceed the maximum pressure faster and remain out of the desired pressure range for a longer period of time. This condition is against the target of operating the plant safely and establishing a forward pressure driven flow of the H_2-rich gas to the GT.

An alternative approach to turn down the GT load is to apply multiple stepwise load changes instead of a single step change, which was investigated so far. Here the results are presented for the cases, where changes in the GT load were applied through a number of multiple smaller changes in a stepwise manner with time lags between the steps. Figs. 14 and 15 compare the results obtained for two different cases of imposing a 30% step change to the GT load through one single step or four steps of 7.5% load change. As shown in Fig. 14, in the case when a single step change of 30% is imposed to the GT load, fuel mass flow rate is decreased by the control system and starts approaching the new set-point value. After about 620 s, it reaches the new set-point value. For the multiple step change strategy, the same pattern is observed and new stable state happens after almost the same time. On the other hand, pressure profile in Fig. 15 shows that the buffer tank pressure behavior is improved when the multiple step change is applied to the GT load. This is due to the fact that it will extend the duration of the GT load change and so make it easier for the gasifier to comply with the relatively quick GT load change.

3.2.4. SEWGS vs. gasification load gradients

The IGCC power plant incorporating the SEWGS process as a pre-combustion CO_2 capture consists of a number of different subprocesses as shown in Fig. 1. To predict performance of the entire IGCC with the SEWGS technology, identifying the dynamic characteristics of each process component is necessary. GT as a turbo machinery unit operation within the IGCC is considered as a component with fast dynamics compared to the components such as gasifier and the SEWGS. Simulation of the SEWGS process at

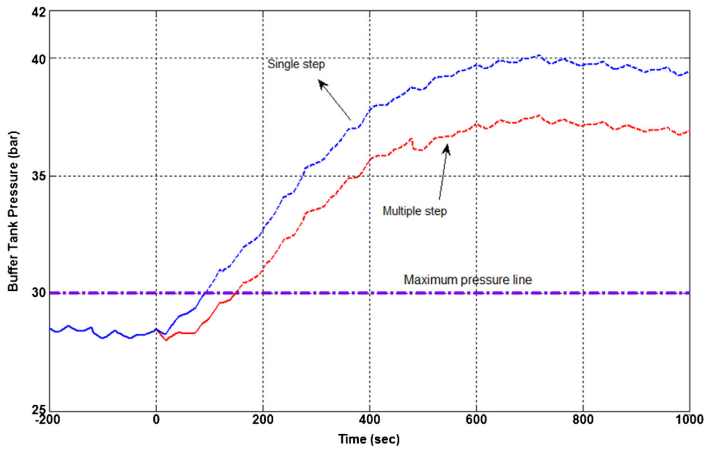

Fig. 15. Buffer tank pressure profile, 30% step change in the GT load via a single step of 30% and four small steps of 7.5%, with 15 s waiting time between the steps.

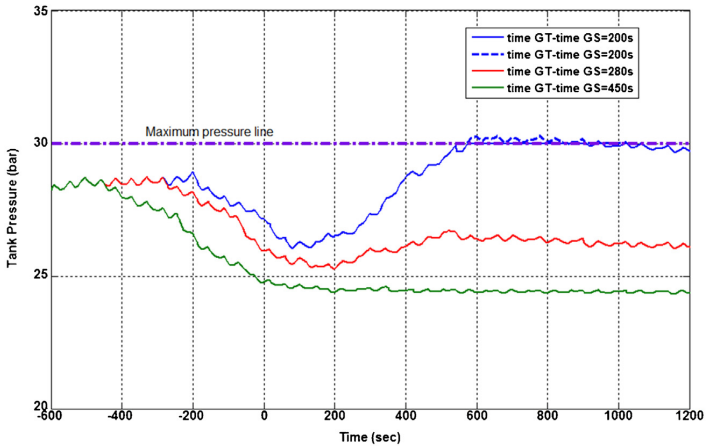

Fig. 17. Buffer tank pressure profile, comparison of three different gasification ramp-down time (time GS) and fixed GT ramp-down time (time GT = 0 s). 40% GT load reduction.

different inlet conditions provides understanding about the dynamic characteristic of this system.

For the gasification process, the typical gasification load gradient of 3% is assumed in this work. Comparing the two processes of gasification and SEWGS with respect to the ramp rates, it is found that the SEWGS system has the slower dynamics compared to the gasification. It is shown schematically in Fig. 16.

3.2.5. Fourth case: planned GT and gasifier load change (ramp)

In this section results are presented for the cases where a ramp rate of 10% is considered for the GT, in contrast to the previous cases of applying sudden step changes to the GT load. This is more realistic to do as the load change in heavy duty GTs may occur in a matter of minutes. Moreover, changing the gasifier load may not necessarily occur once the GT load is ramped down or up. This can be initiated prior to the GT load change, to compensate the inertia of the GT upstream components. Therefore, one solution to avoid too high pressure build-ups in the tank and possibly obtain a satisfactory operation of the system at part-load is to operate the entire system according to a pre-planned strategy for load changes. However, this strategy will not be able to withstand unplanned disturbances which may be experienced during the operation of the system.

3.2.5.1. Gasifier load change time prior to the GT load change. Figs. 17 and 18 show the buffer tank pressure variations and the GT fuel mass flow rate when the GT load ramps down from full-load to 60% load at an arbitrary point of a steady-state operation. The ramp-down time of the GT is assumed to be known (time GT). Different times for ramping down the gasifier load prior to the GT ramp-down time (time GS) were investigated and behavior of the system was observed. Results obtained with three different values of the time difference between the gasifier and GT ramp-down (time GT – time GS) are presented. When (time GT – time GS) equals 280 s, this means the gasifier ramp-down begins 280 s earlier than that of the GT. Turning down the gasifer load, whereas keeping the GT load constant for 280 s, the buffer tank mass balance will be disturbed due to the reduction of the tank inlet flow

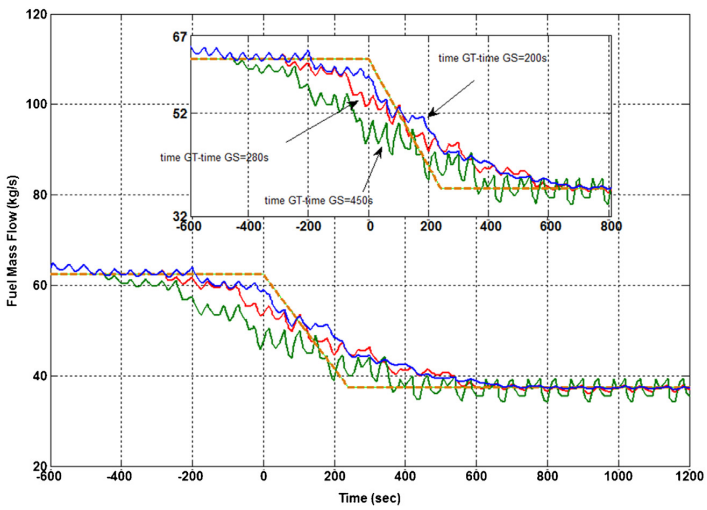

Fig. 18. Fuel mass flow rate profile, comparison of three different gasification ramp-down time (time GS) and fixed GT ramp-down time (time GT = 0 s). 40% GT load reduction.

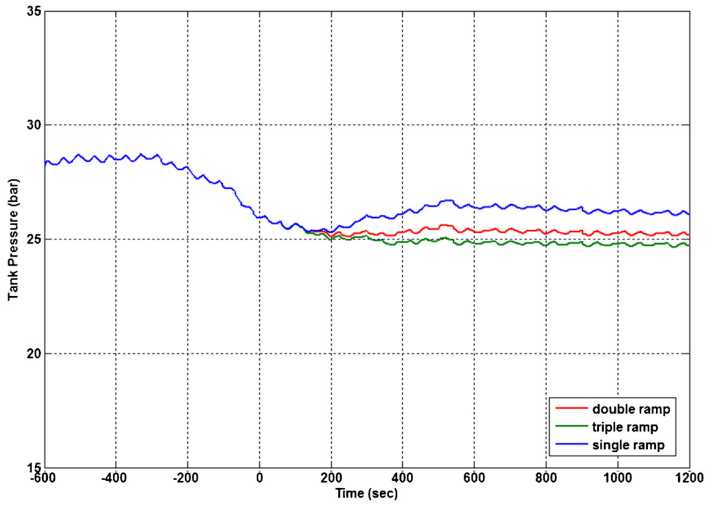

Fig. 19. Buffer tank pressure profile, comparison of single, double, triple GT load ramp-down (40% GT load change) at time GT = 0 s, time GS, 280 s earlier than time GT.

rate, while the exit flow rate is still unchanged. This will lead to a pressure decrease in the tank. When the GT ramp-down time is reached and the GT load starts decreasing, the tank exit mass flow rate will also be ramped down and the tank pressure will start increasing again until the GT load is completely ramped down to 60%. The system then approaches a steady-state mode (Fig. 17). The fuel mass flow rate profile shows quite long transient period before reaching a steady-state again, due to being exposed to two disturbances occurred at different times, once, when the gasifier load changes and second, when the GT load turns down (Fig. 18). The speed of the controller and how fast it adjusts the fuel mass flow rate with any new set-point affects the length of the transient period. The faster the controller, the shorter the duration of the transient state after the load change is. In the case where (time GT – time GS) equals 450 s, meaning that the gasifier ramp-down starts 450 s before starting the GT ramp-down, the pressure reduction in the tank starts earlier than the previously discussed case. The pressure decrease continues until the GT ramp-down time begins. The fuel mass flow rate is then adjusted to the new set-point value. Thereafter the tank pressure will be stabilized. Allowing the gasifier to initiate its load change earlier than the GT, will lead to improved pressure behaviors in the tank (compared to the previous case study of initiating the GT and gasifier load change at the same time), but longer transient behavior of the fuel mass flow rate is observed in return. The closer the gasifier ramp-down time to the GT ramp-down time, the higher the tank pressure and the shorter the transient behavior of the GT fuel mass flow rate are. Among the three cases investigated with different gasifier ramp-down time, the case of starting the gasifier load change 280 s earlier than that of the GT, shows the best results in terms of the fuel flow rate (less oscillating and better following the set-point values, as well as, pressure (within the acceptable range).

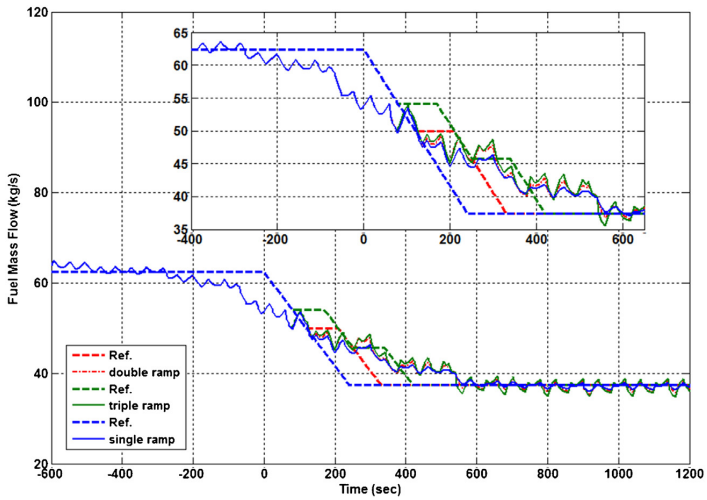

Fig. 20. Fuel mass flow rate profile, comparison of single, double, triple GT load ramp-down (40% GT load change) at time GT = 0 s, time GS, 280 s earlier than time GT.

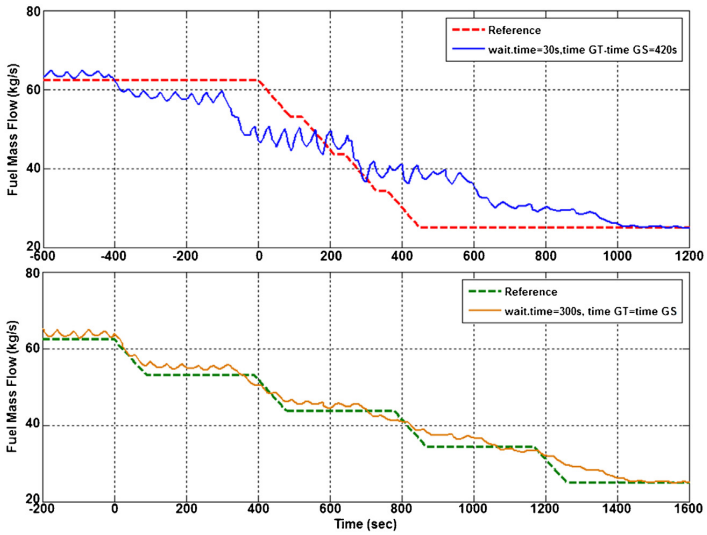

Fig. 21. Fuel mass flow profile, comparison of (time GT – time GS) = 420 s, waiting time = 300 s vs. time GT = time GS, waiting time = 30 s, 60% GT load reduction.

3.2.5.2. Single vs. multiple ramps for the GT load change. There is not one single instruction about load change strategy of GTs. The various manufacturers have their own rules, which are most of the time confidential and not found as available data. One of the objectives of this work is to investigate conditions and operation strategies, which result in smooth operation of the IGCC with the SEWGS technology at part-load. Therefore, an alternative procedure of changing the GT load through multiple smaller ramps instead of applying a single ramp is evaluated to observe load following performance and transient behavior of the entire system.

Allowing the gasifier to initiate the load change 280 s prior to the GT load change (the previously presented results), three different strategies of the GT load ramp-down are investigated and compared to each other. The buffer tank pressure and fuel mass flow rate profile for three cases of single, double and triple GT load ramps down to 60% are demonstrated in Figs. 19 and 20, respectively. Applying multiple ramp change to the GT load, with a time delay of 90 s between the ramps until reaching a new GT load level, provides an opportunity to the gasifier and the following SEWGS system to better follow the GT load changes. This will reduce the imbalances occurred in the system as a consequence of different response time of the process components to the load changes, i.e. fast dynamics of the GT, compared to the slow dynamics of the gasifier and SEWGS. Triple ramp-down strategy shows more stable behavior for the tank pressure profile compared with the double and single ramp-down strategies.

Another operating procedure for the part-load operation of the IGCC with the SEWGS system is shown in Figs. 21 and 22, where the gasifier load change is initiated once the GT load is changed (strategy A). The GT load is ramped down to 40% through four

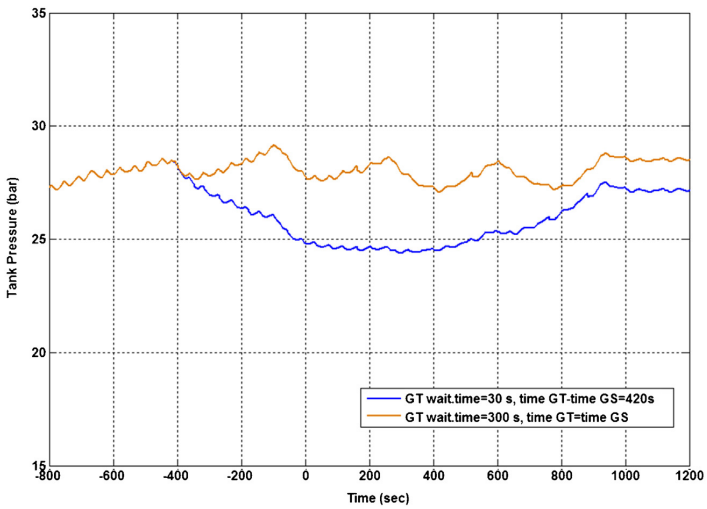

Fig. 22. Buffer tank pressure profile, comparison of (time GT – time GS) = 420 s, waiting time = 300 s vs. time GT = time GS, waiting time = 30 s, 60% GT load reduction.

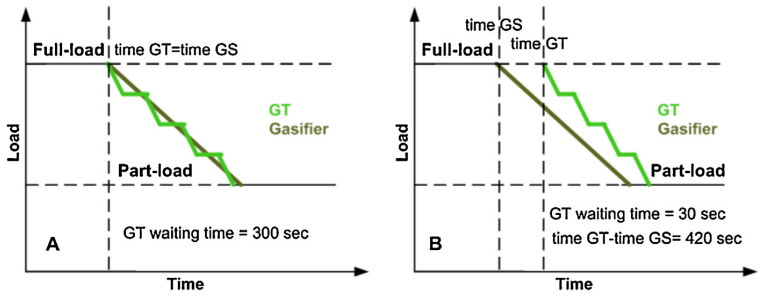

Fig. 23. Comparison of strategy A and strategy B, in terms of the GT and gasifier load gradients.

ramps of 15% with time delay between the ramps (300 s). Prolonging the GT load change with such a strategy reduces the mismatches between the ramp rates of the GT and process components (gasifier, SEWGS). The tank pressure profile of this strategy is shown in Fig. 22 and compared with the other strategy (strategy B), where the gasifier load ramp-down takes place 420 s earlier than the GT, with the waiting time of 30 s between the ramp changes. The pressure profile in the tank for both strategies is acceptable as it remains within the maximum and minimum values during the operation. The results show a more smooth mass flow rate behavior during the transient state for strategy A. A comparison of the two strategies (A and B) in terms of the GT and gasification load gradients is illustrated schematically in Fig. 23. It can be concluded that it is possible to reduce the GT load down to 60%, while operating the plant within a possible operating envelop. The multiple ramps plus waiting time strategy can be effective to maintain the smooth operation of the plant when the GT load is changed either unplanned (disturbance) or planned.

4. Conclusion

Full-load and part-load simulation of an IGCC power plant incorporating a Sorption Enhanced Water Gas Shift (SEWGS) technology for pre-combustion CO_2 capture was investigated. A detailed modeling of the SEWGS system previously developed was used as the base model for simulation in this work (Najmi et al., 2013). A control strategy consisting of a buffer tank followed by a control valve was implemented between the SEWGS and the Gas Turbine (GT) to smooth out the fluctuating H_2-rich fuel, from the SEWGS, with respect to mass flow rate as well as pressure and composition. For full-load operation, it was found that the designed control strategy performs properly and the fuel mass flow rate approaches the set-point after steady-state is reached. Moreover, the buffer tank pressure variations fall within the acceptable range, ensuring sufficient flow rate and pressure of the H_2-rich fuel to the GT. Also the oscillating fuel composition from the SEWGS system is smoothened out after leaving the buffer tank. Part-load performance was investigated in four different cases, with each case presenting a different part-load operation strategy. In the first case, stepwise GT load changes were imposed, while operation of the GT upstream components was kept constant. It was found that using the intermediate buffer tank between the SEWGS and the GT, as part of the fuel control system, improved the operation flexibility of the GT. However, depending on the GT part-load levels, there is a time limit for the flexible and smooth operation of the IGCC with the SEWGS under such a part-load operation strategy. The second case focused on a part-load operation strategy, where the GT upstream components were subject to corresponding load changes (instantaneously), once a stepwise GT load change (disturbance) was applied. Simulation results revealed that the smooth operation of the IGCC with the SEWGS system at part-loads is achievable in the absence of the time delays associated with the transient response of the components to the load changes. Also, it was observed that the designed control system functions properly and controls the fuel mass flow rate with its set-point value(s), while maintaining the buffer tank pressure within the allowed range. In the third case single and multiple step changes to the GT load were imposed. The GT upstream components were changed accordingly, taking into account the transient response of the components to the load changes. A typical gasification load gradient of 3% was used. It was observed that at some part-load operations (more than 10% GT load reduction), undesirable operating conditions in terms of the buffer tank pressure took place for a period of time during the operation. This is due to the slowness of the upstream process components in responding to the load changes compared to the relatively quick response of the GT. Applying multiple stepwise GT load changes, as expected, improved the pressure behavior in the tank vs. the single GT step changes. Simulation of the IGCC integrated with the SEWGS system at different load levels, revealed that the SEWGS system possesses the slower transient dynamics rather than the gasifier. The fourth case was investigated with the intention of reducing the flow rate imbalances as a consequence of different transient dynamics of the gasifier, SEWGS and the GT and thus achieving smooth operation of the IGCC with the SEWGS at part-load. It was assumed that the GT and gasifier load changes were priorly planned. A ramp rate of 10% was considered for the GT load change, instead of stepwise load change strategy. Single and multiple GT load ramp-down (including waiting time before the next ramp) were considered. Assuming a planned GT load change time, different gasification ramp-down times, ahead of the GT, were studied and behavior of the system was observed. It was found that, depending on the time allowed between the gasifier and the GT load change, it is possible to maintain the buffer tank pressure within the acceptable range and achieve a smooth operation of the IGCC with the SEWGS, while mass flow rate is also controlled properly. It was understood that the CO_2 capture process together with the gasification process can follow different GT load changes, when the operating schedule of the part-load for the gasifier and GT is planned. The multiple-ramp plus waiting time strategy appeared as an effective strategy to maintain the smooth operation of the plant when the GT load is changed either unplanned (disturbance) or planned.

References

Allam, R.J., Chiang, R., Hufton, J.R., Middleton, P., Weist, E., White, V., 2005. Development of sorption enhanced water gas shift process. In: Thomas, D., Benson, S. (Eds.), Carbon Dioxide Capture for Storage in Deep Geologic Formations, vol. 1, pp. 227–256.

Astrom, K.J., Hagglund, T., 1995. PID Controllers: Theory, Design and Tuning. Instruments Society of America.

Bakken, E., Cobden, P.D., Henriksen, P.P., Håkonsen, S.F., Spjelkavik, A.I., Stange, M., Stensrød, R.E., Vistad, Ø., Blom, R., 2011. Development of CO_2 sorbents for the SEWGS process using high throughput techniques. Energy Procedia 4, 1104–1109.

2008. Caesar FP7 Project, http://caesar.ecn.nl

Choi, S., Drese, J.H., Jones, C.W., 2009. Adsorbent materials for carbon dioxide capture from large anthropogenic point sources. ChemSusChem 2, 796–854.

Domenichini, R., Mancuso, L., Ferrari, N., Davison, J., 2013. Operating flexibility of power plants with carbon capture and storage (CCS). Energy Procedia 37, 2727–2737.

Franco, F., Anantharaman, R., Bolland, O., Booth, N., van Dorst, E., Ekstrom, C., Sanchez, E., Macchi, E., Manzolini, G., Prins, M., Pfeffer, A., Rezvani, S., Robinson, L., Zahra, A.M., 2010. Common framework and test cases for transparent and comparable techno-economic evaluations of CO_2 capture technologies – the work of the European Benchmarking Task Force. In: Proceedings of GHGT-10, Amsterdam, NL.

Franco, F., Anantharaman, R., Bolland, O., Booth, N., van Dorst, E., Ekstorm, C., Sanchez, E., Macchi, E., Manzoloni, G., Nikolic, D., Pfeffer, A., Prins, M., Rezvani, S., Robinson, L., 2011. Enabling advanced pre-combustion capture techniques and plants. Technical report. Alstom, United Kingdom.

Gazzani, M., Macchi, E., Manzolini, G., 2013a. CO_2 capture in integrated gasification combined cycle with SEWGS – Part A: Thermodynamic performances. Fuel 105, 206–219.

Gazzani, M., Macchi, E., Manzolini, G., 2013b. CO_2 capture in natural gas combined cycle with SEWGS. Part A: Thermodynamic performances. Int. J. Greenh. Gas Control 12, 493–501.

gPROMS, 2007. PSE Enterprise, www.psenterprise.com

GTPro, ThermoFlow, 2011. User's Manual. Release 21.

Halabi, M.H., de Croon, M.H.J.M., van der Schaaf, J., Cobden, P.D., Schouten, J.C., 2012. High capacity potassium-promoted hydrotalcite for CO_2 capture in H_2 production. Int. J. Hydrogen Energy 37, 4516–4525.

Harrison, D.P., 2008. Sorption enhanced hydrogen production: a review. Ind. Eng. Chem. Res. 47, 6486–6501.

Jang, H.M., Lee, K.B., Caram, H.S., Sircar, S., 2012. High-purity hydrogen production through sorption enhanced water gas shift reaction using K_2CO_3-promoted hydrotalcite. Chem. Eng. Sci. 73, 431–438.

Jansen, D., van Selow, E., Cobden, P.D., Manzolini, G., Macchi, E., Gazzani, M., Blom, R., Henriksen, P., Beavis, R., Wright, R., 2013. SEWGS technology is now ready for scale-up. Energy Procedia 37, 2265–2273.

Jarvis, R.B., Pantelides, C.C., 1992. DASOLV – A Differential-Algebraic Equation Solver. Centre for Process Systems Engineering, Imperial College, London.

Lawal, A., Wang, M., Stephenson, P., Yeung, H., 2009. Dynamic modeling of CO_2 absorption for post-combustion capture in coal-fired power plants. Fuel 88, 2455–2462.

Liu, Z., Grande, C.A., Li, P., Yu, J., Rodrigues, A.E., 2011. Multi-bed vacuum pressure swing adsorption for CO_2 capture from flue gas. Sep. Purif. Technol. 81, 307–317.

Lu, H., Lu, Y., Rostam-Abadi, M., 2013. CO_2 sorbents for a sorption-enhanced water–gas-shift process in IGCC plants: a thermodynamic analysis and process simulation study. Int. J. Hydrogen Energy 38, 6663–6672.

Luyben, M.L., Luyben, W., 1997. Essentials of Process Control. McGraw-Hill.

Manzolini, G., Macchi, E., Binotti, M., Gazzani, M., 2011. Integration of SEWGS for carbon capture in natural gas combined cycle. Part A: Thermodynamic performances. Int. J. Greenh. Gas Control 5, 200–213.

Manzolini, G., Macchi, E., Gazzani, M., 2013. CO_2 capture in natural gas combined cycle with SEWGS. Part B: Economic assessment. Int. J. Greenh. Gas Control 12, 502–509.

Martunus, Othman, M.R., Fernando, W.J.N., 2011. Elevated temperature carbon dioxide capture via reinforced metal hydrotalcite. Microporous Mesoporous Mater. 138, 110–117.

Najmi, B., Bolland, O., Westman, S.F., 2013. Simulation of the cyclic operation of a PSA-based SEWGS process for hydrogen production with CO_2 capture. Energy Procedia 37, 2293–2302.

Nikolic, D., Giovanoglou, A., Georgiadis, M.C., Kikkinides, E.S., 2008. Generic modeling framework for gas separations using multi-bed pressure swing adsorption processes. Ind. Eng. Chem. Res. 47, 3156–3169.

Ogata, K., 2010. Modern Control Engineering, fifth ed. Prentice Hall.

Reijers, H.T.J., Valster-Schiermeier, S.E.A., Cobden, P.D., Van Den Brink, R.W., 2006. Hydrotalcite as CO_2 sorbent for sorption-enhanced steam reforming of methane. Ind. Eng. Chem. Res. 45, 2522–2530.

Reijers, H.T.J., Boon, J., Elzinga, G.D., Cobden, P.D., Haije, W.G., van den Brink, R.W., 2009. Modeling study of the sorption-enhanced reaction process for CO_2 capture. II. Application to steam-methane reforming. Ind. Eng. Chem. Res. 48, 6975–6982.

Singh, R., Ram Reddy, M.K., Wilson, S., Joshi, K., Costa, J., Webley, P., 2009. High temperature materials for CO_2 capture. Energy Procedia 1, 623–630.

Siriwardane, R.V., Robinson, C., Shen, M., Simonyi, T., 2007. Novel regenerable sodium-based sorbents for CO_2 capture at warm gas temperatures. Energy Fuels 21, 2088–2097.

Stevens Jr., R.W., Shamsi, A., Carpenter, S., Siriwardane, R., 2010. Sorption-enhanced water gas shift reaction by sodium-promoted calcium oxides. Fuel 89, 1280–1286.

Ulfsnes, R.E., Bolland, O., Jordal, K., 2003. Modeling and simulation of transient performance of the semiclosed O_2/CO_2 gas turbine cycle for CO_2 capture. In: Proceedings of ASME Turbo Expo, pp. 16–19.

Van Dijk, H.A.J., Walspurger, S., Cobden, P.D., van den Brink, R.W., de Vos, F.G., 2011. Testing of hydrotalcite-based sorbents for CO_2 and H_2S capture for use in sorption enhanced water gas shift. Int. J. Greenh. Gas Control 5, 505–511.

Van Selow, E.R., Cobden, P.D., Verbraeken, P.A., Hufton, J.R., van den Brink, R.W., 2009. Carbon capture by sorption-enhanced water–gas shift reaction process using hydrotalcite-based material. Ind. Eng. Chem. Res. 48, 4184–4193.

Van Selow, E.R., Cobden, P.D., Wright, A.D., van den Brink, R.W., Jansen, D., 2011. Improved sorbent for sorption-enhanced water–gas-shift process. Energy Procedia 4, 1090–1095.

Wright, A., White, V., Hufton, J.R., van Selow, E., Hinderink, P., 2009. Reduction in the cost of pre-combustion CO_2 capture through advancements in sorption enhanced water–gas-shift. Energy Procedia 1, 707–714.

Wright, A.D., White, V., Hufton, J.R., Quinn, R., Cobden, P.D., van Selow, E.R., 2011. CAESAR: development of a SEWGS model for IGCC. Energy Procedia 4, 1147–1154.

Yong, Z., Mata, V., Rodrigues, A.E., 2002. Adsorption of carbon dioxide at high temperatures: a review. Sep. Purif. Technol. 26, 195–205.

Paper 4

Available online at www.sciencedirect.com

ScienceDirect

Energy Procedia 63 (2014) 1986 – 1995

Energy Procedia

GHGT-12

Operability of Integrated Gasification Combined Cycle power plant with SEWGS technology for pre-combustion CO_2 capture

Bita Najmi[a]*, Olav Bolland[a]

[a]*Norwegian University of Science and Technology (NTNU), Trondheim, Norway*

Abstract

This paper investigates the performance of an integrated gasification combined cycle (IGCC) power plant incorporating a sorption enhanced water gas shift (SEWGS) process for pre-combustion CO_2 capture at part-load conditions. The multi-train SEWGS process operates on a cyclic manner based on a pressure swing adsorption (PSA) process and reaches a cyclic steady state. Each train consists of eight SEWGS vessels. A H_2-rich stream which is produced at high temperature and pressure is sent to a gas turbine (GT) as an almost carbon-free fuel for power generation. A CO_2-rich stream, the secondary product of the SEWGS process, is released from the solid adsorbent at low pressure. Dynamic mathematical modeling of the SEWGS system developed previously is used to simulate the performance of the SEWGS system at different part-loads. A control strategy including a buffer tank and a closed-loop proportional integral (PI) controller is designed to provide the required amount of the fuel to the GT at full-load and part-load modes of operation. The control system performance is very important to provide a fuel from the SEWGS system that fulfils the requirement of the GT with respect to fuel pressure and heating value variations. Simulation results show when the GT load is changed, the control system functions properly and provides the corresponding GT fuel flow after a new steady-state condition is reached. The H_2-rich stream flow rate fluctuation, associated with the cyclic operation of the SEWGS process, is reduced from ~±14% to ~±1% under the effect of the designed PI controller. On the other hand, when a load change is given to the GT, operation of the entire IGCC plant is dictated by the rate of change of the SEWGS system. The load gradient of the SEWGS process achieved from the part-load simulations is ~2% load/min. The SEWGS system is not able to respond to load changes as rapid as the GT. This will reduce the operation flexibility of the entire IGCC Plant. However, the addition of the intermediate buffer tank improves the operation flexibility of the GT as long as the pressure variation in the tank falls within the acceptable range.

Peer-review under responsibility of the Organizing Committee of GHGT-12

Keywords: SEWGS; H_2-rich; CO_2 capture; GT; IGCC; part-load

* Corresponding author. Tel.: +47-73593697
E-mail address: bita.najmi@ntnu.no

Peer-review under responsibility of the Organizing Committee of GHGT-12
doi:10.1016/j.egypro.2014.11.213

Nomenclature

Abbreviations	
ASU	Air separation unit
CSS	Cyclic steady state
GT	Gas turbine
HP	High pressure
HTC	Hydrotalcite
HTS	High temperature shift
IGCC	Integrated gasification combined cycle
LP	Low pressure
LTS	Low temperature shift
NGCC	Natural gas combined cycle
PI	Proportional integral
PSA	Pressure swing adsorption
SEWGS	Sorption enhanced water gas shift
SP	Set-point
ST	Steam turbine
Symbols	
$\dot{m}_{fuel.measured}$	Measured fuel mass flow rate (kg/s)
$\dot{m}_{fuel.setpoint}$	Fuel mass flow rate set-point value (kg/s)
error	Difference between the measured fuel mass flow rate and its set-point value (kg/s)
K_c	Anti-windup coefficient (-)
K_i	Integral coefficient (-)
K_p	Proportional coefficient (-)
$U_{controller}$	Classical PI controller output (kg/s)
U_i	The integral term (kg/s)
U_p	The proportional term (kg/s)
Xvalve_act	Control valve actuator opening (-)

1. Introduction

Integrated gasification combined cycle (IGCC) is a power production technology in which a solid feedstock such as coal is gasified and converted to syngas. Syngas is basically a mixture of carbon monoxide and H_2 along with some minor components (e.g. carbon dioxide, water vapor, hydrogen sulphide, ammonia, etc.). The syngas is then converted to electricity in a combined cycle power block which consists of a gas turbine (GT), steam turbine (ST) and heat recovery steam generator (HRSG).

IGCC plants can take the advantage of the high pressure of the syngas stream for utilizing a CO_2 capture process to remove the CO_2 from the syngas before combustion in the GT. Physical absorption-based processes by using physical solvents, such as Selexol or Rectisol is the most developed and mature pre-combustion CO_2 capture option. These solvent-based absorption processes operate at a fairly low temperature. Thus, the gas stream entering the absorber must be significantly cooled down. This results in either loss of high amount of the available energy or high capital costs for heat recuperation [1]. It is therefore worth to investigate alternative CO_2 capture processes for IGCC applications with lower energy penalties than the low-temperature capture processes. Recently, solid adsorption-based processes, as an alternative to physical absorption-based processes have attracted growing attentions [2-6]. A novel pre-combustion CO_2 capture concept called sorption enhanced water gas shift (SEWGS) combines both the water gas shift (WGS) reaction and CO_2 capture in one single unit at elevated temperatures typically between ~350-550°C [7]. The CO_2 adsorption on a solid material shifts the equilibrium of the WGS reaction towards higher conversions of the CO into the CO_2. In contrast, conventional pre-combustion CO_2 capture

technologies typically consist of two stages of high temperature shift (HTS) and low temperature shift (LTS) reactors followed by a CO_2 capture unit. The CO_2 capture processes are typically based on physical absorption at low temperature, i.e. a Selexol-based process. Also there are intermediate cooling and reheating stages in such methods to prepare the fuel as per GT requirement [8, 9]. The SEWGS technology has the potential to lower the efficiency penalty of power plants with CCS technologies by combining the WGS reaction and CO_2 capture steps, as well as eliminating the need for cooling and reheating of syngas streams, as is done in conventional processes. Inherently, it is a dynamic process, which operates based on a pressure swing adsorption (PSA) process and undergoes a cyclic operation. The process reaches a cyclic steady state (CSS) after a number of cycles. Then almost an identical pattern of variations in product gas thermodynamic properties is observed repeatedly in each cycle [10, 11]. A H_2-rich stream at high pressure and a CO_2-rich stream at low pressure are produced. To achieve a continuous production of the H_2-rich and CO_2-rich products out of the batch SEWGS single reactor process, it is common to utilize a multiple reactor system for the PSA-based SEWGS process.

Lately, the technology has been attracted a growing interest for pre-combustion CO_2 capture application in power plants. However, it is still far from being considered as a well-developed and mature technology and further investigation and research works are yet to be carried out on different aspects of this technology. A research activity undertook screening studies on a number of potential CO_2 adsorbent materials to select the most suitable adsorbent. Then, a steady-state simulation of a natural gas combined cycle (NGCC) power plant integrated with the SEWGS process for pre-combustion CO_2 capture was carried out using the data achieved from the experimental work on the selected adsorbent material (K_2CO_3 promoted hydrotalcite (HTC)) [12]. Further experimental and theoretical research studies on the SEWGS process, including development of proper CO_2 adsorbent materials were carried out within the CACHET and later CAESAR projects [13, 14]. It was shown that the steam consumption and energy penalty were reduced by using the SEWGS technology for CO_2 capture compared to the conventional solvent-based pre-combustion CO_2 capture technologies [15]. A recent steady-state performance assessment of both NGCC and IGCC power plants integrated with the SEWGS process from thermodynamic and economical points of view was performed within the CAESAR project [7, 16]. The SEWGS system was a multi-train system, where each train was comprised of a number of reactors operating based on a SEWGS cycle configuration. The simulation results were indicated in terms of the efficiency and carbon capture ratio and compared with reference cases. The new K_2CO_3 promoted HTC material developed in the CAESAR project demonstrated catalytic properties and capability of H_2S and CO_2 co-adsorption. The SEWGS reactors were assumed adsorbent-filled reactors [7].

On the other hand, on a system level, there are not works investigating the performance of IGCC power plants integrated with PSA-based SEWGS process at transient and part-load conditions. Moreover, the periodic nature of the SEWGS process, in contrast with many typical processes which reach steady state, needs to be factored in when the process is integrated into an IGCC plant for pre-combustion CO_2 capture.

This work is therefore concerned with further control of the SEWGS process to fulfil the requirements of the GT with respect to fuel pressure and heating value. A dynamic detailed mathematical model of a multi-train SEWGS process which was previously developed is used in this work for simulation of the SEWGS process at different part-loads [17, 18]. A control strategy is designed to control the H_2-rich stream coming from the SEWGS system before it is sent to the GT. The dynamics of the SEWGS is revealed. This facilitates to understand whether the SEWGS process can follow the GT load changes. Also the impact of the SEWGS process on the operation flexibility of the IGCC plant is discussed.

2. IGCC integrated with the SEWGS process

A schematic diagram of an IGCC integrated with the SEWGS process for pre-combustion CO_2 capture is shown in Fig. 1. The IGCC power plant reference model from the European Benchmarking Task Force (EBTF) with two conventional HTS and LTS reactors followed by a solvent-based pre-combustion CO_2 capture unit is used [19]. However, in the present work the conventional HTS and LTS reactors as well as the CO_2 separation unit are replaced by the SEWGS vessels.

The gasification block is composed of an entrained-flow gasifer and air separation unit (ASU). Coal is partially oxidized at high temperature and pressure with oxygen (produced by the ASU) and steam to generate syngas. In the gas clean-up block, the syngas generated by the gasifier is further treated for the particulates and H_2S removal. The H_2S-rich gas is further processed in a claus plant to obtain valuable by-products. A sulphur-free syngas is then fed to the SEWGS process, so called sweet SEWGS. The detrimental effect of H_2S on the stability and long term CO_2

adsorption capacity of the K_2CO_3-promoted HTC considered in this work is the reason for choosing the sweet SEWGS process [9]. Two separate streams of the H_2-rich and CO_2-rich are produced in the SEWGS system. The H_2-rich stream enters the GT within the combined cycle block for combustion. The combined cycle block includes the GT, ST and HRSG. The high temperature of the H_2-rich stream is favoured by the GT from the efficiency point of view. The H_2-rich stream coming from the SEWGS system has almost constant temperature and pressure (~500ºC, ~27 bar), but the mass flow rate fluctuates over time (~±14%) [17].The GT requirement of having a smooth fuel heat input at any given load of operation necessitates further control of the H_2-rich stream before it is sent to the GT.
Low pressure (LP) and high pressure (HP) steam required by the SEWGS system for the rinse and purge steps are supplied from the combined cycle.

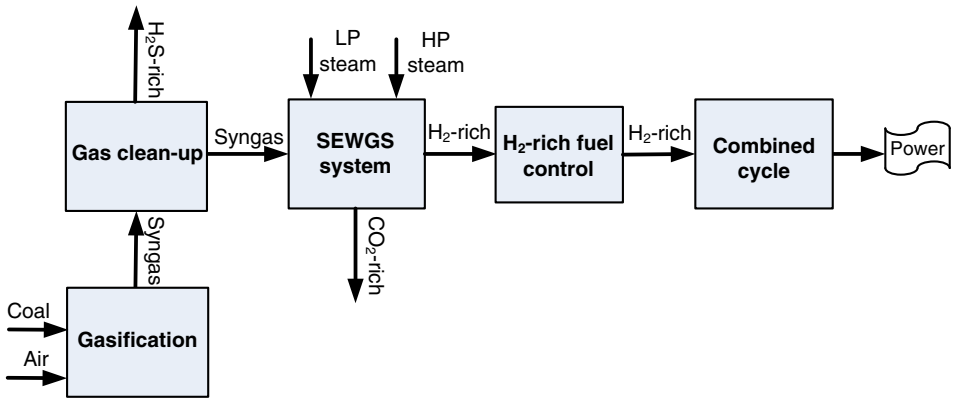

Fig. 1. A block diagram of an IGCC power plant integrated with the SEWGS process for CO_2 capture

2.1. SEWGS system layout

A top view of the SEWGS system is shown in Fig. 2. It consists of ten trains operating in parallel, where each train includes eight SEWGS vessels operating in a cyclic manner based on a PSA process. Each SEWGS reactor is packed with a mixture of the WGS catalyst and K_2CO_3 promoted HTC adsorbent and undergoes a sequence of steps according to a defined cycle configuration [17]. The SEWGS cycle configuration incorporates a sequence of steps including, feed, rinse (counter-current with HP steam), three pressure equalization (by connecting a pair of reactors), depressurization, purge (counter-current with LP steam) and repressurization (counter-current with part of the H_2-rich product gas). The H_2-rich stream is produced during the feed step where the combined WGS reaction and simultaneous CO_2 adsorption take place. The CO_2-rich stream is released during the depressurization and purge steps, through the regeneration of the solid adsorbent at atmospheric pressure. The multi-reactor system makes it possible to achieve close to continuous operation of SEWGS process, even if each reactor vessel functions as a batch process.

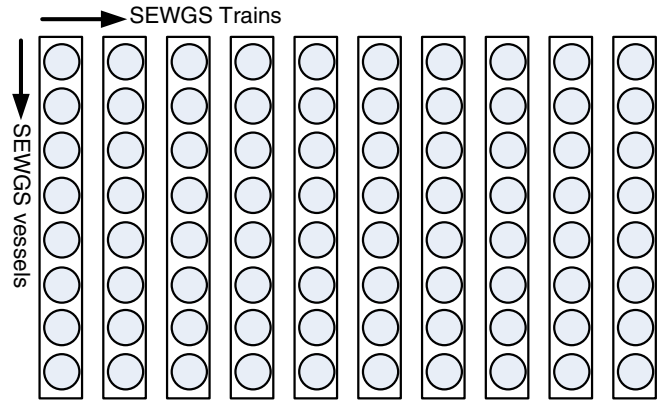

Fig. 2. The SEWGS multi-train system top view; ten trains operating in parallel, eight vessels in each train operating based on a cyclic PSA process

2.2. Fuel control strategy

The cyclic operation characteristics of the PSA-based SEWGS process leads to the production of the H_2-rich stream with repeated fluctuations over time, when the CSS is reached [17]. A closed-loop control strategy is thus designed to smooth out fluctuations in the H_2-rich stream flow rate before it is sent to the GT. As a part of the control system, a buffer tank is placed downstream of the SEWGS process to damp out a large portion of the H_2-rich fuel flow fluctuation (see Fig. 3).

A proportional integral (PI) controller which incorporates a control valve undertakes further control of the H_2-rich fuel with respect to pressure and mass flow rate. The control system is designed to control the H_2-rich fuel mass flow rate according to a set-point value. The set-point value of the fuel mass flow rate is determined based on the GT load. The objective of the control system in addition to smooth out the H_2-rich fuel flow fluctuation is also to adjust the H_2-rich fuel flow when the GT load is changed. The PI controller reduces the difference between the measured fuel mass flow rate and its set point value (error) by changing the valve actuator. Zero steady state error and fast transient response are the main characteristics of a well-functioning PI controller. A tuned anti-windup compensator is added to improve the performance of the closed loop PI controller with respect to the minimized transient response time. The structure of the PI controller including the anti-windup scheme is shown in Fig. 4. It is known that physical systems are subject to actuator saturation or limitation. This is called windup problem, where in the presence of saturation, controller behavior will be greatly deteriorated. However, the method to solve process control design problems in the case of existing input saturation in classical PI controllers is an introduced anti-windup approach [20]. In this paper, an anti-windup scheme is employed to prevent the controller's output, which is the valve actuator opening, X_{Valve_act}, from saturation and reduce the transient response time of the fuel mass flow rate under the effect of the controller.

The output of PI controller before the saturation block can be expressed by Equation (1):

$$U_{controller}=U_p(t)+U_i(t) \quad (1)$$

Where,

$$U_p(t)=K_p\,e(t) \quad (2)$$

$$U_i(t)=U_i\,e(t\text{-}1)+K_i\int U_p(t)\,dt+K_c\left[(X_{Valve\_act}-U_{controller})\right] \quad (3)$$

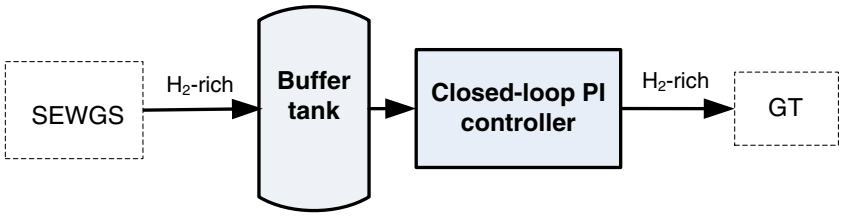

Fig. 3. H_2-rich fuel Control strategy

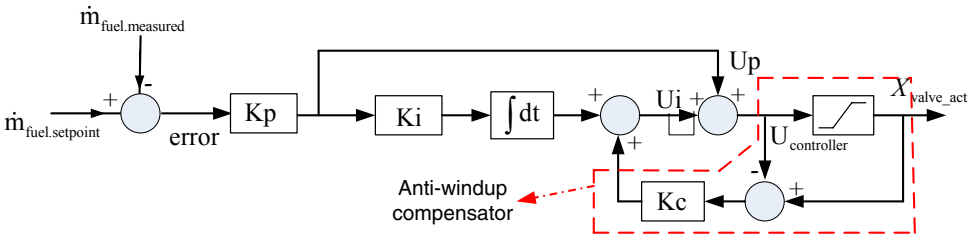

Fig. 4. The structure of PI control with anti-windup scheme

The anti-windup coefficient K_c should be in the same order as K_i (in this work: $K_i = K_c = 2.25\times10^{-4}$). The K_p is the integral coefficient ($K_p = 2.99\times10^{-3}$). The error e(t) is calculated as e(t) = error, which is the difference between the measured fuel mass flow rate at the operating point and its value corresponding to the desired mass flow rate.

3. Results and discussion

An IGCC power plant does not necessarily operate at base load. Following the variations in the electricity demand, the operation of the IGCC plant will be subject to change. In general, the operation of an IGCC plant is less flexible compared to an ordinary combined cycle power plant. This is due to the inertia in connection with its process units mainly gasifier and ASU to generate and prepare the fuel at the conditions required by the GT. The operation flexibility of the IGCC plant is further affected when a CO_2 capture process, i.e. SEWGS process in this case, is introduced to the IGCC plant. To investigate the impacts of the SEWGS system on the operation flexibility of the IGCC plant, understanding of the dynamics of the SEWGS process and how fast it responds to load changes is required. It will provide an insight about the operability and load-following performance of the entire IGCC integrated with the SEWGS system at different part-load. In this section the results related to the dynamics of the SEWGS system as well as the performance of the GT fuel control strategy and operation flexibility of the IGCC integrated with the SEWGS at part-load operation are presented.

3.1. SEWGS dynamic characteristics

The detailed mathematical model which was developed previously is used to simulate the SEWGS system at different loads of the feed syngas [17, 18]. The CO_2 recovery and purity achieved from the simulation of the

SEWGS process at design condition are 95% and 99% respectively. To maintain the part-load performance of the SEWGS system in terms of the CO_2 recovery and purity same as the design condition, in addition to changing the load of the syngas, other parameters should also be varied. Key parameters influencing the performance of the SEWGS system are the cycle time, cycle configuration, number of the vessels, size of the vessels, rinse steam and purge steam consumption. In this work the number and size of the vessels as well as the cycle configuration are fixed when the load of the syngas is changed. On the other hand, amount of the purge and rinse steam as well as the cycle time are changed in a way to produce almost the same CO_2 purity and recovery rate as the design case. Simulation of the SEWGS system at different loads of the feed syngas is performed. Fig. 5 shows the load gradient of the SEWGS system achieved (seven data points). The best fit line to the data-sets is also drawn in Fig. 5 which has a slope of approximately 2.1 load%/min. This represents the load gradient (ramp rate) of the SEWGS system and indicates that the SEWGS process is very slow in responding to load changes compared to the GT. (load gradient of over 10%MW/min).

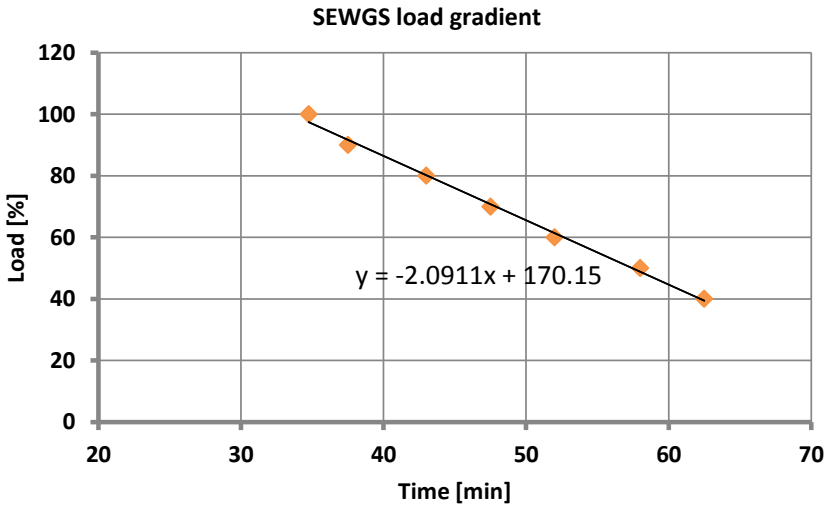

Fig. 5. Load gradient of the SEWGS system achieved from the different part-load simulations

3.2. GT fuel control system performance

The GT fuel mass flow rate is a function of the GT load. At any given load of operation, the control system adjusts the amount of the GT fuel mass flow rate according to its corresponding set-point value. Fig. 6 shows how the control system functions when two disturbances take place in the GT load in a stepwise manner. It is assumed that a 20% load reduction is given to the GT load, while the entire IGCC plant is operating at full-load. The GT then operates at 80% of its full-load for 400 seconds. Again, the load is increased back to the full-load level. Following the GT load changes, the fuel mass flow rate is controlled by the PI controller to approach its set-point value. As shown in Fig. 6 the designed control strategy performs properly and the fuel mass flow rate approaches its set-point after the transient response time is passed and the steady-state is reached. The flow rate fluctuations are reduced by the designed control strategy from ~±14% in the H_2-rich stream leaving the SEWGS system to ~±1-2%. Fig. 7 shows the impact of the anti-windup compensator included in the classical PI controller, as illustrated in Fig. 4, on improving the fuel mass flow rate behavior with respect to the transient response time. When a 20% reduction in the GT load occurs, the fuel mass flow rate is controlled in a way to approach its new set-point value when the new steady state is reached. However, it takes longer for the classic PI controller (without anti-windup) to reach the

steady sate compared to the PI controller with anti-windup compensator. This shows how the anti-windup compensator improves the fuel mass flow rate behavior and reduces the transient state.

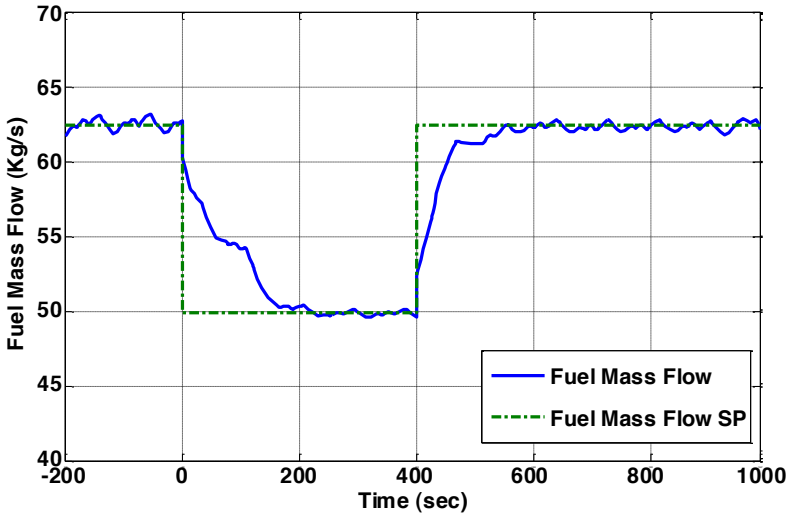

Fig. 6. GT fuel mass flow rate profile, 20% GT load reduction (stepwise) at time=0 seconds, 20% GT load increase (stepwise) at time=400 seconds

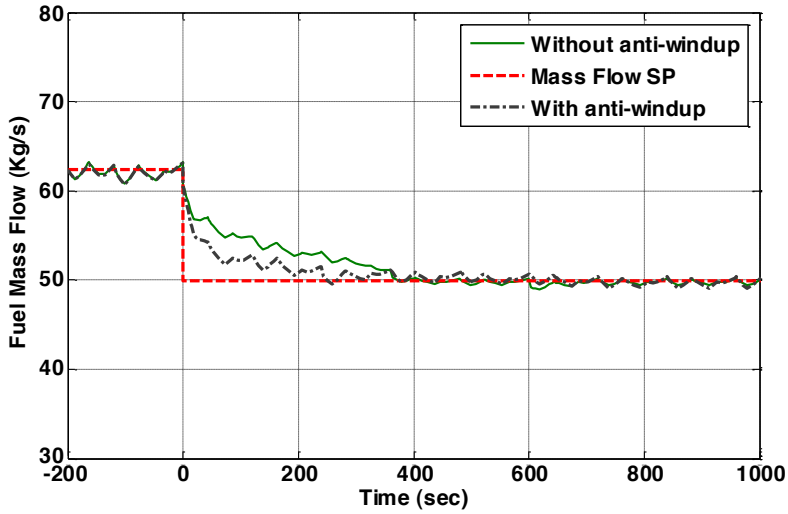

Fig. 7. Comparison of the GT fuel mass flow rate behaviour with and without anti-windup compensator, 20% GT load reduction (stepwise) at time=0 seconds

3.3. Load following capability of the SEWGS system at part-load operation

As mentioned in the previous section, a buffer tank is assumed after the SEWGS system to flatten out a portion of the fluctuations in the H_2-rich stream flow rate produced in the SEWGS system. The variation of the pressure in the buffer tank is important to ensure sufficient flow rate and pressure of the H_2-rich fuel to the GT during the operation. The pressure in the tank should fall within an acceptable range (between the pressure of the upstream SEWGS and downstream GT). Fig. 8 shows the buffer tank pressure variation when the 20% GT load reduction takes place.

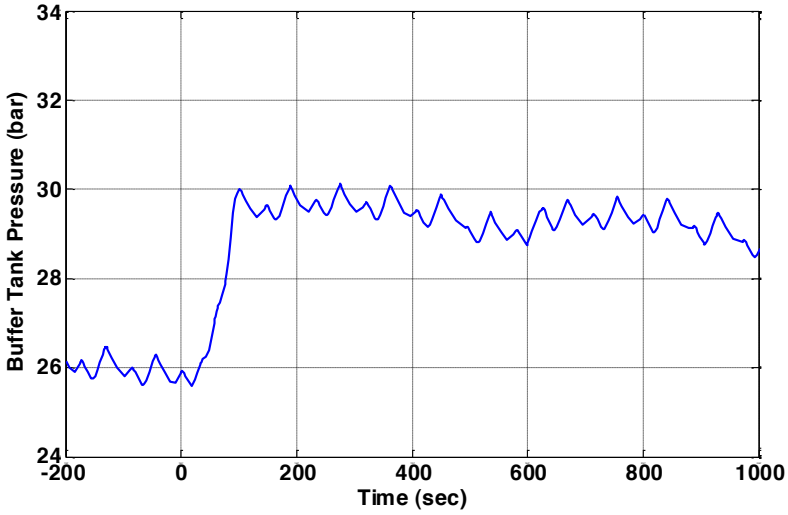

Fig. 8. Buffer tank pressure variation, 20% GT load reduction (stepwise) at time=0 seconds

As indicated in Fig. 8, the buffer tank pressure starts increasing once the 20% step reduction in the GT load is given. This is due to the imbalances occurring in the buffer tank inlet and outlet streams as a consequence of different response time of the process components to the load changes. The GT has a relatively fast dynamics. When the GT load is reduced, the fuel mass flow rate leaving the buffer tank is reduced correspondingly under the effect of the control system. On the other hand, it takes longer for the SEWGS system to respond to the GT load changes due to the slow dynamics. This will thus result in a pressure build-up in the tank, when the GT load is reduced. The tank pressure build-up continues until the transient response time is passed. Using the buffer tank improves the operation flexibility of the GT. As long as the acceptable pressure range in the buffer tank is met, the GT load can change without changing the load of the GT upstream process components. When the pressure in the buffer tank goes beyond the acceptable range, changing the load of the GT upstream process components is also required. In this case, load following capability of the process components which depends on their dynamic characteristics, is one of the main issues.

4. Conclusion

Part-load performance of an integrated gasification combined cycle (IGCC) power plant incorporating a sorption enhanced water gas shift (SEWGS) process for pre-combustion CO_2 capture is investigated. The SEWGS process with the multiple train arrangement operates in a cycle manner based on a pressure swing adsorption (PSA) process.

The H_2-rich stream which is the main product of the SEWGS is used as a gas turbine (GT) fuel. The periodic nature of the SEWGS process leads to the production of the H_2-rich stream with repeated fluctuations when the cyclic steady state is reached. To fulfill the requirements of the GT with respect to fuel pressure and heating value a control strategy including a buffer tank and a closed-loop PI controller is designed. A dynamic detailed mathematical model of the multi-train SEWGS process which was previously developed is used for simulation of the SEWGS process at different part-loads [17, 18]. Simulation results show the H_2-rich stream flow rate fluctuation is reduced from ~±14% to ~±1% under the effect of the designed control system. Also, when a disturbance in the GT load takes place, the fuel control system functions properly and provides the corresponding GT fuel flow rate and pressure after a new steady state is achieved. On the other hand, as a consequence of slow transient response of the SEWGS process to load changes (~2 load%/min as obtained from the part-load simulations), the mass balance of the buffer tank is also disturbed and pressure buildup in the tank is observed. However, addition of the buffer tank improves the operation flexibility of the GT as long as the buffer tank pressure variation is within a desired range. Different part-load operation strategies such as planned GT load changes can be considered to minimize the imbalances occurred in the system during the transient state of the IGCC plant and achieve a smooth operation of the IGCC integrated with the SEWGS process when the GT load is changed.

References

[1] Zan Liu and William H. Green, "Analysis of Adsorbent-Based Warm CO_2 Capture Technology for Integrated Gasification Combined Cycle (IGCC) Power Plants", Ind. Eng. Chem. Res., 53 (2014), 11145−11158.

[2] S. García, M.V. Gil, C.F. Martín, J.J. Pis, F. Rubiera, C. Pevida, "Breakthrough adsorption study of a commercial activated carbon for Pre-combustion CO_2 capture", Chemical Engineering Journal 171 (2011) 549–556.

[3] Armin D. Ebner and James A. Ritter, "State-of-the-Art Adsorption and Membrane Separation Processes for Carbon Dioxide Production from Carbon Dioxide Emitting Industries", Separation Science and Technology, 44 (2009), 1273–1421.

[4] S. Choi, J.H. Drese, C.W. Jones, Adsorbent materials for carbon dioxide capture from large anthropogenic point sources, ChemSusChem 2 (2009), 796–854.

[5] Nathalie Casas, Johanna Schell, Richard Blom, Marco Mazzotti, "MOF and UiO-67/MCM-41 adsorbents for pre-combustion CO_2 capture by PSA: Breakthrough experiments and process design", Separation and Purification Technology 112 (2013), 34–48.

[6] Johanna Schell, Nathalie Casas, Richard Blom, Aud I. Spjelkavik, Anne Andersen, Jasmina Hafizovic Cavka, Marco Mazzotti, "MCM-41, MOF and UiO-67/MCM-41 adsorbents for pre-combustion CO_2 capture by PSA: adsorption equilibria", Adsorption 18 (2012), 213–227.

[7] Giampaolo Manzolini, Ennio Macchi, et.al., "Integration of SEWGS for carbon capture in natural gas 6 combined cycle. Part A: Thermodynamic performances", International Journal of Greenhouse Gas Control 5 (2011) 200–213.

[8] D.P.Harrison, "Sorption Enhanced Hydrogen Production: A review", Industrial & Engineering Chemistry Research, 47 (2008), 6486-6501.

[9] J.R. Hufton, R.J. Allam, R. Chiang, et.al., "Development of a process for CO_2 capture from gas turbines using a sorption enhanced water gas shift reactor system", in Proceedings of 7th International Conference on Greenhouse Gas Control Technologies,1 (2005), 253-262.

[10] Jong-Ho Park, Jong-Nam Kim, and Soon-Haeng Cho, "Performance analysis of four-bed H_2 PSA process using layered beds", AIChE Journal, 46 (2000), 790-802.

[11] Ashok D Dave, Sina Rezvani, Ye Huang, David McIlveen-Wright, Neil Hewitt, "Integration and performance assessment of hydrogen fired combined cycle power plant with PSA process for CO_2 capture in pre-combustion IGCC power plant.", Proceedings of the ASME 2012 Gas Turbine India Conference, December 1, 2012, Mumbai, Maharashtra, India.

[12] R.J. Allam, R. Chiang, et.al., "Development of the sorption enhanced water gas shift process", Carbon 38 Dioxide Capture for Storage in Deep Geologic Formations 1 (2005), 227–256.

[13] Caesar FP7 Project, 2008. http://caesar.ecn.nl

[14] Cachet FP6 Project, http://www.cachet2.eu

[15] A.D. Wright, V. White, et.al.,"CAESAR: Development of a SEWGS model for IGCC". Energy Procedia, 4 (2011), 1147–1154.

[16] Matteo Gazzani, Ennio Macchi, Giampaolo Manzolini, "CO_2 capture in integrated gasification combined cycle with SEWGS – Part A: Thermodynamic performances", Fuel 105 (2013), 206-219.

[17] Bita Najmi, Olav Bolland, Konrad E. Colombo, "Dynamic modeling and simulation of a Sorption Enhanced Water Gas Shift (SEWGS) process for CO_2 capture", submitted manuscript.

[18] Bita Najmi, Olav Bolland, Snorre Foss Westman, "Simulation of the cyclic operation of a PSA-based SEWGS process for hydrogen production with CO_2 capture", Energy Procedia 37 (2013), 2293– 2302.

[19] Franco et al., European Benchmarking Task Force (EBTF), "Common Framework Definition document", 2009.

[20] Peter Hippe, "Windup in Control: Its Effects and Their Prevention," Springer-Verlag, London, 2006.